NASA/TM-2013-217380-REV1

Application of the Brinkley Dynamic Response Criterion to Spacecraft Transient Dynamic Events

Jeffrey T. Somers
Wyle Science, Technology, and Engineering Group

Dustin Gohmert
National Aeronautics and Space Administration

James W. Brinkley
Independent Consultant

National Aeronautics and Space Administration

Johnson Space Center Houston,
Texas 77058

March 2017

NASA STI Program ... in Profile

Since its founding, NASA has been dedicated to the advancement of aeronautics and space science. The NASA scientific and technical information (STI) program plays a key part in helping NASA maintain this important role.

The NASA STI program operates under the auspices of the Agency Chief Information Officer. It collects, organizes, provides for archiving, and disseminates NASA's STI. The NASA STI program provides access to the NASA Aeronautics and Space Database and its public interface, the NASA Technical Report Server, thus providing one of the largest collections of aeronautical and space science STI in the world. Results are published in both non-NASA channels and by NASA in the NASA STI Report Series, which includes the following report types:

- TECHNICAL PUBLICATION. Reports of completed research or a major significant phase of research that present the results of NASA Programs and include extensive data or theoretical analysis. Includes compilations of significant scientific and technical data and information deemed to be of continuing reference value. NASA counterpart of peer-reviewed formal professional papers but has less stringent limitations on manuscript length and extent of graphic presentations.
- TECHNICAL MEMORANDUM. Scientific and technical findings that are preliminary or of specialized interest, e.g., quick release reports, working papers, and bibliographies that contain minimal annotation. Does not contain extensive analysis.
- CONTRACTOR REPORT. Scientific and technical findings by NASA-sponsored contractors and grantees.
- CONFERENCE PUBLICATION. Collected papers from scientific and technical conferences, symposia, seminars, or other meetings sponsored or co-sponsored by NASA.
- SPECIAL PUBLICATION. Scientific, technical, or historical information from NASA programs, projects, and missions, often concerned with subjects having substantial public interest.
- TECHNICAL TRANSLATION. English-language translations of foreign scientific and technical material pertinent to NASA's mission.
- Specialized services also include creating custom thesauri, building customized databases, and organizing and publishing research results.
- For more information about the NASA STI program, see the following:
- Access the NASA STI program home page at *http://www.sti.nasa.gov*
- E-mail your question via the Internet to help@sti.nasa.gov
- Fax your question to the NASA STI Help Desk at 443-757-5803
- Phone the NASA STI Help Desk at 443-757-5802
- Write to:

  NASA STI Help Desk
  NASA Center for AeroSpace Information
  7115 Standard Drive
  Hanover, MD 21076-1320

NASA/TM-2013-217380-REV1

Application of the Brinkley Dynamic Response Criterion to Spacecraft Transient Dynamic Events

Jeffrey T. Somers
Wyle Science, Technology, and Engineering Group

Dustin Gohmert
National Aeronautics and Space Administration

James W. Brinkley
Independent Consultant

National Aeronautics and Space Administration

Johnson Space Center Houston,
Texas 77058

March 2017

Available from:

NASA Center for AeroSpace Information
7115 Standard Drive
Hanover, MD 21076-1320

National Technical Information Service
5301 Shawnee Road
Alexandria, VA 22312

Available in electronic form at https://ston.jsc.nasa.gov/collections/TRS

TABLE OF CONTENTS

Introduction 1
1.0 Background 2
1.1 Focus on the Development and Validation of a Spinal Injury Model 5
1.2 Evaluating the Acceptability of Multi-Directional Acceleration Conditions 6
2.0 Brinkley Dynamic Response Criterion Development 7
2.1 Limitations 7
2.2 -X Axis 7
2.2.1 -X Axis Dynamic Response Model Parameter Estimation 7
2.2.2 -X Axis Injury Risk Level Determination 8
2.2.3 -X Axis Model Limitations 9
2.3 +X Axis 10
2.3.1 +X Axis Dynamic Response Model Parameter Estimation 10
2.3.2 +X Axis Injury Risk Level Determination 10
2.3.3 +X Axis Model Limitations 11
2.4 ±Y Axis 11
2.4.1 Y Axis Dynamic Response Model Parameter Estimation 11
2.4.2 Y Axis Injury Risk Level Determination 12
2.4.3 Y Axis Model Limitations 12
2.5 +Z Axis (Eyeballs Down) 13
2.5.1 +Z Axis Dynamic Response Model Parameter Estimation 13
2.5.2 +Z Axis Injury Risk Level Determination 14
2.5.3 +Z Axis Model Limitations 15
2.6 -Z Axis (Eyeballs Up) 15
2.6.1 -Z Axis Dynamic Response Model Parameter Estimation 15
2.6.2 -Z Axis Injury Risk Level Determination 16
2.6.3 -Z Axis Model Limitations 16
3.0 Brinkley Dynamic Response Criterion Application 17
4.0 Brinkley Dynamic Response Criterion Historical Usage 18
4.1 Evaluation of Mercury Capsule Landings 18
4.2 Evaluation of Apollo Capsule Landings 19
4.3 Evaluation of Soyuz Capsule Landings 19
5.0 Brinkley Dynamic Response Criterion Application Rules 19
5.1 Transient Accelerations 19
5.1.1 Verification Method 19
5.2 Proper Restraint 20
5.2.1 Required Restraint 20
5.2.2 Pelvic Restraints 21
5.2.3 Torso Restraints 21
5.2.4 Negative-G Restraints 21
5.2.5 Verification Method 21
5.3 Flail Considerations 22
5.3.1 Verification Methodology 23
5.4 Seating Support 23
5.4.1 Verification Method 24
5.5 Occupant Response Amplification 24
5.5.1 Verification Method 25
5.6 Suit Considerations 26
5.6.1 Chest Mounted Equipment 26
5.6.2 Rigid Suit Elements 26

5.6.3 Head Protection 26
5.6.4 Helmet Mass 26
5.7 Spaceflight Deconditioning 27
5.7.1 Verification Method 28
6.0 Limitations 28
6.1 Sex Differences 28
6.1.1 Required ATD Assessments to Address Sex Differences 29
6.2 Age Effects 29
6.3 Anthropometry Effects 30
6.3.1 Verification Methodology 30
6.4 Military Training 30
7.0 ATD Supplementary Test and Analysis 31
7.1 ATD Specifications 31
7.1.1 Head Specification Revision 31
7.1.2 Pelvis and Spine Specifications 31
7.2 Neck Injury Assessment 32
7.2.1 Current HSIR Limits - Individual Limits 32
7.2.2 Proposed HSIR Limits - N_{ij} Neck Injury Criteria 33
7.2.3 Proposed HSIR Limits -Neck Axial Force Injury Criteria 37
7.2.4 Limitations of the Proposed Neck Injury Assessment 40
7.3 Head Injury Metrics 40
7.3.1 Linear Head Acceleration 41
7.3.2 Rotational Head Acceleration 43
7.3.3 Limitations of the Proposed Head Injury Assessment 44
7.4 Flail Limit 45
7.5 Lumbar Axial Compression Force 45
7.6 Summary 45
8.0 Design Validation Approach 46
8.1 Case Selection Approach 48
8.2 Model Development Approach 50
8.3 Model Validation Approach 51
8.4 Design Compliance Approach 52
8.4.1 Design Compliance Testing 52
8.4.2 Design Compliance Analysis 52
8.4.3 Human Volunteer Testing Requirement Verification 53
8.5 Adverse Outcomes 56
9.0 Forward Work 56
10.0 Conclusion 57
11.0 References 58
APPENDIX A - Summary of Occupant Protection Impact Tests Conducted to Support Joint USAF and NASA Spacecraft Landing Studies 67
APPENDIX B - NASA Sign Convention 74
APPENDIX C - Acronyms and Abbreviations 75
APPENDIX D - Documentation 76

INTRODUCTION

Currently, the National Aeronautics and Space Administration (NASA) occupant protection standards are primarily based on the Multi-Axial Dynamic Response Criteria, which NASA refers to as the Brinkley Dynamic Response Criterion (BDRC). The BDRC was developed by the United States Air Force (USAF) and adopted by NASA in the mid-1990s during the development of the Assured Crew Return Vehicle (ACRV) [1] and evaluation of the Soyuz three-person crew vehicle landing impact tests [2-6].

During this period, NASA developed the X-38 vehicle that would remain docked to the International Space Station (ISS) to provide emergency return capability for the ISS crew. The vehicle was designed to land on unprepared terrain instead of landing on the runway as with the Space Shuttle.

In addition, NASA contracted with NPO Energia (developers of the Soyuz spacecraft) in the early 1990s to modify and evaluate the Soyuz vehicle for use to transport U.S. astronauts to and from the ISS.

This BDRC eventually was incorporated into the NASA-STD-3001, Space Flight Human-System Standard document, which applies to all new manned vehicle programs at NASA.

The BDRC criterion includes a dynamic model, which is used to evaluate the risk of injury using a series of lumped parameter models with mass, spring, and damping properties. The individual model units are arranged orthogonally to respond to linear accelerations and linear components of angular accelerations measured on the vehicle occupant seat. During the BDRC development, these model responses were related to human injury data to develop low, medium, and high injury risk limits. Because of the simplicity of the BDRC, it is very attractive to designers, as it is very simple to evaluate for many design cases with only seat accelerations. However, because of these simplifications and the specific characteristics of the seating systems used, there are application criteria or rules that are necessary to correctly apply the model and interpret the results. In addition, because of the subjects used in the development of the BDRC and some unique considerations for NASA's applications, several limitations have been identified that limit the injury prediction capabilities of the model.

The purpose of this document is to review the BDRC development, document the rules necessary to apply the BDRC, identify limitations for NASA's application, and describe additional testing and analysis methods necessary to supplement the BDRC.

1.0 BACKGROUND

The BDRC was developed as a result of an evolutionary process to define the human dynamic response (DR) to, and exposure limits for, short-duration accelerations (i.e., ≤500 ms) associated with spacecraft landing and emergency escape system performance. The initial database that was used to associate injury risk to short-duration acceleration exposures was developed in the mid to late 1940s and early 1950s by the USAF research authorities such as Stapp and his contemporaries [7-10]. These data were used in the guidance and standards for design, development, and performance evaluation of aircraft emergency ejection seats. Accelerations during ejection seat and occupant catapulting from an aircraft cockpit and their aerodynamic deceleration were controlled by use of limits defined in terms of acceleration amplitude, rate of acceleration onset, and duration presuming a trapezoidal waveform [11, 12]. Injury risks were defined in terms of areas of voluntary tolerance, medium injury, and severe injury. This approach worked well for open ejection seat design as the acceleration-time profiles could be easily controlled by those limited parameters.

In the mid 1950s to early 1960s, escape systems designers developed aircraft enclosed escape systems to provide very high-speed escape and high-altitude protection capabilities such as those provided by the B-58 capsule, the XB-70 capsule, and the F/FB-111 crew escape cockpit. These aircraft escape systems were each designed to land with the occupants on the Earth's terrain or water. The landing impact profiles did not meet the acceleration limit criteria due to the high rates of acceleration onsets and multi-directional nature of the landing impacts.

In the late 1950s, the USAF and NASA undertook the design of manned spacecraft. USAF programs included Dyna-Soar and the Manned Orbiting Laboratory (1958 to 1967) and NASA successfully developed the Mercury, Gemini, and Apollo space flight programs [13]. The initial acceleration limits were established [11, 12] in terms of rate of onset, acceleration amplitude, and duration for acceleration profiles known to be within voluntary tolerance and those known to cause medium to severe injury. However, the fitting of the trapezoidal acceleration-time histories was inadequate to assess the injury risk due to the complex multi-directional landing impact acceleration-time histories associated with these crew systems.

These systems shared a common design constraint; they were limited in terms of the distance available for deceleration of the vehicles during landing. For example, the B-58 capsule landed on the seatback bulkhead with only inches available for the stroke of its four metal cutting impact attenuation devices [14]. The Mercury capsule would normally land on water using an airbag skirt around its heat shield to attenuate impact under normal recovery conditions. However, if the capsule was to be safely lifted away from the main launch rocket during an emergency abort on the launch pad, the skirt could not be deployed and inflated quickly enough to protect the capsule occupant during land or water landing. Only a small column of crushable aluminum honeycomb under the astronaut's seatback would be available to attenuate the landing impact.

In contrast, ejection seats could be accelerated over a distance of about 3 feet by its ejection catapult, thereby permitting a more gradual rate of acceleration onset to meet the relatively low rate of onset limits enforced at that time by the USAF and Navy.

As a result of this problem, the USAF began experimental studies to investigate the effects of rapid rate of onset accelerations that would occur during escape capsule landings. The studies were also designed to investigate how the human body responded as a mechanical system to extremely high rate of acceleration onset in the range of thousands of G/s [15]. Due to the parallel investigations and development of spacecraft by the USAF and NASA, this line of investigation was tackled jointly, both experimentally [16-19] and analytically, using existing empirical data and a mechanical dynamic systems approach [20-23].

Examples of other key experimental research results include that of Beeding and Mosely [24, 25] who conducted experiments using a horizontal deceleration facility to study the responses of volunteers to impact in forward-facing and rearward-facing seats as well as off-axis conditions [25] with lap belt and shoulder harness restraints. They reported severe shock and repeated syncope with myalgia requiring one volunteer to be hospitalized for 5 days following his exposure to a 40-G sled deceleration with a rate of onset of 2,139 G/s and a velocity change of 48.5 ft/s in a rear-facing seat. Mosley reported that the subject may not have survived without immediate medical care. Prior exposures of volunteers in this position ranged from 25 to 40 G at onset rates from 1,034 to 2,139 G/s for durations of 50 to 190 ms. Impact velocities were below 50 ft/s. The acceleration-time histories could be defined in terms of the existing trapezoidal acceleration-time profile, although a half-sine pulse shape more approximated the applied acceleration.

The experimental efforts were soon expanded to investigate the effects of multidirectional accelerations necessary to support the development of the Apollo crew module. The initial multidirectional impact studies were conducted with volunteer military subjects using a vertical deceleration tower to demonstrate the safety of impact conditions expected during the Apollo crew module landings [26]. These were the first controlled multidirectional impact experiments to study the human response to impact directions other than impacts in the X axis and Z axis. Special concern was focused upon the responses of the volunteers to sideward acceleration since the Apollo impact attenuation system was limited to a stoke distance of less than 8 inches in that direction. Prior to this research, volunteers had not been exposed to sideward impact. Impact levels were gradually raised by increments of direction and impact level until the NASA goals of impact level were reached. Acceleration levels ranged from 3 to 26.6 G with rates of onset ranging from 300 to 2000 G/s and impact velocities up to 28 ft/s.

U.S. Navy researchers conducted impact tests with volunteers using a horizontal track at a Naval facility in Philadelphia to provide the initial investigations of the effects of impacts in the -Z axis to support the Apollo program [27].

The USAF experimental research was expanded using the horizontal deceleration facilities at Holloman Air Force Base (AFB) [28-30] to partially replicate the work of Weis et al. and to increase the investigation to include tests conducted including -Z axis components that were not considered feasible using the vertical deceleration facility at Wright-Patterson AFB. More than 500 tests were performed at Wright-Patterson AFB and Holloman AFB to support the objectives of these multidirectional impact investigations.

Later impact tests were conducted at Holloman AFB with volunteers to study the influence of developmental seats, restraints, and pressure suits, as shown in Figures 1 and 2. Complete test plans, medical protocols, test data recordings, and photogrammetric records of these tests have not been located.

During these later impact tests of full pressure suit prototypes, one of two subjects exposed to +Z axis impact conditions incurred a seventh thoracic vertebra fracture as a result of the tests being conducted with the pressure suit partly inflated [31]. The details of these tests remain unknown.

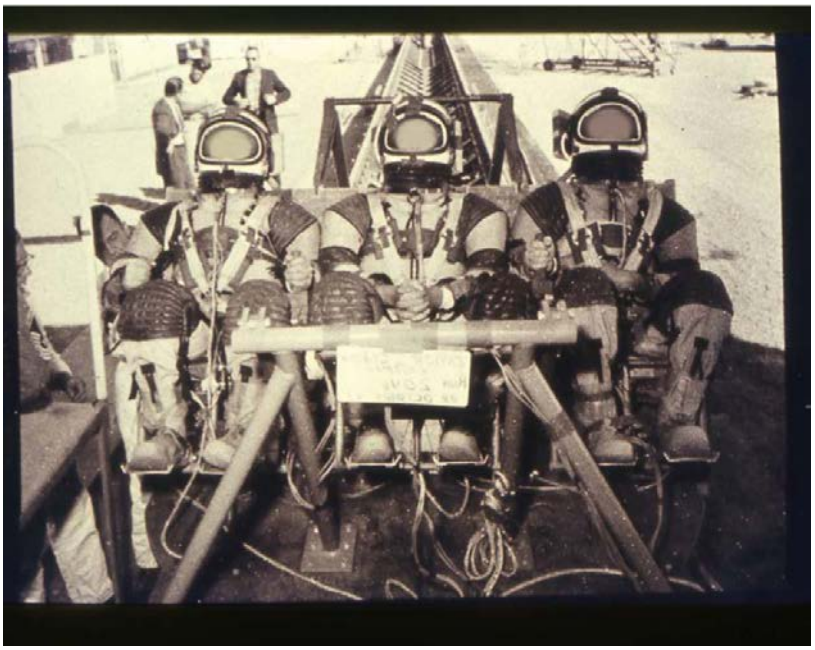

Figure 1. Volunteers undergoing an impact test in developmental pressure suits, lap belts, shoulder harness, and seating system. (Credit: USAF)

Figure 2. A volunteer being tested in a developmental pressure suit using a lap belt, shoulder straps, and inverted-V, negative-G straps. (Credit: USAF)

Payne [22] further developed numerical models of human body dynamics and studied the effects of body support and restraint systems in a research effort jointly funded by the USAF and NASA. Important analytical results influencing the design of restraint systems included studies of the influence of restraint system slackness and preload using lumped-parameter models of human dynamic impact response.

The results of the hundreds of impact tests with volunteer subjects and of the analytical modeling efforts were used to support the design and development the Apollo crew module and its occupant protection system. The module successfully recovered each crew without injuries after every landing impact throughout the entire Apollo program. The final design of the body support and restraint system used in the Apollo crew module was simpler that the body support system initially used in the multidirectional impact research experiments with volunteers. More details of these research efforts are provided in Appendix A.

1.1 FOCUS ON THE DEVELOPMENT AND VALIDATION OF A SPINAL INJURY MODEL

Payne had suggested that two lumped parameter models could be used to describe the human responses to spinal (+Z-axis) and transverse (X-axis) impact conditions. NASA and the Air Force Research Laboratory (AFRL) sponsored a more detailed study of these models [23] using data from tests with human cadavers, and available impact as well as vibration tests with volunteers [32].

The spinal injury model was used on an experimental basis to evaluate the performance of the F/B-111 crew-escape cockpit system during developmental and qualification ejections from a rocket-propelled sled. Using the spinal injury model referred to as the Dynamic Response Index (DRI), Brinkley estimated the ground landing of the F/B-111 escape system to have a probability of spinal injury greater than 20%. After the system was operational, the spinal injury rate was found to be 29.5%(23/78) by Hearon et al. [33].

Brinkley [34] and colleagues [35] conducted laboratory impact studies and evaluation of the spinal injury rates associated with operational USAF ejection seats using the DRI model developed by Steck and Payne [23]. Using the operational ejection seat data, Brinkley and Shaffer [35] validated the model using the injury probability distribution from the work of Steck and Payne [23], but adjusting it to match the higher resistance to crew spinal injury shown in Figure 3 [35].

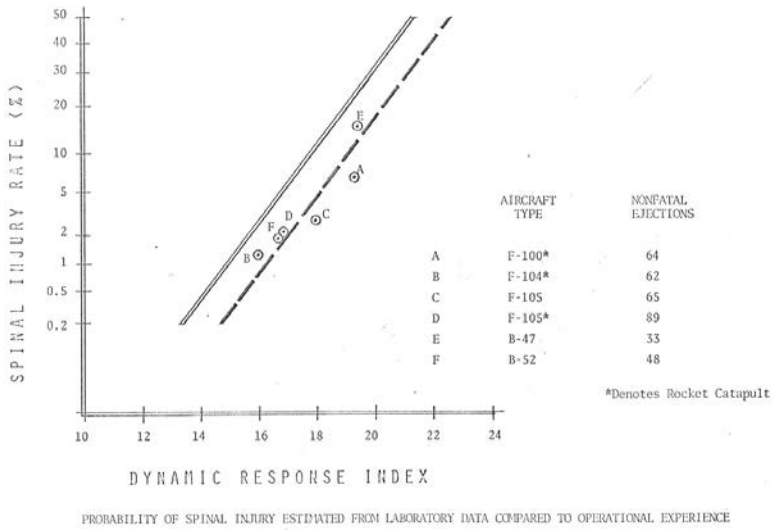

Figure 3. Probability of spinal injury estimated from operational ejection seat experience [35].

The DRI model estimates combined with ejection tests on volunteers were used to correct an extraordinarily high spinal injury rate associated with the ejection seat used in the F-4 aircraft. The complex curvature of the seat back and headrest caused the seat occupant to be forward of the ejection catapult thrust vector [35, 36]. This caused the occupant's head and upper body to flex forward and the lumbar spine and pelvis to rotate backward during ejection, lowering the threshold of compression injury to the thoracic spine and coccyx [37]. To correct the high injury rate, the ejection catapult thrust was reduced and a rocket was added to the seat bottom to sustain the acceleration after the seat separated from the aircraft. The seat-back geometry and thrust vector alignment could not be accomplished without a major seat redesign or replacement (see Figure 4). Because of the feasible changes, the spinal injury rate was reduced from 34% attributed to catapult force to 8% as shown in Figure 5 [35].

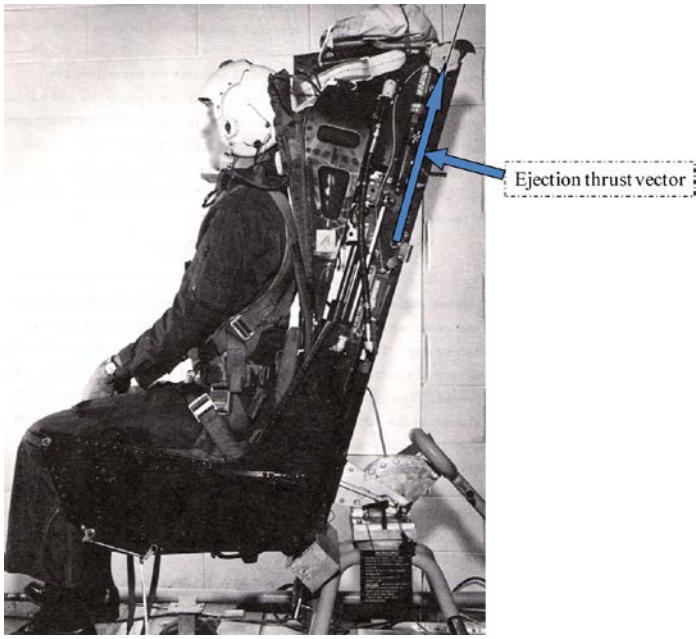

Figure 4. Seat-back geometry and spine alignment to the ejection thrust vector [36].

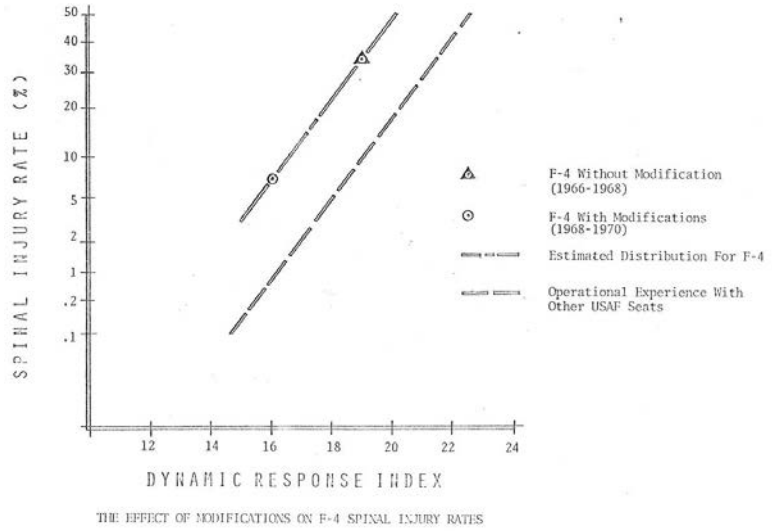

Figure 5. The F-4 ejection seat injury rates associated with the DRI [35].

The ability of the spinal column to withstand +Z-axis acceleration without injury may be significantly increased with proper spinal column alignment prior to impact.

1.2 EVALUATING THE ACCEPTABILITY OF MULTI-DIRECTIONAL ACCELERATION CONDITIONS

During the 1970s, the USAF used a method to evaluate multi-directional acceleration environments that incorporated the DRI with a method to assess the magnitude of accelerations in the other principal axes that occurred within a moving 62-ms analysis window. A computer program was developed to accomplish this analysis incorporating look-up tables to assess the effects of the X-, Y-, and -Z-axes. While this method provided a consistent means to evaluate the performance of relatively conventional ejection seats, it did not provide a means to evaluate a new generation of ejection seats. These new ejection seat designs incorporated an array of attitude, altitude, and airspeed sensors; digital flight control; ejection catapult thrust control; and rocket thrust vector control. In situations where the conditions at ejection were benign, the escape system performance would be controlled to produce a low injury risk. Where the conditions presented a higher risk to the seat occupant, the ejection seat would produce accelerations with a higher injury risk, but a higher likelihood of a successful escape.

This concept led the USAF to generate a strategic plan for a development program to demonstrate the technologies required to demonstrate an advanced ejection seat that would have such flight control features, and would be capable of safe escape at aircraft speeds up to 700 knots equivalent airspeed. The new technologies required to evaluate the performance of such an ejection seat included a test manikin capable of measuring specific forces and moments at key internal locations and extremity joints, a rocket sled capable of providing adverse attitudes and roll motion of an aircraft forebody at the time of an ejection test, and a means to sense and assess the injury risk associated with the escape system's performance [38].

2.0 BRINKLEY DYNAMIC RESPONSE CRITERION DEVELOPMENT

Brinkley [39] proposed a means to evaluate the performance of an escape system using a whole body acceleration exposure limit method. Its primary objective was to compute a set of DRs that could be used to estimate the injury risk levels. The computations would be based on measurements of linear acceleration and angular velocities at a known point. Brinkley proposed that if the linear acceleration at a point on the seat and the angular velocity were known, then the seat motion would be uniquely defined and the linear acceleration at any point in the seat coordinate system could be calculated. Brinkley proposed that a 6 degree-of-freedom (DOF), lumped-parameter model could be used to assess the DR of the human body in each orthogonal axis. The DRs of the three orthogonal axes could be used to calculate a general whole body injury risk in terms of an ellipsoidal approximation. Model parameters, natural frequency, and damping coefficients were selected on the basis of available laboratory data and existing lumped-parameter models. Injury risk levels were chosen on the basis of operational escape system experience, injury-free and minimal injury military laboratory tests, research using anesthetized animals, experiments with post-mortem human surrogates, and accidental injuries that had occurred in experiments in government laboratories and during impact tests conducted by aerospace companies.

For each axis, two separate analyses are needed: determining the DR parameters (natural frequency and damping coefficients) and determining the injury risk levels based on available injury data.

2.1 LIMITATIONS

In general, although the model simplicity allows for straightforward injury evaluation, simplification of the human-vehicle interface to the acceleration input to a set of lumped-parameter models may not protect the occupant from a variety of injurious causes. Because the dynamics are intimately related to the specific test setup used in development, extrapolation of the data to different configurations may necessitate additional testing with the configuration and recalculating the model parameters [40]. As noted, much of the injury data used to develop the injury risk limits for each axis have not been reported in detail. Without exact knowledge of the conditions and configurations of these cases, it is unclear how robust the limits are for predicting the true risk of injury using future seat, restraint, pressure suit, and helmet designs.

Brinkley reports that the limits for ±X, ±Y, and -Z were assigned without statistically based methods [40]. Nevertheless, the results of the many hundreds of tests with investigators and volunteers willing to explore previously unexplored impact levels at high risks of injury are highly unlikely to be repeated in the future. Limitations specific to each axis are further discussed below.

2.2 -X AXIS

2.2.1 -X Axis Dynamic Response Model Parameter Estimation

Initially the DR_x model parameters were developed from a variety of data not specifically collected for that purpose from various military experiments. The -X (eyeballs out, frontal impact) data consisted primarily of data with rise times between 25 to 160 ms [41]. Brinkley et al. [41], using data from Study 198402 in the Wright-Patterson Air Force Base Collaborative Biodynamics Network

(CBDN) [42], recalculated the model parameters based on data from 17 male subjects all tested at varying rise times at 10G (Table 1) for a total of 85 runs.

TABLE 1. SUBJECT DATA USED TO DETERMINE -X AXIS (EYEBALLS OUT) DYNAMIC RESPONSE MODEL

Subject	Subject Height [cm]	Subject Weight [kg]	Subject Age	Subject Sex	Nominal G	Rise Time [ms]	Pulse Duration [ms]	Number of Tests
D-3	185.4	90.2	24	M	10	23-35	48-84	3
G-4	186.9	73.0	23	M	10	17-29	30-65	3
H-7	184.9	88.8	27	M	10	18-117	34-252	6
H-8	178.8	66.7	28	M	10	17-34	30-83	5
K-2	172.7	90.1	23	M	10	17-119	34-251	8
L-3	182.4	84.8	34	M	10	18-120	34-247	8
L-4	182.9	83.3	23	M	10	16-114	31-246	7
M-15	166.1	63.6	25	M	10	16-112	29-246	5
M-16	177.8	91.2	29	M	10	23-35	48-84	3
R-6	174.9	72.6	34	M	10	14-119	30-252	5
R-8	189.7	76.7	26	M	10	24-33	49-83	3
S-3	176.7	75.8	35	M	10	16-119	32-247	4
S-7	174.0	77.2	24	M	10	18-32	31-83	5
S-8	184.7	95.2	26	M	10	18-34	31-84	4
T-1	167.9	74.8	30	M	10	15-114	31-244	5
T-3	170.9	74.5	22	M	10	34-113	80-245	3
W-4	178.1	89.1	27	M	10	15-113	29-252	8

This new analysis estimated the natural frequency for the -X model as 56.0 rad/s versus 62.8 rad/s in the initial model. The damping coefficient estimate was significantly different (0.04 versus 0.2 in the initial model). Brinkley et al. suggested that the original computations be recomputed.

2.2.2 -X Axis Injury Risk Level Determination

The high risk level (5% - 50%) limits are based on volunteer data collected on the rocket propelled sled at Muroc Lake, CA (now Edwards AFB) [7, 8], the Daisy Decelerator Track [7, 8, 24, 25] at Holloman AFB, NM, and multi-axis testing conducted at the Wright-Patterson AFB and Holloman AFB [26, 28, 29]. The computed DR data are shown in Figure 6. Additional information about these studies can be found in Appendix A. Injuries for the -X axis for the high risk level include cardiovascular shock, retinal hemorrhage, and fracture of the subject's neck-hyoid bone and severe cardiovascular shock requiring hospitalization [43].

The low risk (<0.5%) limits are based on acceleration levels routinely tolerated by volunteers in laboratory experiments. High impact volunteer testing has been conducted with volunteers up to 40 G in the -X axis with robust restraints including shoulder straps, a lap belt, and two crotch straps attached from the lap belt buckle to each corner of the seat reference line of the seat pan [43]. Note that during the rocket sled tests, the subject's head and neck were flexed forward due to pre-impact rocket sled deceleration. Injuries that occurred were not considered to be major by medical investigators such as Stapp [7]. However, the helmets that were used were lighter than pressure suit helmets that may be used by astronauts. The heavier helmets may increase the risk of injuries in case of significant -X axis impacts.

The medium injury risk (0.5% to 5%) limits were chosen as the mid-point between the low- and high-risk limits.

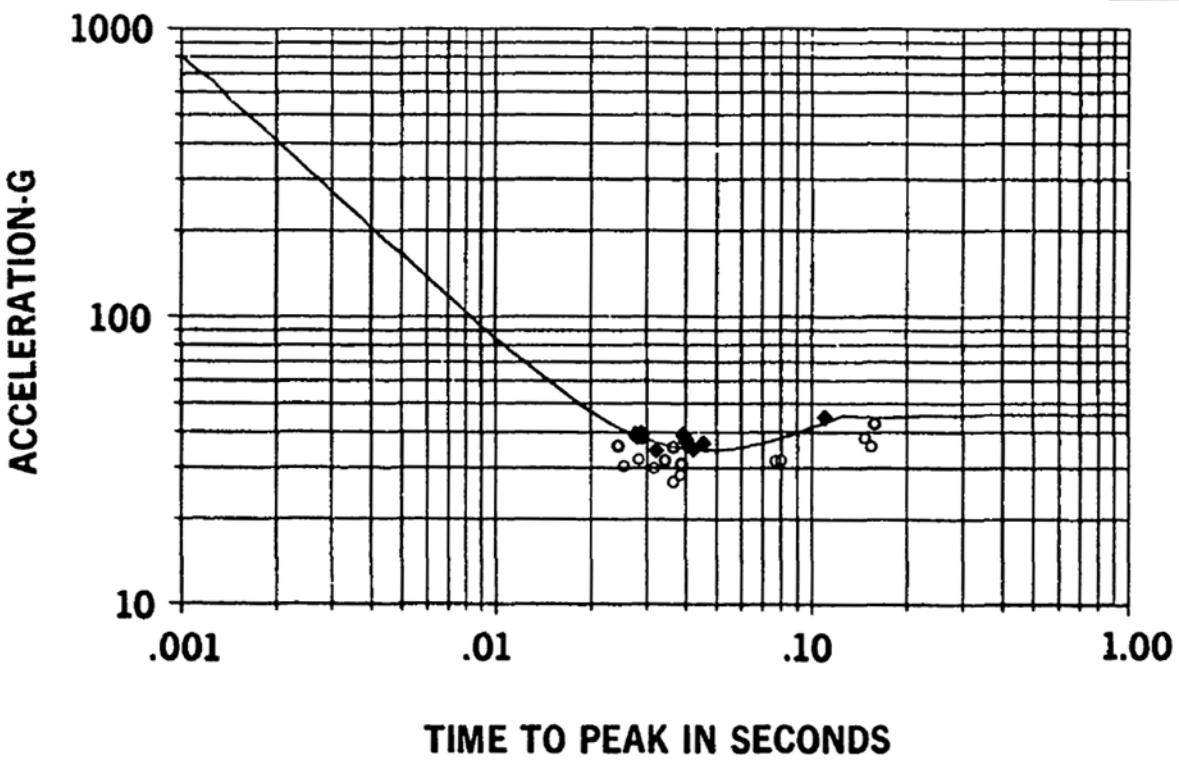

Figure 6. -X model high injury risk level determination [39]. Data points were derived from volunteer tests. Injury or serious symptoms are designated by black diamonds. Non-injury cases are designated by open circles. The curve represents the high injury risk limit (estimated to approximate a 50% risk of injury for male subjects with conventional flight helmets and a 5-point restraint system).

2.2.3 -X Axis Model Limitations

In addition to the limitations described in Section 2.1, there are several additional limitations related to these models.

Data were only collected at 10 G. Although many different pulse widths were used in the development, it is unclear how well the model extends to other G-levels. The rise time of the pulses used was varied, allowing a better estimation of the frequency response of the human, but it is unclear if the rate-sensitive nature of the human response is completely captured in this limited data set. This may account for the differences seen between the original models and the re-analysis.

First, the subjects used were all male. It is unclear how the models would change for female occupants. In regard to age, the subject ages range from 22 to 35, well below the current NASA astronaut population range of 32 to 56. Although the current age ranges may not be indicative of the flight population for a particular vehicle, historically astronauts tend to be older than military populations used for USAF research efforts. For anthropometry, the subjects used to develop the -X axis model ranged in stature from 166 to 190 cm, whereas the NASA requirements cover a range of 149 to 195 cm. Although the model data do not cover the entire range, the range covered is a significant portion of the population. For weight, the subjects included in the model ranged from 66.7 to 91.2 kg versus 42.6 to 110.2 kg in the NASA requirements.

In regard to the injury risk limits, as mentioned earlier, very little information is given to determine the adequacy of the limits chosen. Figure 6 shows data used to develop the high (5% to 50%) risk limits for both the ±X models for the original model parameters. In the reanalysis, the limits weren't changed and it is unclear whether the original injury cases were recalculated using the new model. Another concern with the injury risk limits is the difference in data sets. The model parameters were selected based on one set of data, and the injury data were taken from different tests that may have had

differing configurations. Again, without more information on the exact tests and setup used when injury occurred, it is impossible to determine the adequacy of the limits.

2.3 +X AXIS

2.3.1 +X Axis Dynamic Response Model Parameter Estimation

Initially the DR_x model parameters were developed from a variety of data not specifically collected for that purpose from various military experiments. The +X (eyeballs in, rear impact) data consisted primarily of rise times between 20 to 50 ms, with only a few cases between 80 to 100 ms.

Brinkley [39] reports both a -X and +X model. Because the +X data were insufficient to adequately estimate model parameters, the -X model fit the data reasonably well to allow the same model to be applied to both X directions. Since then, experimental human response data became available in the -X axis, and the coefficients in that direction were changed to reflect the new data (see section 2.2). It's uncertain whether the +X coefficients were intended to be revised as well, thus the previous model parameters will be used [44]. The natural frequency was previously estimated as 62.8 rad/s and the damping coefficient as 0.2. No additional information is available related to the development of this model, nor is there information about what +X data were used to determine the fit was adequate.

2.3.2 +X Axis Injury Risk Level Determination

The high risk level (5% to 50%) limits are based on volunteer data collected on the rocket propelled sled at Muroc Lake, CA (now Edwards AFB) [7, 8], the Daisy Decelerator Track [7, 8, 24, 25] at Holloman AFB, NM, and multi-axis testing conducted at the Wright-Patterson AFB and Holloman AFB [26, 28, 29]. The computed DR data are shown in Figure 7. Additional information about these studies can be found in Appendix A. The low risk (<0.5%) limits are based on acceleration levels routinely tolerated by volunteers in laboratory experiments. The medium risk (0.5% to 5%) limits were chosen as the mid-point between the low- and high-risk limits.

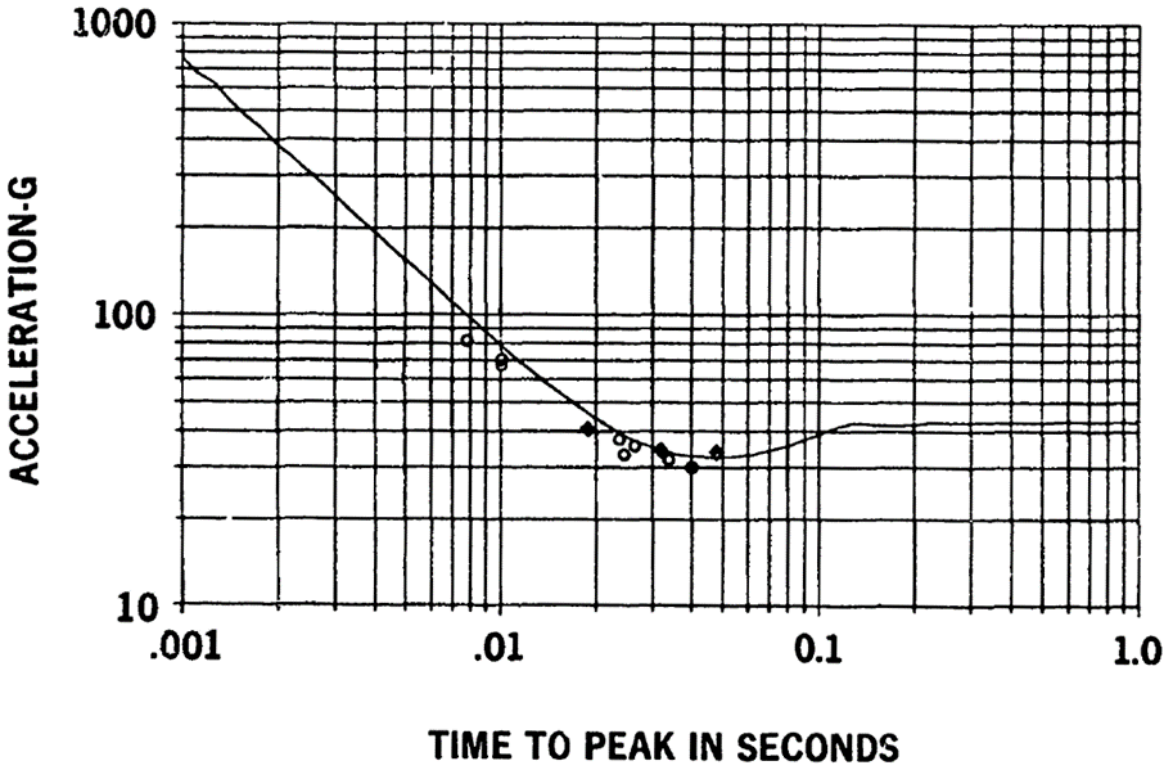

Figure 7. +X model high injury risk level determination [39]. Data points were derived from volunteer tests. Injury or serious symptoms are designated by black diamonds. Non-injury or minor injury cases are designated by open circles. The line represents the high injury risk limit (estimated to be a 50% risk of injury)

2.3.3 +X Axis Model Limitations

For the +X model, very limited data were used in the initial model showing the ±X models were similar. Since then, no additional analysis of the +X model dynamics has been performed to validate this assumption. Because +X axis loading is one of the primary loading directions expected in spacecraft landings, this uncertainty in the validity of this +X model is concerning. Data are available to develop an updated model, but the work was not completed due to funding changes.

The subject demographics are another limitation. Because the previous model's demographics were not stated, it is unclear how the subject demographics compare to the astronaut population.

2.4 ±Y AXIS

2.4.1 Y Axis Dynamic Response Model Parameter Estimation

Selection of model parameters for the Y axis proved to be the most difficult due to the limited data. One set of sideward impact data was selected to be suitable for analysis [45]. Using data collected from 13 subjects at 8 G (a total of 15 runs) from Study 197901 [42] (Table 2), the natural frequency was estimated as 58.0 (±1.7 SD) rad/s and the damping coefficient was estimated as 0.07 (±0.04 SD).

TABLE 2. SUBJECT DATA USED TO DETERMINE Y AXIS DYNAMIC RESPONSE MODEL

Subject	Subject Height [cm]	Subject Weight [kg]	Subject Age	Subject Sex	Nominal G	Rise Time [ms]	Pulse Duration [ms]	Number of Tests
D-1	186.9	90.9	23	M	8	100	204	1
E-1b	185.4	84.5	39	M	8	98	194	1
F-2	170.2	71.4	24	M	8	99	207	1
F-3	174.0	70.9	24	M	8	95	212	2
G-2	160.0	54.5	22	F	8	99	199	1
J-1b	179.1	72.7	25	M	8	99	218	1
M-10	167.0	63.6	22	M	8	101	213	1
M-5	183.9	76.8	34	M	8	97	211	1
M-9	180.1	76.8	25	M	8	96	212	1
R-1	180.1	91.4	34	M	8	94	213	2
S-3	176.8	74.1	30	M	8	100	221	1
S-5	178.0	78.6	27	F	8	98	221	1
W-1	186.9	70.5	22	M	8	100	218	1

2.4.2 Y Axis Injury Risk Level Determination

Injury risk levels could not be developed with high confidence as few injuries had been observed beyond adverse cardiovascular responses [26, 28-30] knee injury [45], bradycardia, and syncope [30]. The injury risk levels (including data with side panels) were determined based on expert opinion and available data [26, 28, 30, 45]. Additional information about these studies can be found in Appendix A. Data from a larger number of Y axis impact tests with volunteers conducted at AFRL were analyzed to study the loads measured on rigid shoulder support panels and related those dynamic impact responses to the probability of clavicle fractures and shoulder joint injuries from in NASCAR crashes. This work was also not completed due to funding constraints.

The high risk (5% to 50%) injury level was determined by determining the DR for known injurious acceleration conditions. Injurious conditions were adverse cardiovascular responses due to stretching the receptors within the carotid arteries of the neck. When side supports are used, there have been minor but adverse cardiovascular responses at high impact levels. At higher levels expected injuries would include fractures within the cervical spine and rupture of the aorta; however, these injuries were fortunately not observed in testing.

The low risk (<0.5%) level was determined from human tolerance based on numerous non-injurious volunteer tests.

The medium risk (0.5% to 5%) level was assigned as a mid-point between the low and high-risk levels.

2.4.3 Y Axis Model Limitations

As with the ±X model, the ±Y model is based on a limited data set. The model relies on data collected on a very limited number of subjects and test runs. The model is based on 15 cases tested at only 1 G-level and rise-time. Applicability beyond this dynamic condition is not known.

Subject demographics for this model have some limitations. It is encouraging that 2 females were included in the ±Y model, but is not a sufficient number to account for sex differences. As for anthropometry, the range of subject stature was 160 to 189 cm compared to the NASA requirements range of 149 to 195 cm. Although the model data do not cover the entire range, the range covered is a significant portion of the population. For weight, the subjects included in the model ranged from 54.5 to 91.4 kg versus 42.6 to 110.2 kg in the NASA requirements. The subject ages ranged from 22 to 34, which is well below the current NASA astronaut population range of 32 to 56. It is not known if age, gender, and anthropometry are factors for lateral impact tolerance.

Although the test cases were conducted without side supports, it is assumed that the model parameters are the same for these two conditions; however, there are no data supporting this assumption. The damping coefficient in the model is lower due to the poorer coupling with the restraints, so it would be expected that better restrained occupants (with side supports) would have a higher damping coefficient, resulting in an underestimation of the human response.

Injury limits are reported for conditions with and without side supports with very little explanation of the source of the side-supported limits. As with the ±X case, the data used to determine the injury limits were from different cases than those used to develop the dynamic model and it is unclear what configuration was used to collect those data. It is also unclear what data were used (if any) to develop the limits. In regards to the case where side supports are not included, Brinkley has stated that the injury risk limits are not appropriate and are insufficient to mitigate injury [32]

2.5 +Z AXIS (EYEBALLS DOWN)

2.5.1 +Z Axis Dynamic Response Model Parameter Estimation

The +Z axis DRI is the most validated axis of the model, and was adopted for use in the BDRC [23, 34, 35]. The damping coefficient was estimated from 8 male subjects shown in Table 3 [46].

The natural frequency determination in the +Z axis, however, is a bit more complicated. Yorra [47] determined the load deflection curves for the fourth lumbar vertebrae (L4 spine level) on a 57.5-year-old cadaver, whereas Ruff [48] measured vertebral breaking strength in cadavers (19 to 46 years old) for various lower vertebrae between the thoracic spinal bodies at T8 and L5. Stech and Payne assumed a linear relationship between breaking strength and stiffness [23]. Based on this assumption, Stech and Payne extrapolated the stiffness characteristics of the remaining vertebrae using the percentage of body weight carried by each vertebrae related to the breaking strength reported by Ruff. The results were extrapolated to account for age differences based on experiments of additional cadaveric specimens [49]. From these data, the natural frequency is determined for a variety of ages.

TABLE 3. SUBJECT DATA USED TO DETERMINE +Z AXIS DAMPING COEFFICIENT

Subject	Subject Height [cm]	Subject Weight [kg]	Subject Age	Subject Sex
W.B.	182.9	89.8	34	M
R.C.	188.0	83.9	47	M
B.D.	193.0	99.3	30	M
W.E.	175.3	70.3	29	M
W.G.	180.3	81.6	40	M
R.H.	180.3	90.7	35	M
E.M.	182.9	94.3	29	M
G.Z.	170.2	71.7	29	M

Recently, Buhrman and Mosher reported +Z axis model parameters based on tests conducted on 14 males and 12 females [50]. Male subject mass range was 64.8 to 103.4 kg (83.5-kg average) and sitting height range of 84.3 to 97.5 cm (93-cm average). Female subject mass range was 45.4 to 70.3 kg (57.6-kg average) and sitting height range of 81.2 to 89.4 cm (87.1-cm average). A total of 157 test runs were available, but the number used is not reported (at least 52 tests). See Table 4 for subject demographics (determined from the CBDN) [42]. The model parameters estimated from the +Z-axis chest acceleration data are similar the parameters reported by Stech and Payne (Table 5). The damping coefficients are somewhat lower, probably due the location of the measurement with respect to the spine.

TABLE 4. BUHRMAN AND MOSHER SUBJECTS

Subject	Subject Height [cm]	Subject Weight [kg]	Subject Age	Subject Sex	Nominal G	Rise Time [ms]	Pulse Duration [ms]	Number of Tests
B-16a	165.8	57.9	31	F	10	75	150	2-6
B-17	170.2	60.9	26	F	10	75	150	2-7
B-18	163.8	45.6	24	F	10	75	150	2-5
C-15	161.4	57.8	25	F	10	75	150	2-3
C-16	158.3	54.4	21	F	10	75	150	2-1
J-11	166.9	69.9	22	F	10	75	150	2-6
J-9	155.5	58.3	25	F	10	75	150	2-6
K-9	167.3	62.6	28	F	10	75	150	2-6
O-5	166.5	63.5	24	F	10	75	150	2-6
R-20	161.5	49.9	26	F	10	75	150	2-7
S-20	171.2	56.8	27	F	10	75	150	2-7
V-3	162.2	52.7	26	F	10	75	150	2-7
B-11	184.7	104.0	35	M	10	75	150	2-6
C-12a	172.9	83.2	35	M	10	75	150	2-6
C-17a	177.2	72.6	29	M	10	75	150	2-6
E-4	181.6	96.6	35	M	10	75	150	2-7
G-11	176.6	78.1	29	M	10	75	150	2-7
H-15	175.7	79.8	24	M	10	75	150	2-6
J-10	175.4	88.1	23	M	10	75	150	2-7
J-7	171.9	74.1	28	M	10	75	150	2-6
M-21b	167.4	68.4	37	M	10	75	150	2-7
M-30	177.9	81.3	35	M	10	75	150	2-6
O-3	158.9	65.6	27	M	10	75	150	2-6
P-11	188.0	84.4	25	M	10	75	150	2-6
R-21	181.1	101.8	35	M	10	75	150	2-7
S-11b	180.8	94.9	32	M	10	75	150	2-7

TABLE 5. BUHRMAN AND MOSHER MODEL PARAMETER ESTIMATES

	Males	Females	Stech & Payne
ω_n	61.1 ± 5.78	63.2 ± 6.3	52.9
δ	0.11 ± 0.15	0.04 ± 0.07	0.224

2.5.2 +Z Axis Injury Risk Level Determination

To determine the injury risk associated with +Z axis accelerations, operational ejection seat injury experience was related to estimated DRI values for the following aircraft: F-100 (with and without a rocket catapult), F-105 (with and without a rocket catapult), B-47 and B-52. Each data point represents the injury rate associated with at least 25 successful nonfatal ejections (Figure 8) [34]. The DRI values were estimated from representative catapult qualification test performance at 70°F (nominal operating temperature) with a 50th percentile male with personnel equipment. Once the DRI was estimated for each ejection seat, the results were related to the operational occurrence of thoracolumbar spinal injuries and the resulting injury risk is given by Equation 1. The injury occurrence rates are derived from fit, military male pilots. The average age of the flying population at the time was 28 years old, although it is not known the ages of the injured pilots. Only compression fractures (AIS≥2) attributable to the ejection acceleration were considered [34, 35].

Equation 1. Risk of Thoracolumbar Spinal Injury

$$p(inj|DR_z) = 10^{\left(\frac{DR_z - 15.8}{3.73}\right)}$$

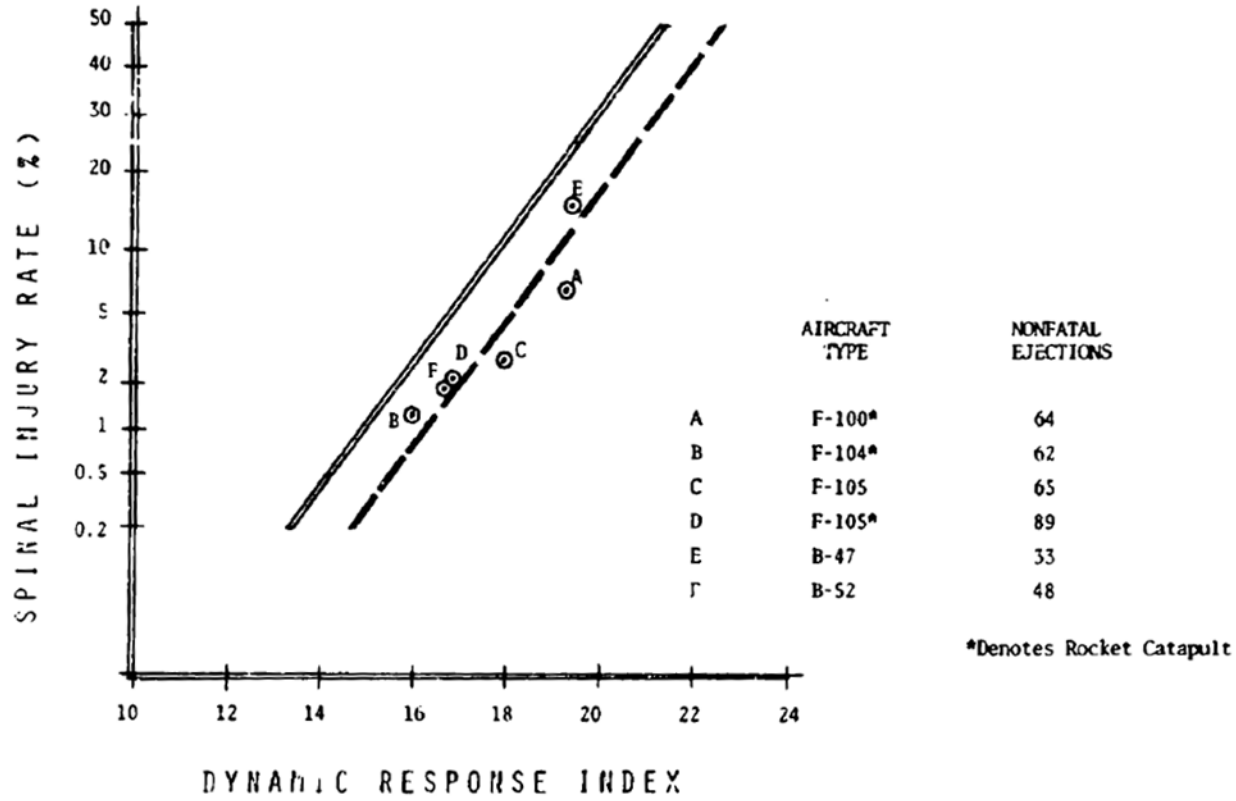

Figure 8. Risk of thoracolumbar spinal injuries. The symbols denote the operational injury rate for various aircraft ejection seats. The solid line denotes the injury risk based on laboratory data and the dashed line is the risk of injury based on operational data [35].

2.5.3 +Z Axis Model Limitations

The model used for the +Z direction is based on a very limited number of subjects and cadaveric studies. The natural frequency was determined from a single 57.5-year-old cadaver and natural frequency was determined from a small set of male subjects. A recent study using chest acceleration data showed that the damping coefficient may be slightly overestimated and the natural frequency slightly underestimated [50]. The study found little difference between males and females for the model parameters; however, Buhrman and Mosher propose that the injury limits may differ for males and females due to differences in vertebral stresses.

Injuries for the +Z axis are compression fractures of the vertebrae within the lumbar and thoracic spine. The +Z axis model does not consider injuries to other regions of the body, particularly the neck; although no injuries to the neck were attributed to operational ejection catapult force. For injuries to the lower spine, the injury risk is well validated through operational data; however, the risk is based on male, military subjects with an average age of 28, which may not be indicative of the NASA astronaut population.

2.6 -Z AXIS (EYEBALLS UP)

2.6.1 -Z Axis Dynamic Response Model Parameter Estimation

Initially, data from Schulman et al. [27] were used to estimate the model parameters. The natural frequency was found to be slightly lower than the +Z model and the damping coefficient was nearly identical. Because of the similarity, the +Z axis model parameters were adopted for both Z axis directions.

Later, Brinkley et al. [41] recomputed the -Z axis model using data from Study 198504 in the CBDN [42]. These data consisted of 12 subjects (11 male and 1 female) tested at 10 G and various rise times (a total of 52 runs). These data were used to estimate the natural frequency of 47.1 rad/s (versus 52.9 rad/s in the initial model) and a damping coefficient of 0.24 (versus 0.224 in the initial model).

TABLE 6. SUBJECT DATA USED TO DETERMINE -Z AXIS DYNAMIC RESPONSE MODEL

Subject	Subject Height [cm]	Subject Weight [kg]	Subject Age	Subject Sex	Nominal G	Rise Time [ms]	Pulse Duration [ms]	Number of Tests
B-1	179.1	77.8	28	M	10	17-112	33-252	5
D-5	185.4	79.5	24	M	10	18-112	34-252	5
H-8	178.8	69.7	30	M	10	18-111	33-251	3
L-3	182.4	85.5	36	M	10	17-120	33-252	5
M-16	177.8	90.2	32	M	10	17-114	33-253	2
M-19	188.5	83.8	26	M	10	17-112	33-253	5
M-21a	167.6	56.1	27	M	10	17-114	33-253	5
P-5	174.0	83.5	25	M	10	18-113	34-251	5
S-3	176.8	71.5	37	M	10	23-117	65-240	3
T-4	180.3	85.8	31	M	10	18-114	33-253	5
Z-1	163.8	48.2	22	F	10	18-114	34-240	4
Z-2	172.7	64.7	25	M	10	17-115	33-252	5

2.6.2 -Z Axis Injury Risk Level Determination

The methodology used to develop the ±X and +Z axes models produced higher confidence than that produced for the -Z. The results of -Z-axis accelerations explored by investigators such as Shaw [10] and Schulman et al. [27], and the USAF experience with downward ejection seats, were initially used to estimate the medium risk (0.5% to 5%) level. Schulman et al. data were also used to estimate the high risk (5% to 50%) level.

Upon estimation of the new dynamic model parameters, these limits were revised. The low injury risk (<0.5%) limit was revised to a DR value of -13.4 based upon the maximum values computed from the experimental input acceleration conditions. The medium injury risk limit (DR_{-z} = -16.5) was calculated based on the maximum allowable acceleration condition of MIL-S-9479B, Military Specification Seat System, Upward Ejection, Aircraft, General Specification, [51]. The high injury risk limit (DR_{-z} = -20.5) was determined using the worst-case impact condition tested with volunteers by Schulman et al. Additional information about these studies can be found in Appendix A.

2.6.3 -Z Axis Model Limitations

For the -Z model, several limitations exist. In regard to the dynamics used for model parameter estimation, only 10 G peak acceleration pulses were used; however, a range of rise times were tested, with multiple runs per subject. It is unclear how well the model extends to other G-levels because of the rate-sensitive nature of the human response.

In addition, the model is based on the responses of 11 males and 1 female, which may not account for a wide enough range of subject variability and sex differences. The subject ages ranged from 24 to 37 years old, whereas the current astronaut age range is 32 to 56 years old. Thus the data do not cover the upper range of ages seen currently in the astronaut corps and expected for future missions. The subject stature ranged from 164 to 189 cm, whereas the NASA requirement range is 149 to 195 cm. For weight, the subjects ranged from 64.7 to 90.2 kg versus 42.6 to 110.2 kg in the NASA requirements.

As stated above, there is very little documentation on the injuries used to calculate the high injury risk limits including what injuries were induced, and the conditions in each case. The low risk (<0.5%) limit was reported without any explanation about it derivation. As with each of the previous models, the

data used to determine the injury risk limits were different than the data used to develop the model parameters.

3.0 BRINKLEY DYNAMIC RESPONSE CRITERION APPLICATION

Because statistical uncertainty remains for many of the BDRC axes, the probability of injury is provided as a relative scale as follows in Table 7.

TABLE 7. APPROXIMATE RISK ASSOCIATED WITH EACH BDRC CATEGORY

Category	Approximate Risk
Low	0.5%
Medium	5.0%
High	50%

The injury risk criterion (IRC), β, is calculated according to Equation 2.

Equation 2. Injury Risk Criterion Calculation

$$\beta(t) = \sqrt{\left(\frac{DR_x(t)}{DR_x^{lim}}\right)^2 + \left(\frac{DR_y(t)}{DR_y^{lim}}\right)^2 + \left(\frac{DR_z(t)}{DR_z^{lim}}\right)^2}$$

Where DRx(t), DRy(t), and DRz(t) are calculated using the BDRC. The dimensionless DR in each of the three axes is given by Equation 3.

Equation 3. Dynamic Response (DR) Formulation

$$DR(t) = \frac{\omega_n^2 \cdot \delta(t)}{g}$$

Where δ(t) is defined by the spring deflection of the dynamic system (consisting of the seat and the body) along each axis given by Equation 4.

Equation 4. DR Differential Equation

$$\ddot{\delta}(t) + 2 \cdot \zeta \cdot \omega_n \cdot \dot{\delta}(t) + \omega_n^2 \cdot \delta(t) = A(t)$$

Where:

- g Acceleration of gravity
- $\ddot{\delta}(t)$ Occupant's acceleration in inertial frame
- $\dot{\delta}(t)$ Occupant's relative velocity with respect to the critical point shown in the seat coordinate system (Figure 9)
- $\delta(t)$ Displacement of the occupant's body with respect to the critical point shown in the seat coordinate system in Figure 9 (A positive value represents compression of the body)
- ζ Damping coefficient ratio defined in Table 8
- ω_n Undamped natural frequency of the dynamic system defined in Table 8
- A(t) The measured acceleration, per axis, of the seat at the critical point shown in Figure 9. Because the seat axis is not an inertial frame, rotational acceleration must be considered in terms of the linear components of the angular motion.

TABLE 8. MODEL COEFFICIENTS*

	X		**Y**		**Z**	
	Eyeballs out	**Eyeballs in**	**Eyeballs left**	**Eyeballs right**	**Eyeballs up**	**Eyeballs down**
	x < 0	**x > 0**	**y < 0**	**y > 0**	**z < 0**	**z > 0**
ω_n	56.0	62.8	58.0	58.0	47.1	52.9
ζ	0.04	0.2	0.07	0.07	0.24	0.224

*Note: Equation 4 is nonlinear since the parameters ω_n and ζ change with the sign of the displacement, δ.

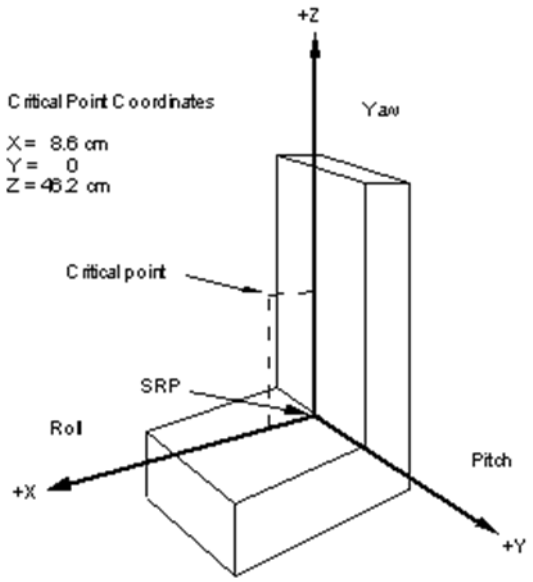

Figure 9. Critical point definition of a seated occupant.

To determine the risk of injury in a particular axis, the following procedure is used with limits, DR^{lim}, given in Table 9. The appropriate risk level will be determined by the Projects and concurred by the Program.

1. Determine the transient acceleration (A(t)) of the occupant at the critical point, in a body fixed coordinate system that is fixed to the seat and rotates along with any seat rotations, in each axes (X, Y, and Z). A(t) is normally obtained by test or analysis.
2. Solve the second order differential equation for the displacement (δ(t)) of the occupant (Equation 4).
3. Determine the DR(t) for each axis at time (t) (Equation 3).
4. Determine β(t) using Equation 2.
5. Find the maximum β(t). This is the IRC.
6. If the IRC is > 1.0, repeat steps 1-5 with the next highest DR limits.
7. If IRC <1.0, then stop and this is the risk level for the applied acceleration.

TABLE 9. DYNAMIC RESPONSE LIMITS

Axis	Direction	Low (<0.5%)	Medium (0.5% to 5%)	High (5% to 50%)
X	**Eyeballs out**	$-28 \le DR_x < 0$	$-35 \le DR_x < -28$	$-46 \le DR_x < -35$
	Eyeballs in	$0 \le DR_x < 35$	$35 \le DR_x < 40$	$40 \le DR_x < 46$
Y	**Eyeballs left**	$-15 \le DR_Y < 0$	$-20 \le DR_Y < -15$	$-30 \le DR_Y < -20$
	Eyeballs right	$0 \le DR_Y < 15$	$15 \le DR_Y < 20$	$20 \le DR_Y < 30$
Z	**Eyeballs up**	$-13.4 \le DR_Z < 0$	$-16.5 \le DR_Z < -13.4$	$-20.4 \le DR_Z < -16.5$
	Eyeballs down	$0 \le DR_Z < 15.2$	$15.2 \le DR_Z < 18.0$	$18.0 \le DR_Z < 22.8$

Table values were derived based on a review of the following: AGARD CP-472, NASA-TM-2008-215198, NASA-TN-D-7440, and NASA-TN-D-6539.

4.0 BRINKLEY DYNAMIC RESPONSE CRITERION HISTORICAL USAGE

The BDRC has been used in numerous research and development applications related to spaceflight. A summary of each activity is given here.

4.1 EVALUATION OF MERCURY CAPSULE LANDINGS

The BDRC was used retrospectively to investigate the risk of injury during Mercury capsule landings. In actual landings, no injuries were reported; however, this analysis gives a point of comparison to previous experience to evaluate future risk.

The BDRC was applied to drop tests with zero-horizontal velocity and zero-pitch attitude. Cases with and without heat shield airbag were evaluated. The results found a low probability of injury for land and water touchdowns (Table 10) [43].

TABLE 10. MERCURY DROP TEST EVALUATION RESULTS

Case	Velocity	BDRC	
Water impact; with skirt	9.1 m/s [30 ft/s]	0.32	low risk
Land impact; with skirt	9.1 m/s [30 ft/s]	0.60	low risk
Water impact; no skirt	9.1 m/s [30 ft/s]	0.55	low risk
Land impact; no skirt	9.1 m/s [30 ft/s]	0.99	low risk

4.2 EVALUATION OF APOLLO CAPSULE LANDINGS

In addition to the Mercury landing analysis, the BDRC was also used retrospectively to evaluate Apollo drop test data. These test data were collected with zero-horizontal velocity and zero-pitch attitude as well. The tests compared two heat-shield designs and two vertical-velocity conditions. The model showed low probability of injury for all test cases (Table 11) [43].

TABLE 11. APOLLO DROP TEST EVALUATION RESULTS

Case	Velocity	BDRC	
Rigid-shell theory impact	5.4 m/s [17.7 ft/s]	0.25	low risk
Flexible heat shield	5.4 m/s [17.7 ft/s]	0.24	low risk
Rigid-shell theory impact	6.8 m/s [22.2 ft/s]	0.34	low risk
Flexible heat shield	6.8 m/s [22.2 ft/s]	0.32	low risk

4.3 EVALUATION OF SOYUZ CAPSULE LANDINGS

The BDRC was used to evaluate tests of the Russian Soyuz vehicle to determine the risk of injury to U.S. crewmembers [2-6]. The MIR-era vehicle (Soyuz-TM) and the newly redesigned vehicle (Soyuz-TMA) were both evaluated using a probabilistic model. The analysis included BDRC limits for deconditioned crewmembers [43].

5.0 BRINKLEY DYNAMIC RESPONSE CRITERION APPLICATION RULES

The BDRC is based on data from volunteer experiments and operational ejection seat experience. Because the model is based on single DOF dynamics, interactions between the occupant and the seat are not directly assessed; thus, operationally equivalent configurations are necessary for application of the model. The application rules and standards stated here are intended to ensure that inappropriate extrapolation to other environments is not made. All the stated application rules must be met to assess a system using the BDRC.

5.1 TRANSIENT ACCELERATIONS

The BDRC has only been validated by test for up to 0.5-second epochs. If the acceleration duration is longer than 0.5 seconds, the sustained acceleration limits (as defined in NASA-STD-3001, Volume II, Space Flight Human-System Standard Volume 2: Human Factors, Habitability and Environmental Health) are applicable and must be met [52].

5.1.1 Verification Method

Identify by analysis all transient accelerations during dynamic phases of flight at each occupant location. All identified accelerations exceeding the sustained acceleration limits for less than 0.5 seconds must be assessed as described in this document.

5.2 PROPER RESTRAINT

5.2.1 Required Restraint

Crewmembers, at a minimum, must be restrained by a restraint system that includes pelvic, torso, and negative-G restraints. The restraint system must provide at least a 5-point harness occupant restraint. Restraints must meet or exceed the requirements defined in SAE AS-8043B, Restraints Systems for Civil Aircraft, [53]. If other requirements conflict with the standard, the most conservative requirement is to be followed. Additional guidance and best practices can be found in SFI Specification 16.1, Driver Restraint Assemblies, [54] and MIL-S-58095A, Military Specification Seat System: Crash-Resistant, Non-Ejection, Aircrew General Specification, [55].

The volunteer tests conducted to demonstrate the safety of impact accelerations were numerous. They ranged from the two 3-inch shoulder straps, subaxillary cross chest strap, 3-inch lap belt, and inverted-V crotch straps used by Stapp [7] to the similar but narrower restraint webbing configurations used by Weis et al., Taylor and Stapp, and Brown et al. [26, 28, 29] to explore the safety of numerous impact directions without creating major injury (see Figure 10). These restraint configurations exceed the capabilities of the 5-point harness that is recommended for spacecraft applications that will not operate above low injury risk levels. Use of the 5-point restraint configuration may result in an underestimation of the injury risk for high-risk levels. The 5-point harness was used for most of the more recent impact tests with volunteers where the data were used to compute DR model coefficients.

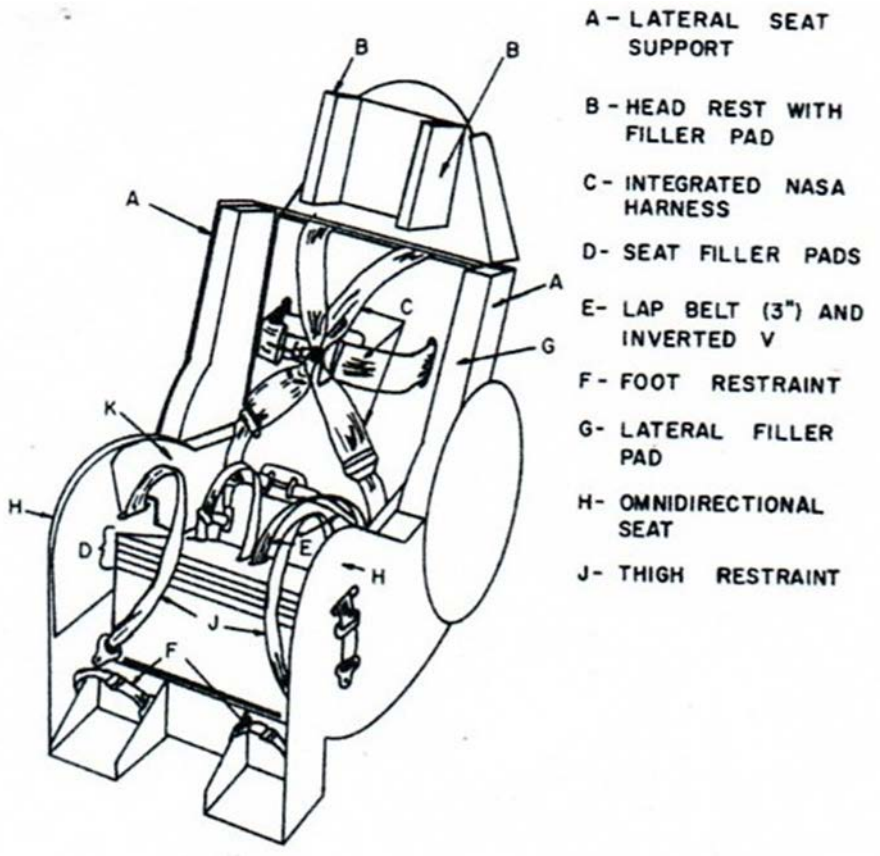

Figure 10. Seat and restraint system [29].

During the experimental efforts, the restraint system was pretensioned to eliminate slack. The capability of being tensioned by the crewmember (whether manual or automatic) to at least 45 N (10 lbf) per strap is required to apply the BDRC in all directions. Payne [22] notes that "a slack of only half an inch in the spinal mode would increase the DRI of a continuous 20-G acceleration pulse (with zero rise time) by as much as 100%." Such a pulse is used for analytical purposes, but is not feasible using any impact test facility. However, Payne also notes that additional preloading, beyond that required to

eliminate restraint slack, is of little value. A value of 45 N (10 lbf) was chosen to ensure elimination of slack.

Positioning of the restraint system with respect to the body is of critical importance. Incorrect placement of restraints has been shown to dramatically increase injury risk and is not reflected in the BDRC [56, 57]. Verification must demonstrate proper belt positioning for the smallest and largest occupant sizes as shown in Figure 11.

5.2.2 Pelvic Restraints

Proper restraint of the pelvis is necessary for protection of the crew. Because the pelvis provides a large contact area on bony structures, it is an ideal location for restraints; however, improper placement can cause injury to the abdomen [56, 57]. Because of this injury risk, lap belts must ride within the curvature of the pelvic bone preferably just below the iliac crest. The harness buckle must be centered on the body 25 to 50 mm (1 to 2 inches) below the belly button when all belts are tensioned [58]. As shown in Figure 11 in blue, belt anchors must be located laterally within 25 mm (1 inch) of the outside of the thigh for all occupant sizes with the suit [59]. This assists in controlling pelvis motion during lateral accelerations. In addition, the belt angle must be between 45° to 55° from horizontal [60].

5.2.3 Torso Restraints

Control of the torso not only protects the ribs and internal organs, but also protects the spine from induced forces and moments [61].

As shown in Figure 11 in black, the shoulder belts are ideally positioned across the trapezius/clavicle, running orthogonal to the seatback across the top of the shoulder. If necessary (but not ideal) the belt may run at an upward angle of up to 30° above this point; however, in no circumstances should the shoulder belt run downward. Ideally, shoulder belt must fall between the mid-clavicular line and the acromion for all occupant sizes with the suit [59]. Critical anthropometric ranges for crewmembers in unpressurized suits are given in Table F1.0-2 in the Human-System Integration Requirements (HSIR) document [62].

5.2.4 Negative-G Restraints

In addition to pelvic and torso restraints, a negative-G restraint is required. The negative-G strap provides two critical functions. First, by tethering the negative-G strap to the forward part of the seat, it prevents the lap belt from moving up and over the anterior superior iliac spines of the pelvis, pressing into the abdomen to cause serious internal injuries [63]. Complete transection of the rectus abdominal muscles and hepatic lacerations have occurred in anesthetized baboon subjects as a result of submarining during high -Z-axis impacts [64]. Stapp [7] also reported that “the forward motion of the shoulders during impact applies traction to the shoulder straps, raising the lap belt, permitting the lower half of the body to begin bending around it. The upper edge of the belt lodges against the lower margin of the ribs and against the upper abdomen.” Second, the negative-G strap prevents the pelvis from moving upward during -Z-axis acceleration. Schall [65] reported that a USAF RF-4 aircraft pilot suffered a cervical vertebrae fracture and transient paralysis as a result of -Z-axis aircraft acceleration causing canopy contact and cervical flexion during a subsequent +Z-axis acceleration.

To function correctly, the belt must exit at an angle in line with the chest to 20° (forward) as shown in red in Figure 11 [58]. Depending on the dynamics of the expected impacts, additional anti-submarining belts (so called 7-point harness) may also be appropriate.

5.2.5 Verification Method

Verify that each is true for the system:

1. Verify restraints are equivalent to 5-point harness or better and adjustable to allow for proper body positioning for minimum and maximum applicable subject anthropometric ranges.

2. Verify by inspection or analysis that belt positioning meets above specifications for minimum and maximum applicable subject anthropometric ranges for the specified critical anthropometric dimensions.
3. Verify by demonstration or test restraint pretensioning to a minimum of 45 N (10 lbf) can be accomplished by the minimum and maximum sized suited crewmembers.
4. Verify restraint meets SAE AS-8043B.

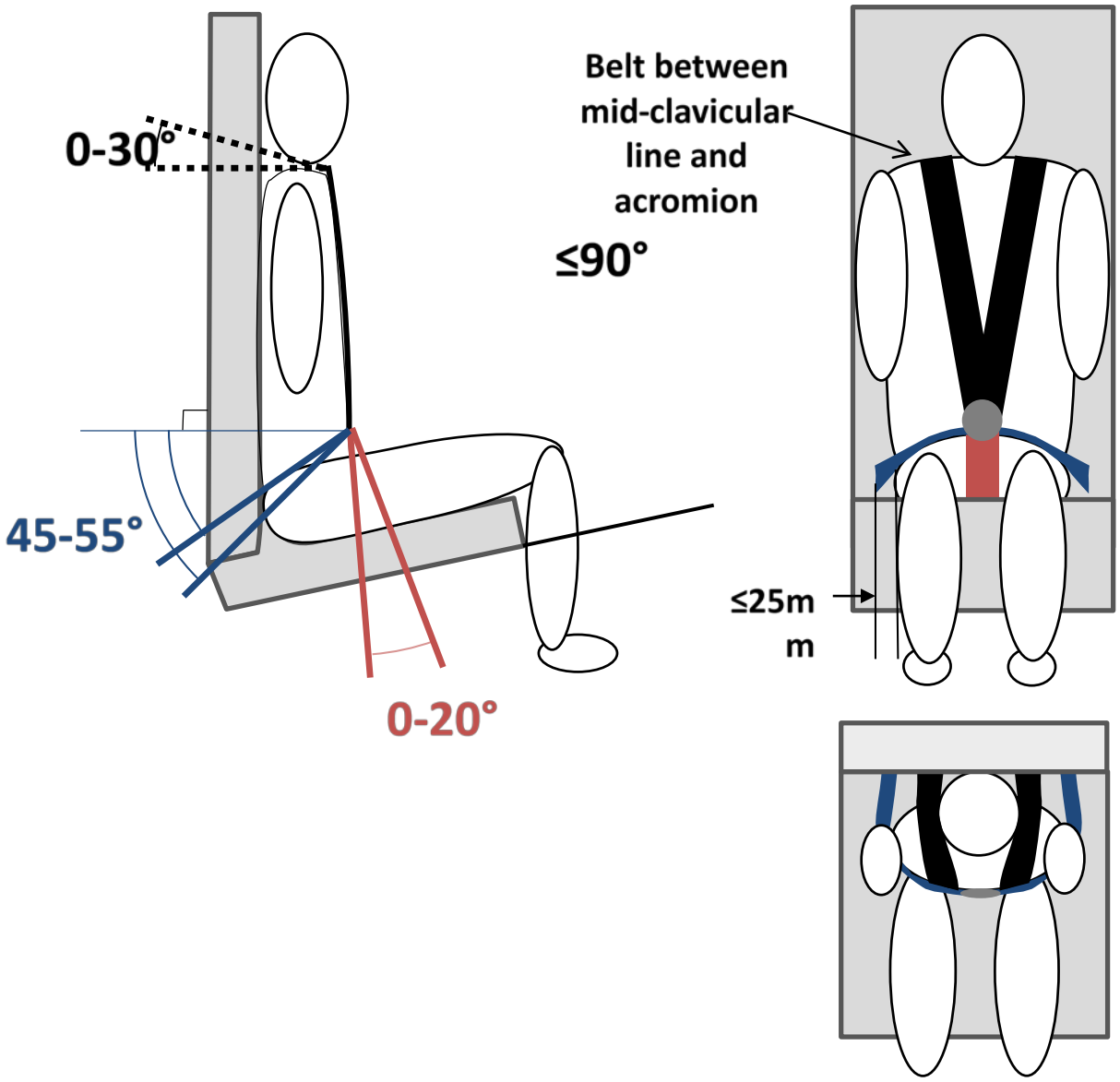

Figure 11. Restraint configuration. Torso restraints are shown in black, pelvis restraints are shown in blue, and the negative-G restraint is shown in red.

5.3 FLAIL CONSIDERATIONS

During dynamic flight phases there is potential for extremity flail injury, which includes crewmember extremities impacting vehicular surfaces or objects, hyper-extending, hyper-flexing, hyper-rotating, fracturing, or dislocating without proper design consideration. Features such as harnesses, form-fitting seats, hand holds, foot holds, and tethers may help maintain the proper position of the

crewmember's body and limbs to reduce movement or contact with vehicle surfaces that would produce flail injury. In addition, the design of the suit may contribute to reducing flail injury to the crew. Preventing the inadvertent contact of extremities with vehicular structure or interior components will significantly reduce the likelihood of limb fracture or soft tissue injury during a dynamic flight event. Extremity guards, tethers, garters, and hand holds have been used to reduce extremity flail in other spacecraft, aircraft, and automotive vehicles. Limiting limb motion to within the seat envelop reduces the likelihood of hyperextending, hyperflexing, and hyperrotating the limbs. Limiting and preventing contact with surrounding structure reduces the likelihood of blunt trauma injuries to the limbs.

5.3.1 Verification Methodology

Verify by analysis and test that flail doesn't occur per Section 7.4.

5.4 SEATING SUPPORT

The testing used to develop the BDRC includes a supportive seat. Similar seating must be used for the BDRC to be applicable.

Alignment of the spine within 5° of the Z-axis acceleration vector is desired to minimize the risk of injury to the spinal column. This spinal alignment condition is important, since having the head bent forward during Z axis (eyeballs down) dynamics can induce thoracic spinal injury not predicted by the model [36]. To achieve this spinal alignment, the back of the head should not project forward more than 5° from the plane of seatback. Offsets caused by suit elements, the helmet, and headrest should be accounted for in this angle. The head offset should not be less than 0° from the plane of the seatback (neck in extension). These design recommendations will improve the safety of the design and reduce bending moments in the neck (see Section 7.2.2).

The seat back and seat pan must support the entire posterior surface of the body without gaps. Any gaps can contribute to amplification of the dynamics (see Section 5.5), which may lead to higher probabilities of occupant injuries. For lateral seating surfaces, care must be taken to minimize gaps between the seat and occupant. Gaps up to 25 mm are allowed laterally, but are not recommended.

In addition, a seat pan to seatback angle of >90° may cause pelvic submarining increasing the risk of injury. Both angles must be ≤90° as shown in Figure 11.

A seat reclined at the same angle to 2° forward with respect to the impact vector would have no effect on injury risk, a seat reclined 20° with respect to the impact vector decreases risk of spinal/neck injury by 5% to 10%, and the seat back perpendicular to the impact vector (crewmember in recumbent position) substantially decreases risk of spinal/neck injury [45, 66-68].

For -Z axis accelerations, the initial conditions at impact initiation must be met for the model to be applied. The sustained acceleration vector must be such that the occupant is in contact with seating surfaces, and not supported primarily by the 5-point restraint. In the original testing conducted by Schulman, et al. to develop the -Z axis model, the subjects were elevated 5° from supine, thus causing the gravity vector to press the subject into the seatback and seatpan [27]; however, Brinkley et al. [41] conducted testing with the subjects completely supine, resulting in the subjects only have positive contact with the seatback. In this case, the subjects used hand-holds to hold themselves into the seat prior to the impact, again assuring proper positioning in the seat.

The seating system used in the development of the ±Y DR (eyeballs left and right) had minimal gap between the subject and the seat support surfaces. To apply the ±Y axis BDRC, supports are required to support the head, shoulder, pelvis, knee, and ankle/foot at a minimum. Gaps between the occupant and side panels are allowed but recommended to be minimized as possible to prevent injury due to closing velocity impacts. Figure 12 shows an example of proper side supports.

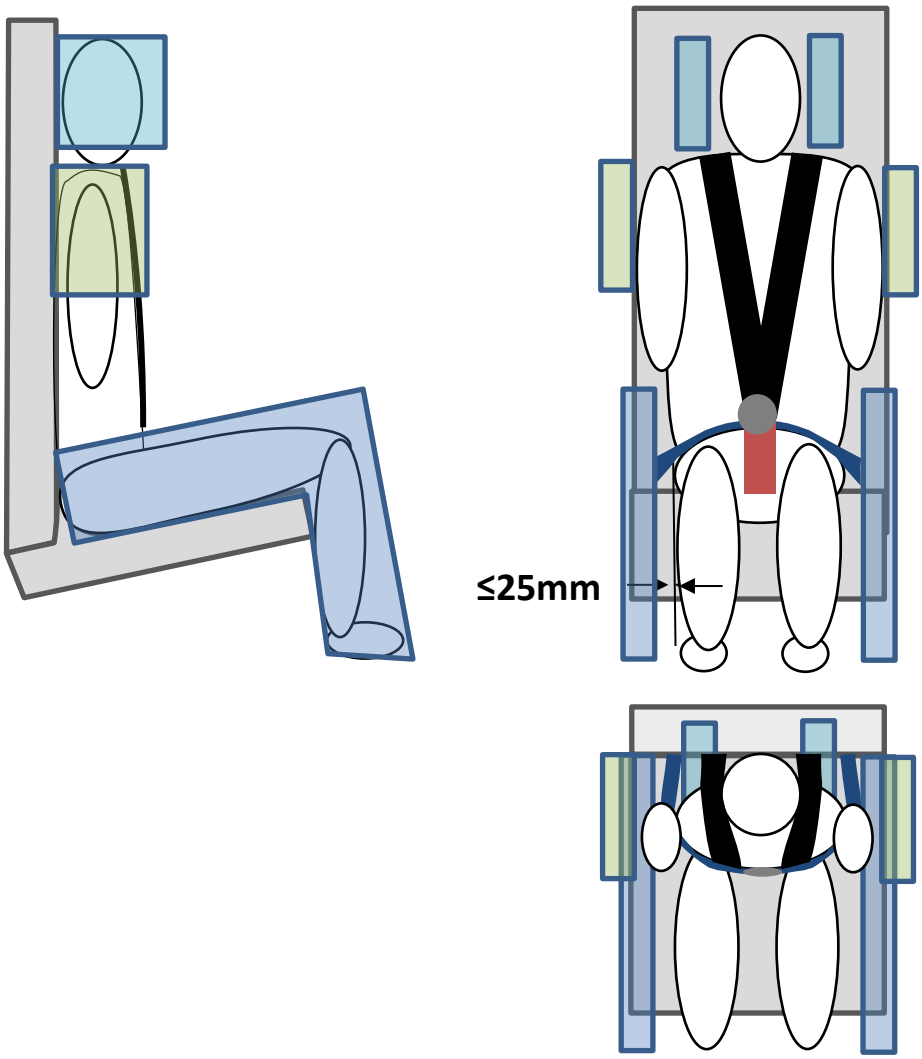

Figure 12. Side Support Example

5.4.1 Verification Method

Verify that each is true for the system:

1. Verify by inspection or analysis that seat back and seat pan provide full support of the body surface and gaps between seat and body are minimized (less than 25 mm) for all applicable anthropometric sizes.
2. Verify by inspection and/or analysis that seat pan angle relative to the seatback is ≤90°.
3. Verify by test and/or analysis side supports arrest lateral movement beyond the plane of the restraint surface for the head (or helmet), shoulder, pelvis, knee, and leg.

5.5 OCCUPANT RESPONSE AMPLIFICATION

Amplification of the DR is a concern, as the model was developed with rigid seat back, side supports, and seat pan structures and may not adequately predict injury risk for seats with insufficient rigidity. To address this risk, NASA has specified a minimum modal response of 15 Hz for Orion [69]. Thus, any vehicle design will be required to have a modal response above 15 Hz for the pallet, strut, seatback, and seat pan structure.

Seat padding or cushion design may also lead to amplification of the occupant transient accelerations due to dynamic overshoot effects. Amplification of the occupant response increases the risk of injury, but is not reflected in the model predictions. Cushioning that can store energy and can quickly restore that energy back to the occupant should be avoided. For lateral supports, seatback and head rest, crushable foam or rate sensitive foam are recommended. Amplification in +Z axis accelerations are of primary concern, as energy absorption is the only mitigation strategy for spinal injury in this axis. In previous vehicles, rate-sensitive foam has been used and has been shown to be beneficial for protecting crew [70]. Perry compared the original B-2 ejection seat cushion made of a 0.63" Confor® foam layer over a 0.375" layer of polyethylene foam to a thicker comfort cushion composed of a 0.5" C-45 Confor® foam in the contoured buttock contact area over a 1.0" thick layer of C47 Confor® foam. In addition, the cushion included a raised area at the back, sides and thigh with an additional 1.0" layer of C-45 Confor® foam between the top and bottom layers. The raised layers were credited with providing additional comfort (Figure 13).

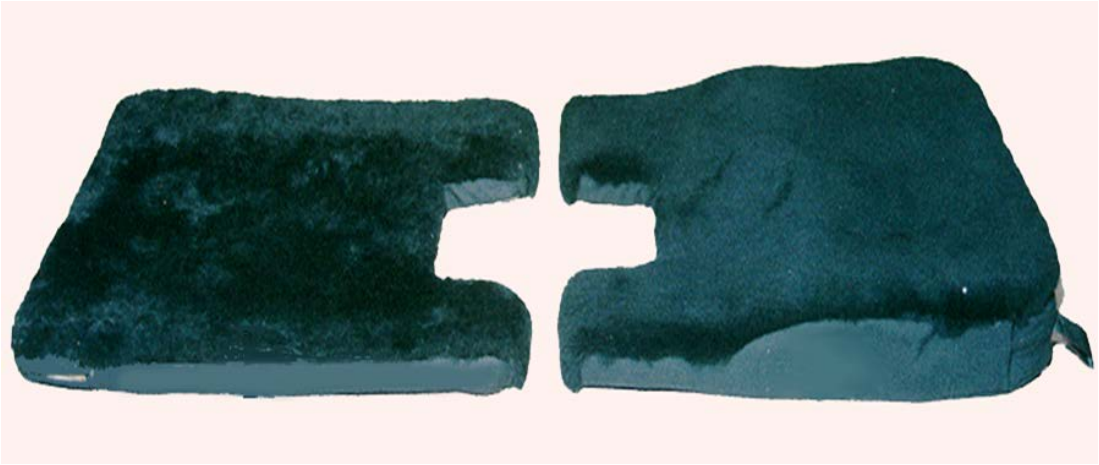

Figure 13. Comparison of B-2 ejection seat cushions. Original cushion (left) and proposed cushion (right) are shown [70].

Hearon and Brinkley [71] also showed that rate-dependent foam was more benign in +Z axis impact. Cheng and Pellettiere [72] report on a broader set of cushions using the mid-size male Hybrid III. Although differences were observed (presumably due to the shape as well as material properties), the authors conclude that lumbar spinal force is a better measure than specifying a specific type of foam. Finally, Miller and Morelli [73] compared several additional configurations with small female and large male Anthropomorphic Test Devices (ATDs). These tests included a 2 in (51 mm) C-47 Confor® foam cushion. The authors concluded that it is safe to include 1 or 2 in (25 or 51 mm) Confor® foam in ejection seats.

Minimization of loads in the lumbar spine is the primary mitigation for preventing spinal injury, thus the use of rate-dependent foam in seat cushions is recommended, because it reduces +Z axis loads transmitted to the lower spine. However, foam in the seat pan should not exceed 51 mm (2").

5.5.1 Verification Method

Verify that each is true for the system:

- Verify the pallet, strut, seatback, and seat pan structure has a modal response is above 15 Hz.
- Verify that no seat cushioning is used, or the seat cushioning material is similar to the Confor® foam tested in the above references and does not exceed 51 mm in thickness. Alternate Verification Method
- For cases where the seat pan cushioning does not meet the specifications above, verify by analysis and test the design meets the Peak Axial Lumbar Compression Limits using the small female and large male anthropomorphic test device (ATD) as described in Section 7.5.

5.6 SUIT CONSIDERATIONS

5.6.1 Chest Mounted Equipment

Chest mounted equipment have been shown to increase injury risk and this increase risk is not reflected in the BDRC prediction [74]. To apply the BDRC in the +X (eyeballs in) direction, chest mounted equipment are not allowed. This includes rigid suit elements.

5.6.1.1 Verification Method

Verify by inspection/analysis that the suit design has no rigid elements located over the chest (elements with masses greater than 0.5 kg).

5.6.2 Rigid Suit Elements

Rigid suit components or seat/cockpit hardware that may impinge upon the occupant are not explicitly considered in the BDRC [75, 76]. Components that impinge upon the torso and or head/neck during transient loading are considered to create the highest potential for model invalidation and require inspection and/or analysis to ensure that no blunt trauma effects are induced. Rigid components on extremities must also be inspected and/or analyzed as required, but generally are considered less detrimental provided that they do not cause fracture, immobilization, or overall compromise of occupant restraint during acceleration exposure.

5.6.2.1 Verification Method

Verify by inspection and/or analysis that no rigid elements are within or could move within the load path (between the crewmember and seat/restraints) during dynamic events.

5.6.3 Head Protection

Protecting the head from blunt impact is critical to protecting the crew. Head injury from contact with surrounding seat and vehicle structures and helmet interior can induce significant loads leading to mild traumatic brain injury (MTBI), diffuse axonal injury (DAI) or skull fractures [77]. To provide adequate protection needed to validate the injury risk prediction of the BDRC, head protection must be included in the design. In impact tests with volunteers used to develop the BDRC helmets except those +X axis reported by Brinkley [18], helmet liners were used within the helmets, which padded the head and lessened the impact magnitude.

Helmets used in the development of the BDRC Confor®med to ANSI Z90.1 [78]. For spacecraft design, instead of relying on certification tests requiring additional design constraints that may not have direct applicability or may overly constrain the design, test and analysis with an ATD is preferred. This testing will ensure head contact with surrounding structures is not injurious directly instead of relying on a generic standard.

5.6.3.1 Verification Method

Verify the following metrics by analysis and test using the small female and large male ATD as specified in Table 15:

1. Head Injury Criterion (HIC15) (see Section 7.3.1).
2. Head Rotational Acceleration (see Section 7.3.2).

5.6.4 Helmet Mass

The experiments used to develop the BDRC included a helmet. The maximum helmet mass tested was the Mercury program helmet with a weight of 2.7 kg. The model may only be valid for designs with a helmet mass ≤2.7 kg unless special provisions are provided to prevent axial loading and increased bending moments to the neck during impact. Such provisions may include design aspects of the pressure suit helmet that allow the helmet pressure seal ring to be supported by wearer's shoulders

and straps from the suit prevent the helmet from rising upward with respect to the wearer's head. However, the head and helmet should not be restrained to the seat structure.

5.6.4.1 Verification Method

Analysis and test results showing helmet mass does not increase injury risk related to the N_{ij} and neck axial force (see section 7.2) to the occupant using the small female and large male ATD as specified in Table 15.

5.7 SPACEFLIGHT DECONDITIONING

Crewmembers experience varying levels of deconditioning related to exposure to microgravity. This includes changes to the musculoskeletal system [79-88]. Figure 14 shows example bone mineral density (BMD) losses after long-duration spaceflight. Data were collected on crewmembers before the use of the advanced resistive exercise device, and may be conservative compared to today's crewmember losses.

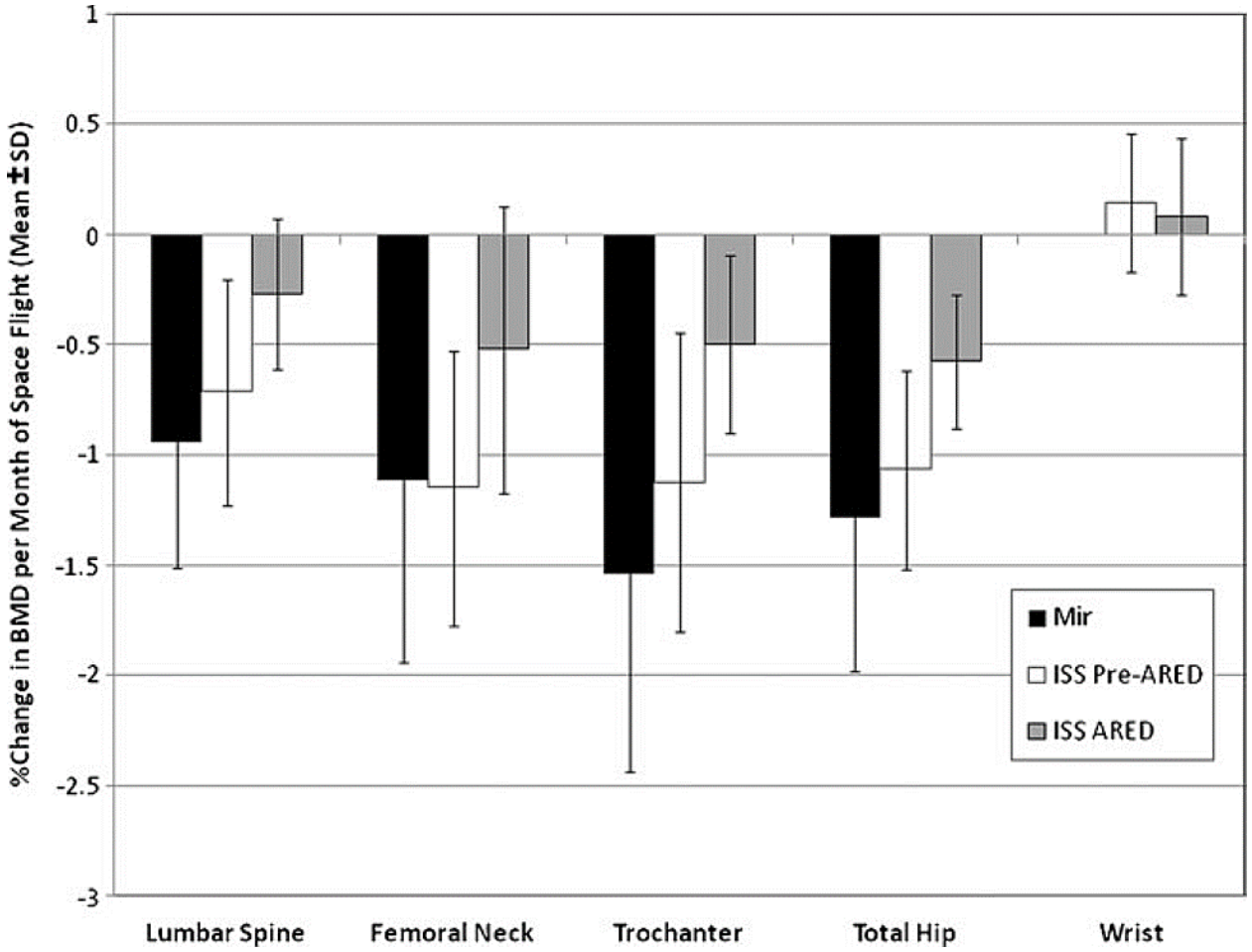

Figure 14. Changes in BMD after long-duration spaceflight [89].

To account for changes in injury risk due to microgravity exposure, scaling factors have been developed to reduce the BDRC limits for specific regions of the body. Additional information can be found in Lewendowski et al. and the HSIR Document [62, 90]. Table 12 shows the factors determined for regions of the body. These factors are to be applied to any dynamic event occurring after 1 month of reduced gravity exposure. These limits are an estimation of the necessary reduction in human tolerance to protect deconditioned crewmembers after up to 6 months in space. For longer missions, deconditioning limits should be discussed and agreed to by a panel of medical experts.

TABLE 12. DECONDITIONING FACTORS

Anatomical Region	Deconditioning Factor
Spine	0.86
Lower Extremities (including hip)	0.75
All Other Regions	1.0

To account for the effects of spaceflight deconditioning, the spinal elements deconditioning factor has been applied to the DR_z limits shown in Table 13. To protect for femoral head and neck fractures in lateral impact conditions, the lower-extremities deconditioning factor has been applied to the DR_Y limits as well. This was done to address the concern that pelvic restraint designs may not contact the iliac crest, concentrating the load on the femoral head and neck that is at a greater risk of fracture after spaceflight [91]. These values are to be used in cases where crewmembers have been exposed to reduced gravity for more than 1 month.

TABLE 13. DR LIMITS FOR SPACEFLIGHT DECONDITIONING

Axis	Direction	Low	Medium	High
Y	**Eyeballs left**	$-11.3 \leq DR_Y < 0$	$-15 \leq DR_Y < -11.3$	$-22.5 \leq DR_Y < -15$
	Eyeballs right	$0 \leq DR_Y < 11.3$	$11.3 \leq DR_Y < 15$	$15 \leq DR_Y < 22.5$
Z	**Eyeballs up**	$-11.5 \leq DR_z < 0$	$-14.1 \leq DR_z < -11.5$	$-17.5 \leq DR_z < -14.1$
	Eyeballs down	$0 \leq DR_z < 13.0$	$13.0 \leq DR_z < 15.4$	$15.4 \leq DR_z < 19.5$

5.7.1 Verification Method

Verify that each is true for the system:

1. Verify by test and analysis that all cases meet the BDRC for X values in Table 9.
2. Verify by test and analysis that all abort cases meet the BDRC for Y and Z values in Table 9.
3. Verify by test and analysis that all non-abort cases meet the BDRC for Y and Z values in Table 13.

6.0 LIMITATIONS

As discussed in Section 2.0, the limited data used to develop the models and the limitations imposed by the simplifications are inherent to the model. Even if all of the above application rules are met, there are limitations of the BDRC. Supplemental ATD and human testing is required to reduce the risk of injury to the crew.

6.1 SEX DIFFERENCES

The BDRC was developed with primarily young, male military volunteers (see Section 2.0). Buhrman et al. found male and female DRs in -X axis were not significantly different [92]; however, it is unclear whether a difference exists in the other model directions.

Recent evidence indicates that small female occupants are at greater risk of injury due to dynamic loads, particularly in certain anatomical regions [93-95]. Because the BDRC does not predict the increased risk to female crewmembers, ATD assessments are required.

Female occupants have an increased risk of neck injury due to loading [96-99]. Pintar et al. report a 600 N decrease in neck compression loading tolerance for females compared to males [96]. Failure loads in post-mortem human subjects due to pure compression were 1.2 ± 0.5 kN for females and 2.5 ± 0.9 kN for males [100].

In addition to neck compression tolerance changes, neck bending moment tolerance is also lower. Nightingale reports failure moments of 23.7 ± 3.4 Nm for flexion and 43.3 ± 9.3 Nm for extension in females [101]. For males, the failure moments were 29.0 ± 6.3 Nm and 49.5 ± 17.6 Nm for flexion and extension respectively [102]; a 12% to 18% decrease in tolerance between females and males.

Finally, lateral neck bending tolerance is lower for female subjects. Perry et al. measured neck moments were 29% higher in female subjects compared to the same conditions for males (25.2 Nm versus 19.3 Nm) [103].

Although no significant differences in cervical lumbar BMD exist between healthy males and females [98, 104], when normalized for weight, lumbar and cervical spine stress is 15% greater in females [99]. The effect of an increase in cervical stress on the DRI probability of injury curve has not yet been established, but would be expected to lead to a slight increase in the probability of neck injury [99].

6.1.1 Required ATD Assessments to Address Sex Differences

To account for the differences in sex, the following metrics are required to be assessed to ensure safety for female crewmembers. Depending on the chosen design implementation, the small female ATD may be the driving case for injury mitigation. If this is not the case, sufficient rationale should be provided as to why they chose ATD size or sizes are necessary to adequately bound the problem.

Assess by test and analysis using the small female ATD as specified in Table 15. Assess the following metrics:

1. Nij (see Section 7.2.2).
2. Peak Neck Axial Force Limits (see Section 7.2.3).

6.2 AGE EFFECTS

During the aging process, physical changes affect a person's tolerance to loading. Published literature shows injury risk increases with age, due to effects such as decrease in bone strength, disc degeneration, ligament strength, and muscle strength and reaction [77, 105, 106].

The BDRC is based on volunteer test data from subjects aged 18 to 58; however, a majority of the subjects were less than 30 years old. Currently, the astronaut corps ranges in age from 32 to 56-years old, suggesting that the model may not sufficiently protect older crewmembers from injury.

Table 14 shows a comparison of lumbar vertebra breaking strength related to age 30 [104, 107-109]. This change in strength is related to decrements in bone density in the vertebra. These changes would be in addition to any changes or loss of vertebral strength due to spaceflight. These results are based on a general population as compared to the astronaut corps, where adequate BMD is required for selection for flight [110].

TABLE 14. COMPARISON OF LUMBAR FAILURE STRENGTH BY AGE - VALUES ARE COMPARED TO AGE 30

	Age 40	**Age 50**	**Age 60**
Lumbar Failure Force [104, 107]	-11%	-22%	-35%

The DRI does include an age factor, which shows that the DR_z response decreases with age [23]. Although the BDRC does not adopt the age factor, it uses a 27.9-year-old male as the basis for this axis (median USAF aviator age) [23]. Changes in model dynamics related to age are shown in Figure 15 for a 50% risk of spinal fracture. Maximum tolerable acceleration decreases with increased age.

However, because age-related BMD loss is controlled through crew selection criteria, no additional age-related decrement factor is included for the +Z axis. In addition, there are currently not sufficient data available to propose limits based on age, nor to include supplemental ATD metrics.

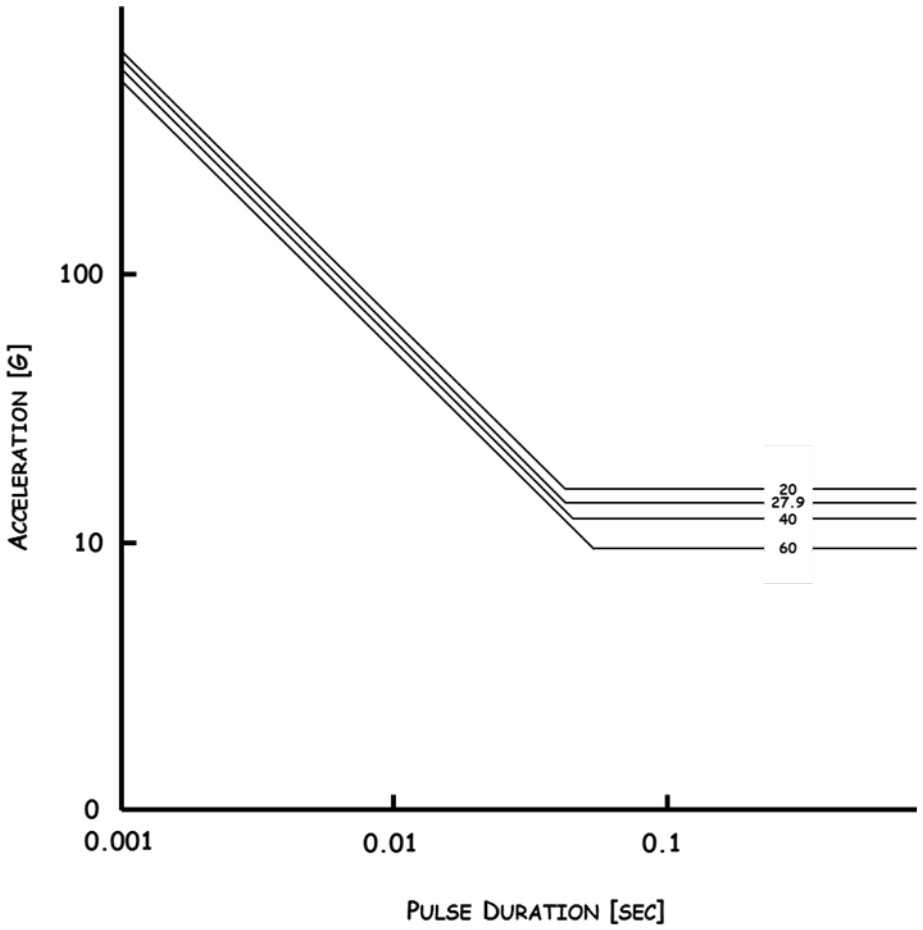

Figure 15. Dynamic Response Index (DRI) age effects. Shown are the 50% probability of spinal injury for various ages [23].

6.3 ANTHROPOMETRY EFFECTS

Anthropometry affects injury risk during dynamic events. Smaller crewmembers are at a greater risk of neck injury. Although smaller occupants have lower mass, the cross-sectional area of the cervical vertebra are smaller, causing significantly higher vertebral stress. No significant lumbar stress correlations were found with height or sitting height for either males or females [99]. In addition, because different size crewmembers interact with the seat, suit, and restraints differently, testing with a small and large ATD is necessary to assess unique design specific interactions.

6.3.1 Verification Methodology

Conduct test and analysis using the small female and large male ATD as specified in Table 15 to assess the following metrics:

1. Nij (see section 7.2.2)
2. Peak Neck Axial Force Limits (see Section 7.2.3)

6.4 MILITARY TRAINING

Military personnel (males and females) have been found to have 15% to 20% greater BMD than non-military personnel [99]. BMD is correlated to breaking strength, indicating that non-military personnel may be at a greater risk of injury due to dynamic loads. Because the BDRC is based on data collected from military test subjects, the injury limits may be under-conservative for non-military subjects. Because astronaut fitness levels preflight are similar to military personnel, this limitation is believed to be controlled for NASA's uses.

7.0 ATD SUPPLEMENTARY TEST AND ANALYSIS

In addition to the BDRC, the following assessments must be conducted to show the vehicle meets the requirements. Testing is to be conducted per SAE J211/1 for test procedures, channel polarity and signal filtering [111].

7.1 ATD SPECIFICATIONS

All ATD tests must be conducted with the ATDs as specified in Table 15, with the appropriate size selected to meet the injury assessment reference values (IARV) shown in each table. Summary Table 34 provides the required and additional ATD assessments. Depending on the vehicle, seat and suit configuration, all 3 ATDs may not be required for design verification.

TABLE 15. ATD SPECIFICATIONS

ATD	Description
Small Female	5th percentile female automotive Hybrid III with a straight spine (default configuration) and articulated pelvis
Mid-size Male	50th percentile male automotive Hybrid III with a straight spine and articulated pelvis
Large Male	95th percentile male automotive Hybrid III with a straight spine and articulated pelvis

7.1.1 Head Specification Revision

The Joint Strike Fighter (JSF) heads were originally selected because they are more representative of real human heads. For the small female, the standard Hybrid III head is undersized, whereas the 8.1 lbf JSF headform is a much more realistic representation of the true head mass. Similarly, for the large male Hybrid III, the 11.0 lbf JSF head is more representative of a large male. For JSF both heads, anatomical features are also included such as a chin and ear auricle.

After publishing the initial specifications for the Hybrid III configurations, it was decided that the JSF heads are not necessary. The reasons are threefold. First, the original injury metrics (Head Injury Criteria, head rotational acceleration, neck axial forces, and N_{ij}) were not developed with the JSF heads, but instead were developed with the standard Hybrid III headforms. The JSF headforms are heavier than the Hybrid III heads, so the predicted neck loadings are expected to be larger than for the Hybrid III headform; however, the head accelerations might be lower with heavier JSF heads. The second reason for the change is because numerical models of the JSF headforms are not available. One of the advantages of selecting the Hybrid III standard headforms is the availability of numerical models. The third reason for returning to the Hybrid III headforms is because of availability of the physical headform. Although they may be procured, they are not commonly available at testing facilities.

7.1.2 Pelvis and Spine Specifications

Table 15 specifies the use of the articulating pelvis and straight spine (mid-size and large male) options for the Hybrid III. This requirement was made for several reasons. First, for seat designs with an acute seat pan angle, the sitting pelvis does not typically fit. Because ATD fit in the seat is critical for obtaining realistic responses, this was considered an important addition. For seats that do not have a significant acute seat pan angle, the sitting pelvis may be acceptable; however, without further test data, it is unclear if the pelvis configuration will result in differences in head and neck responses. So for consistency, the sitting pelvis was disallowed. The straight spine specification for the mid-size and large male ATD is required if the optional lumbar axial force limit is invoked, as the automotive curved spine is not adequate for generating lumbar forces for assessing injury risk for seat cushioning. In addition, similar to the differences in pelvis design, it is unclear if differences between the two spines will affect other ATD responses, so the curved spine option is also disallowed during physical testing. In addition, NASA experience with ATD testing has shown that ATDs with the sitting pelvis are extremely difficult to fit into a pressure suit, and may even be difficult to fit into a spacecraft-type seat or full-scale vehicle test.

In regards to numerical modeling of the Hybrid III, there are not currently models of the articulating pelvis for all sizes and straight spine for the large male Hybrid III. Because of this, use of a sitting pelvis and curved spine Hybrid III model is allowed; however, care must be taken to adequately position the ATD in the seat and minimize gaps. NASA experience has shown that even if the physical ATD does not fit properly in the seat, it is possible to manipulate the models into a spacecraft type seat using gravity and belt tensioning to preload the ATD. Care must be taken to not over-preload the ATD model and generate large initial preloads in the model. In addition, if the seat cushioning exceeds the ground rule in section 5.5, alternate methods of assessing the lumbar load, which is beyond the scope of this report, are needed (such as using DRI to select the worst case lumbar load case and then conduct testing with the straight spine).

7.2 NECK INJURY ASSESSMENT

7.2.1 Current HSIR Limits - Individual Limits

7.2.1.1 Neck Axial Compression Force

Neck compression is of particular concern during spacecraft landing, because there can be a significant +Z acceleration (eyeballs down) causing neck compression from the inertial effects of the head. In addition, any head mounted mass, such as a helmet, could increase the load on the neck. The upper neck compressive force limits chosen for the HSIR have been derived from the automotive injury biomechanics and injury assessment literature and as codified in the NHTSA FMVSS 208, *Occupant Crash Protection* [112]. Mertz [113] does not give risk curves for neck compressive loading or neck shear loading. Lacking that information, a conservative estimate of low risk (approximately 0.5%) can be made by taking the data on volunteer static loading of the neck from Mertz [114] as a surrogate for low-risk dynamic loading in compression and shear (Table 16).

TABLE 16. HSIR PEAK UPPER NECK AXIAL COMPRESSION FORCE IARVs

Peak Neck Axial Compression Force (N)	Nominal			Off-Nominal		
	Small Female	Mid-size Male	Large Male	Small Female	Mid-size Male	Large Male
Non-Deconditioned	693	1,100	1,328	2,520	4,000	4,830
Deconditioned	596	946	1,142	2,167	3,440	4,154

7.2.1.2 Neck Axial Tension Force

In analyzing the biomechanical database for upper neck tension, the Alliance of Automobile Manufacturers noted there was one fatal neck lesion at the 5% risk level. As a result, the 3% risk level for neck tension was chosen for implementation in FMVSS 208 [112]. The worst case for neck tension loading is considered to be when the neck muscles are tensed only to the degree required to keep the head upright. Mertz [113] shows neck tension risk curves for serious neck injury limits with minimum muscle tone (see Table 17).

TABLE 17. HSIR PEAK UPPER NECK AXIAL TENSION FORCE IARVs

Peak Neck Axial Compression Force (N)	Nominal			Off-Nominal		
	Small Female	Mid-size Male	Large Male	Small Female	Mid-size Male	Large Male
Non-Deconditioned	734	1,097	1,323	2,513	4,000	5,030
Deconditioned	631	943	1,138	2,161	3,440	4,326

7.2.1.3 Neck Bending Moments

The concept of predicting neck injuries due to bending has been studied for almost as long as head injury prediction. The present bending moment limit criteria for fore and aft bending (i.e., flexion and extension) are based on the work of Mertz and Patrick [115] in which the necks of volunteers and cadavers were inertially loaded by head motion in sled tests where the subjects were restrained by belt

restraints or seatbacks without head support. The concept of neck injury due to bending is based on the concern for excessive bending motion (in flexion, extension, or lateral bending) causing ligamentous and boney damage as the vertebrae impinge in extreme motion. Since neck motion is difficult to measure with transducers in an ATD, the bending-moment levels associated with excessive motion in cadaver tests was used by Mertz and Patrick as an indicator of potential impingement. Mertz [113] does not give risk curves for neck bending moments. Lacking that information, a conservative estimate of low risk (~0.5%) can be made by taking the data on volunteer static neck loading from Patrick and Chou [116] as a surrogate for low-risk dynamic loading in neck flexion and lateral bending. Mertz [113] presents a risk curve for extension moment values related to serious injury for the case of minimum muscle tone in various sized dummies. Values are shown in Table 18.

TABLE 18. HSIR UPPER NECK BENDING MOMENTS

Peak Neck Moments [Nm]		Nominal			Off-Nominal		
		Small Female	Mid-size Male	Large Male	Small Female	Mid-size Male	Large Male
Extension	**Non-Deconditioned**	17	39	49	33	65	87
	Deconditioned	15	34	42	28	56	75
Flexion	**Non-Deconditioned**	49	96	96	104	190	258
	Deconditioned	42	83	83	89	163	222
Lateral	**Non-Deconditioned**	38	75	75	72	143	143
	Deconditioned	33	65	65	62	123	123

7.2.2 Proposed HSIR Limits - N_{ij} Neck Injury Criteria

Previous studies have shown that combined axial loading and bending moments have a higher injury potential than for pure axial loading [117-120].

The N_{ij} expanded upon the research of Prasad and Daniel to address injury risk in all four combinations of loading and bending. NHTSA first published this revision in 1996 [121]. The "ij" refers to each combination of axial force and sagittal plane bending moment: N_{TE} for tension-extension, N_{TF} for tension-flexion, N_{CE} for compression-extension, and N_{CF} for compression-flexion. In addition, lateral bending moments combined with axial force are also included: N_{TL} for tension-lateral and N_{CL} for compression-lateral. Each combination is calculated using Equation 6 for each ATD size based on critical values (Table 19). The maximum of each combination determines the final N_{ij} score (Equation 7). In addition, pure tension and compression axial load limits are also specified.

The N_{ij} critical values have been revised several times since the first NHTSA proposal [122-124]. A more detailed explanation of the development of the criteria and associated critical values can be found in these references.

The moment used in the N_{ij} calculation (Equation 6) is the effective moment at the occipital condyle and is determined by Equation 5.

Equation 5. Effective Moment at the Occipital Condyle

$$M_{oc}(t) = M_y(t) - F_x(t) \cdot d_{LC}$$

Where:

$M_{oc}(t)$ Is the effective moment at the occipital condyle
$M_y(t)$ Is the sagittal plane moment measured at the upper neck load cell
$F_x(t)$ Is the x-axis shear force measured at the upper neck load cell
d_{LC} Is the height of the upper neck load cell above the condyles

Equation 6. N_{ij} Calculation

$$N_{ij} = \frac{F_z(t)}{F_{int}} + \frac{M_{oc}(t)}{M_{int}}$$

N_{ij} Is the normalized neck injury risk for each combination ($N_{TE}, N_{TF}, N_{CE}, N_{CF}$)
$F_z(t)$ Is the axial force in the prescribed direction
F_{int} Is the critical axial force limit in the prescribed direction
$M_{oc}(t)$ Is the effective moment at the occipital condyle in the prescribed direction
M_{int} Is the critical sagittal moment limit in the prescribed direction

Equation 7.

$$N_{ij} = \max(N_{TE}, N_{TF}, N_{CE}, N_{CF}, N_{TL}, N_{CL})$$

It is important to note that the maximum N_{ij} value may not occur at the same time point as the maximum of either the axial load or sagittal moment, since it is the combined value at any time point that is correlated to injury. In addition, the spinal element deconditioning factor shown in Table 12 must also be applied to the N_{ij} when necessary.

TABLE 19. NASA PROPOSED CRITICAL VALUES

N_{ij} Critical Values	Small Female Hybrid III	Mid-size Male Hybrid III	Large Male Hybrid III
F_c Tension	4,287 Nm	6,806 Nm	8,216 Nm
F_c Compression	3,880 Nm	6,160 Nm	7,440 Nm
M_c Extension	67 Nm	135 Nm	179 Nm
M_c Flexion	155 Nm	310 Nm	415 Nm
M_c Lateral	67 Nm	135 Nm	179 Nm

The maximum N_{ij} limits were determined by expert consensus (Table 20). Currently, the Department of Defense (DoD) uses a limit 0.5 for the F-35 crew escape system [125]. Based on the existing injury risk functions, this corresponds to approximately a 10% risk of an AIS≥3 injury risk; however, this level was deemed acceptable for two reasons:

1. the injury risk is based on a general population, so crewmembers may not be at as great a risk, and
2. there is uncertainty in the injury risk function at this level (an N_{ij} = 0 equates to a 4% risk of AIS≥3 due to the statistical model used).

This injury risk level differs from the levels denoted in Table 23 because of the limitations discussed above.

In addition, the spinal element deconditioning factor shown in Table 12 must also be applied the N_{ij} when necessary. The regions of acceptable neck dynamics are shown in Figures 16, 18 and 20 for the small female, mid-size male, and large male Hybrid III ATDs respectively.

TABLE 20. NASA PROPOSED IARVs

N_{ij} Limit	Non-Deconditioned		Deconditioned	
	Nominal	Off-Nominal	Nominal	Off-Nominal
Small Female	0.5	0.5	0.4	0.4
Mid-size Male	0.5	0.5	0.4	0.4
Large Male	0.5	0.5	0.4	0.4

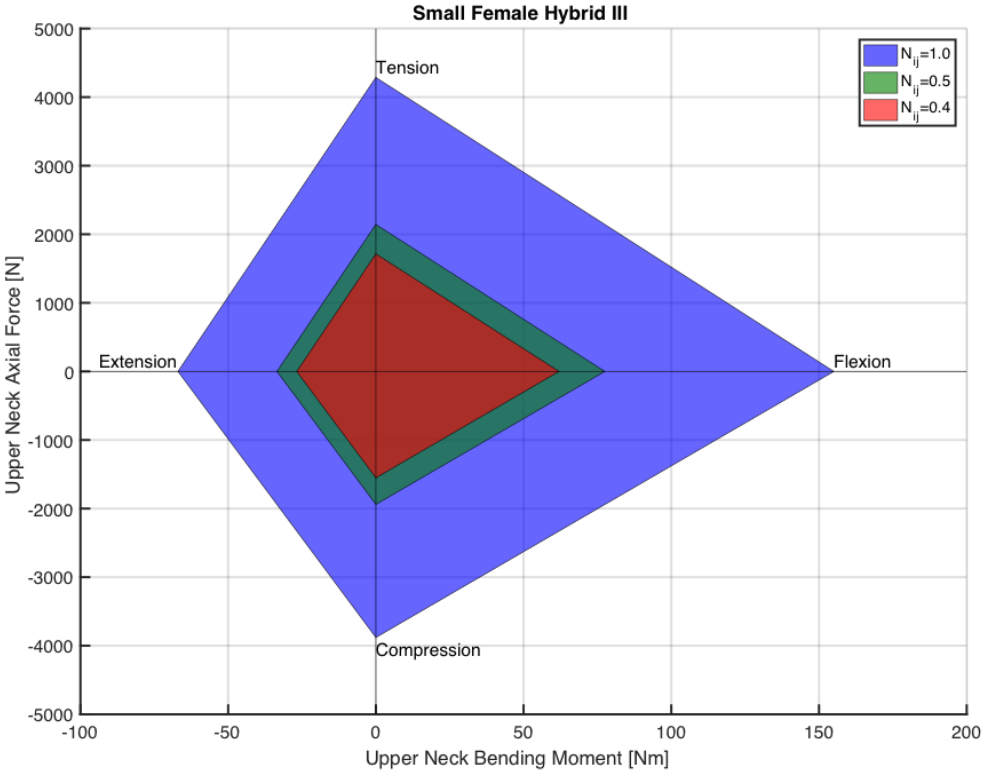

Figure 16. Small female Hybrid III sagittal N_{ij} regions.

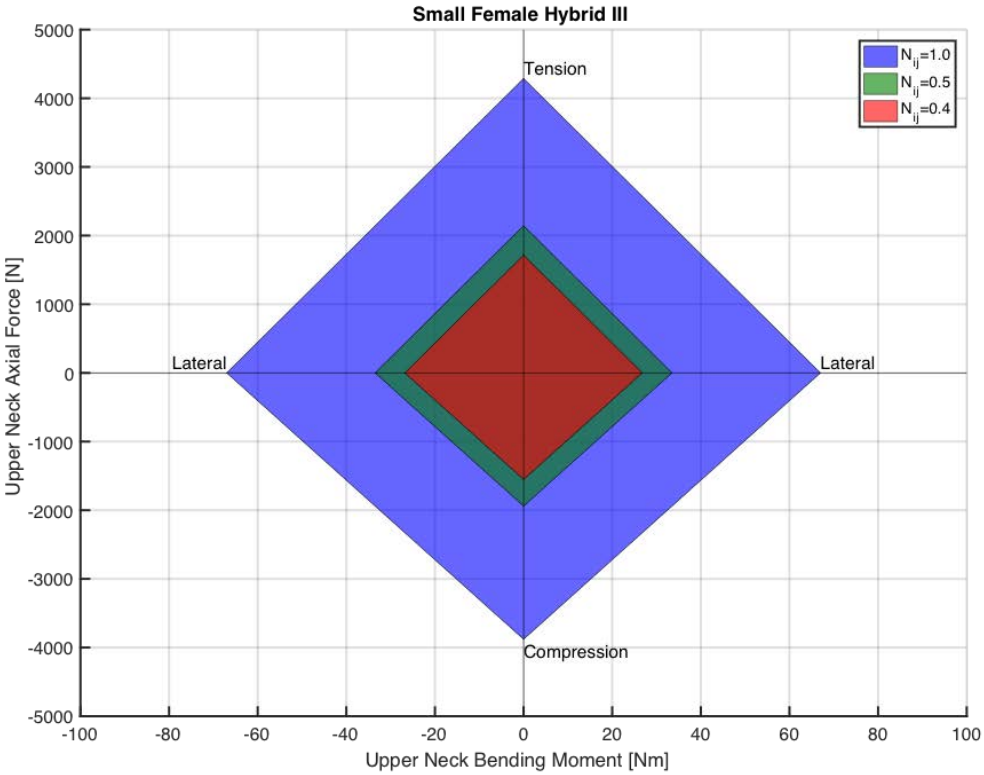

Figure 17. Small female Hybrid III lateral N_{ij} regions.

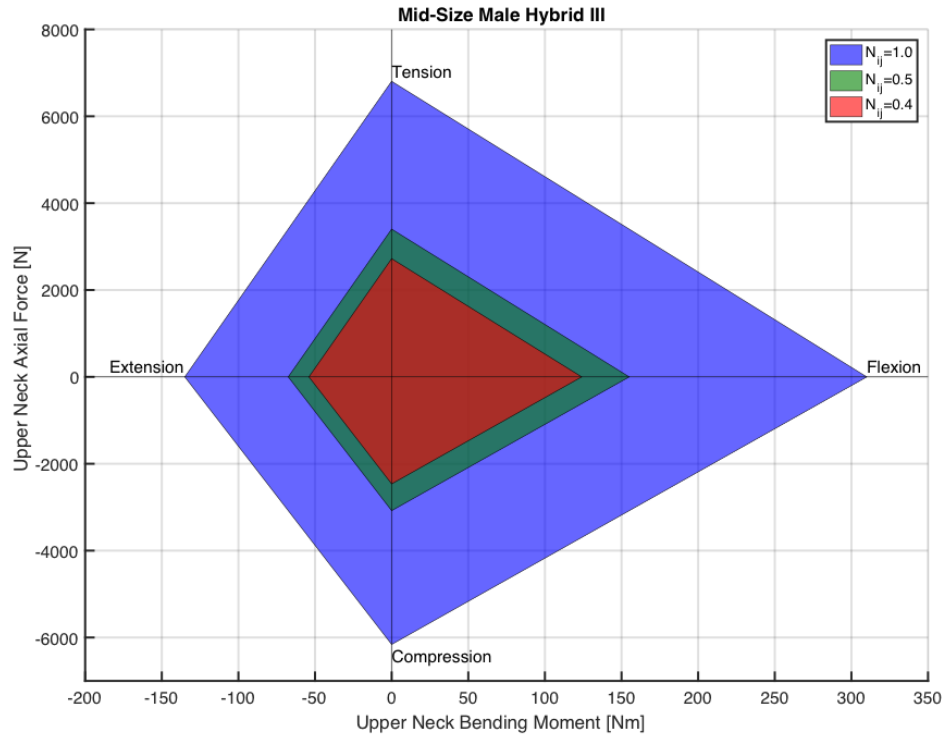

Figure 18. Mid-size Male Hybrid III sagittal N_{ij} regions.

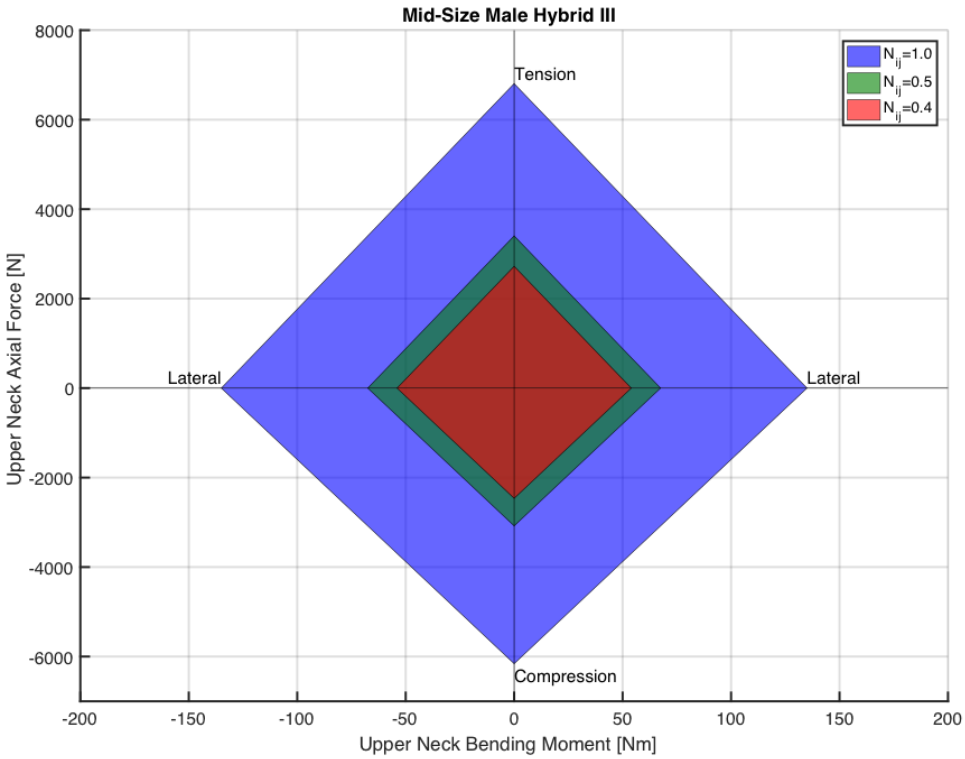

Figure 19. Mid-size Male Hybrid III lateral N_{ij} regions.

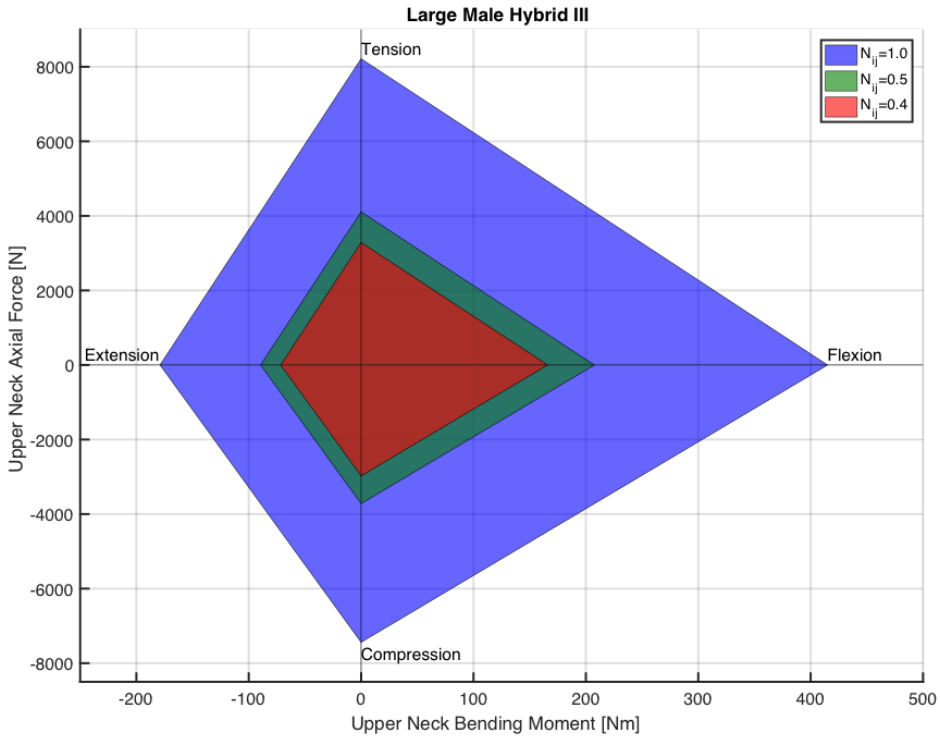

Figure 20. Large male Hybrid III Nij regions.

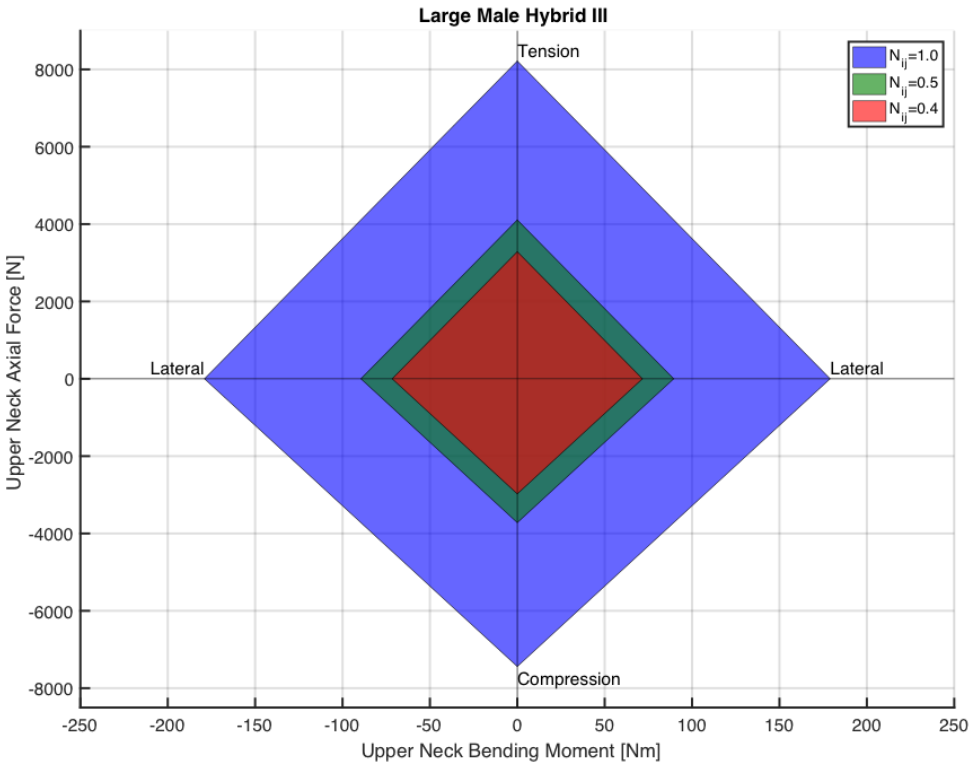

Figure 21. Large male Hybrid III lateral Nij regions.

7.2.3 Proposed HSIR Limits -Neck Axial Force Injury Criteria

In addition to the N_{ij}, maximum neck load limits are also required. The values and method reported here are currently in use by the DoD for the F-35 crew escape system, as described by Nichols

[125]. Figure 22 shows how to determine the peak-duration values for a particular waveform with the resulting amplitude-duration curve shown in Figure 23. Table 21 and Figure 24 show the limits for upper neck axial tension force in Newtons. Table 22 and Figure 25 show the limits for upper neck axial compression force in Newtons.

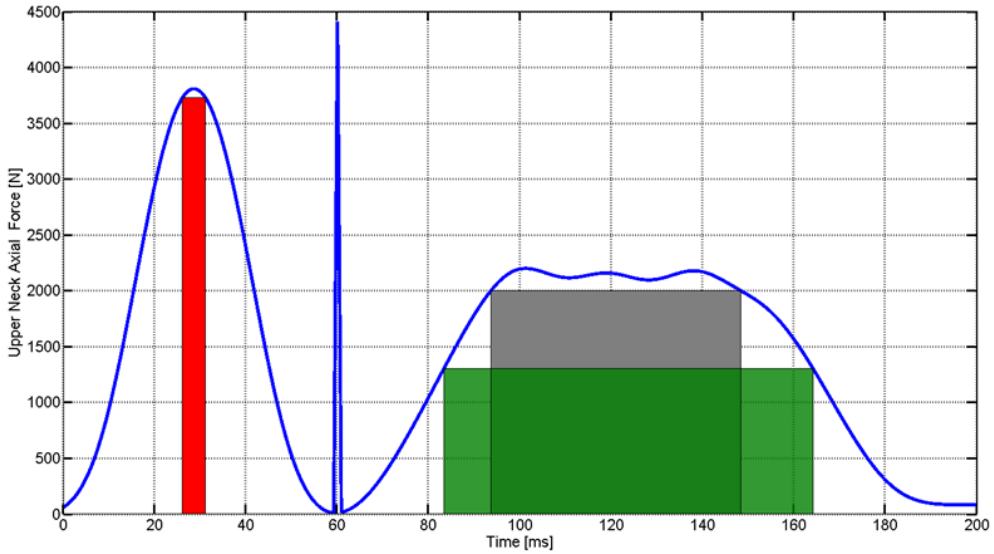

Figure 22. Neck force peak-duration determination. The red box shows a 5-ms sustained force above 3,700 N, the gray box shows a 55-ms sustained force above 2,000 N, and the green box shows an 80 ms sustained force above 1,300 N. Note that although the spike at 60 ms is very large in amplitude, it is less than 5 ms and is ignored.

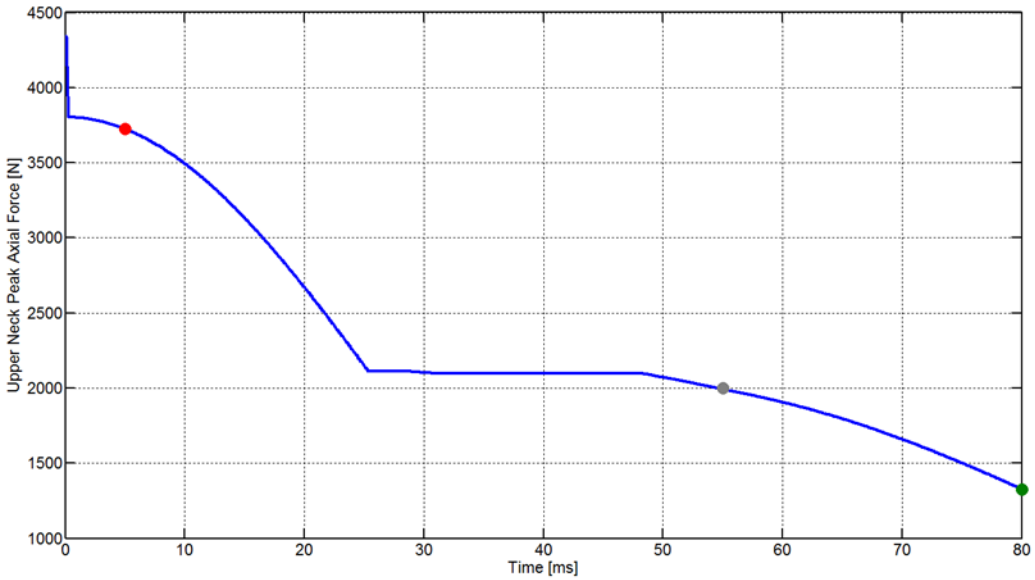

Figure 23. Resulting peak axial force by duration from waveform shown in Figure 22. The colored dots correspond with the boxes shown in Figure 22.

TABLE 21. PEAK NECK AXIAL TENSION VALUES

		Time [ms]	Conditioned	Deconditioned
Neck Axial Tension Force Duration Limits [N]	**Small Female**	5	1,840	1,580
		31	1,840	1,580
		40	890	765
		80	890	765
	Mid-size Male	5	2,750	2,360
		35	2,750	2,360
		45	1,420	1,220
		80	1,420	1,220
	Large Male	5	3,390	2,910
		37	3,390	2,910
		48	2,000	1,720
		80	2,000	1,720

TABLE 22. PEAK NECK AXIAL COMPRESSION VALUES

		Time [ms]	Conditioned	Deconditioned
Neck Axial Compression Force Duration Limits [N]	**Small Female**	5	2,310	1,990
		27	890	765
		80	890	765
	Mid-size Male	5	3,510	3,020
		30	1,420	1,220
		80	1,420	1,220
	Large Male	5	4,360	3,750
		32	2,000	1,720
		80	2,000	1,720

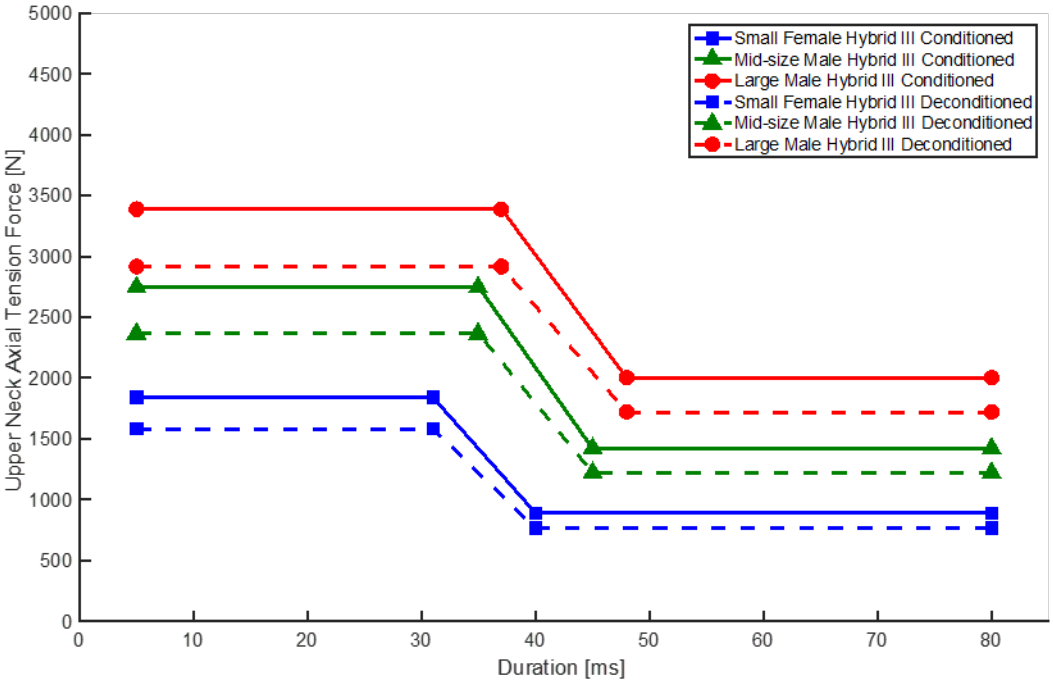

Figure 24. Peak neck axial tension limits.

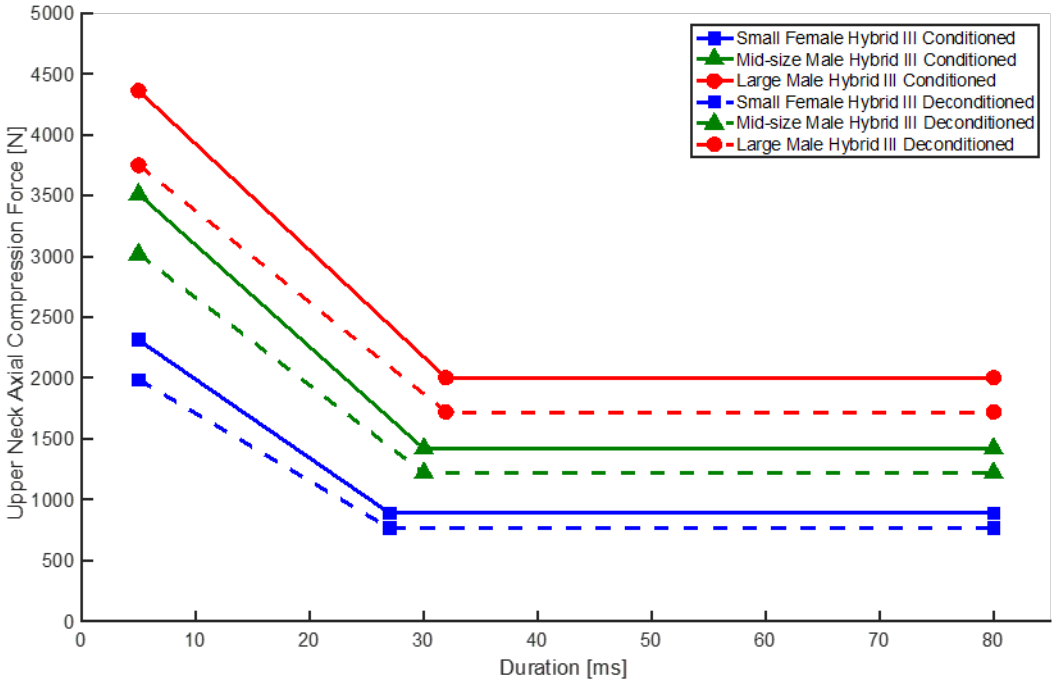

Figure 25. Peak neck axial compression limits.

7.2.4 Limitations of the Proposed Neck Injury Assessment

Although these neck injury assessments are based on current methods in the injury biomechanics field, there are limitations associated with the injury predictions.

First, the Hybrid III neck is not biofidelic in its response. In tension, recent results by Dibb et al. show it to be much stiffer than a human neck. In forward flexion, the head and neck response is also stiffer than in live human testing [126]. In the lateral direction, the neck is not biofidelic and has been shown to also be very stiff [127].

In regard to the IARVs related to neck injury, the N_{ij} work is based on injury to juvenile pigs with the 3-year-old Hybrid III ATD tested in matching conditions [120]. The 3-year-old values were then scaled to the different ATD sizes [122]. In addition, the lateral bending moment limits were selected based on the extension moments, with the assumption that this selection is conservative.

For the axial force limits, the limits presented in Figures 24 and 25 have been revised from the original work published by Mertz [114]. Changes were made by the U.S. Navy and USAF to raise the long-duration limits and limit the maximum allowable force to 5 ms based on previous experience [125].

7.3 HEAD INJURY METRICS

Because the BDRC does not require head restraint, measures to protect the head are appropriate. Brain injury is more concerning for spaceflight (as opposed to skull fracture that may occur from higher loads), since conservation of emergency self-egress capability is required. Recent studies of football players have established MTBI risk related to both linear and rotational head acceleration. Linear acceleration has been shown to cause injury and the HIC is a validated metric for assessing injury risk. As recent work in the automotive community has shown that rotational head acceleration contributes to risk of head injury, this metric is included to enhance the protection provided by the BDRC.

Because head injury risk is highest for cases in which head impacts occur, suitable testing conditions must be used. For example, if head impact may occur with surrounding vehicle structure, a mock-up of the structure must be included during test to ensure any derived head injury metric is not

exceeded. The mock-up must ensure sufficient fidelity to replicate the dimensions and nature of injurious forces imparted to the head so as to ensure the preventative measures are adequate.

The updated limits are based on the injury risk limits shown in Table 23. This allows consistent risk estimates for each metric.

TABLE 23. ACCEPTABLE RISK LIMITS

Injury Level	Nominal	Off-Nominal
AIS1+	5%	19%
AIS2+	1%	4%
AIS3+	0.3%	1%
AIS4+	0.03%	0.1%

7.3.1 Linear Head Acceleration

Assessing the potential for head injury (e.g., brain and skull injury) has been a primary focus in injury biomechanics research for more than 40 years. The pioneering efforts by researchers to predict brain injury from head acceleration measurements led to the Wayne State Tolerance Curve (WSTC) [128]. Using the observation that most emergency room patients admitted with simple linear skull fractures were concussed (although not all concussed patients had skull fractures), they hypothesized that determining the translational head accelerations associated with the initiation of linear skull fractures in drop tests of embalmed cadaver heads would give an estimate of concussion occurrence. The extreme association of the limit accelerations with the durations of impact found in those tests for contact durations below 4 ms led Gadd [129] to plot the data on a logarithmic scale that exhibited a linear relationship with a slope of -2.5 between the peak acceleration and time duration on a log-log plot. Gadd proposed the Gadd Severity Index (GSI), a weighted impulse criteria in which the integral of the measured head acceleration over time, raised to the 2.5 power was a measure of head injury potential based on the WSTC. Because the time interval for calculating the GSI was not specified, this led to confusion over the interpretation of more complex head acceleration waveforms. Versace [130] proposed an optimization method to search for the acceleration time interval, (t_2-t_1) that would maximize the GSI. This is referred to as the Head Injury Criteria (HIC) and codified by the NHTSA. All passenger cars sold in the U.S. must meet a designated level of HIC in a 35-mph barrier crash test for the vehicle occupants. Equation 8 is used to calculate the HIC. The HIC is most valid for head accelerations due to contact with a generally rigid surface [131], so the 15 ms time interval was selected.

Equation 8. Head Injury Criteria (HIC) Formula

$$HIC_{15} = \max_{0 \le t_2 - t_1 \le 0.015} \left((t_2 - t_1) \left[\int_{t_1}^{t_2} a(t)dt \; \frac{1}{t_2 - t_1} \right]^{2.5} \right)$$

7.3.1.1 Current HSIR Limits

Currently, the HSIR limits are based on an extrapolation of the injury risk curve published by Mertz [113]. These values are related to an AIS≥4 brain injury.

TABLE 24: HSIR HIC 15 IARVs

HIC 15	Nominal			Off-Nominal		
	Small Female	**Mid-size Male**	**Large Male**	**Small Female**	**Mid-size Male**	**Large Male**
	300			700		

7.3.1.2 Proposed HSIR Limits

Recent studies of MTBI in football players can be very useful for determining the appropriate threshold for head injury. As AIS 1 and 2 injuries to the brain are of primary concern, the HIC injury risk functions from Funk, et al. will be used (Equation 9) [132]. These data were chosen over the Virginia Tech data reported by Funk in 2012 because the HIC values from the 2007 study are more

conservative [133]. Because concussion injury risk determined from NASCAR head injury modeling resulted in much higher allowable HIC values [134], the Funk HIC 15 curve will be used since these limits are more conservative.

Equation 9. Head Injury Criteria Injury Risk Model

$$p(inj|AIS \geq 1) = 1 - e^{-\left(\frac{HIC}{\beta}\right)^{\alpha}}$$

Where:

A is the cut point for the specified AIS level
β is the regression coefficient

TABLE 25: HIC 15 INJURY RISK MODEL COEFFICIENTS

Variable	A	β
AIS≥1	4.34	671

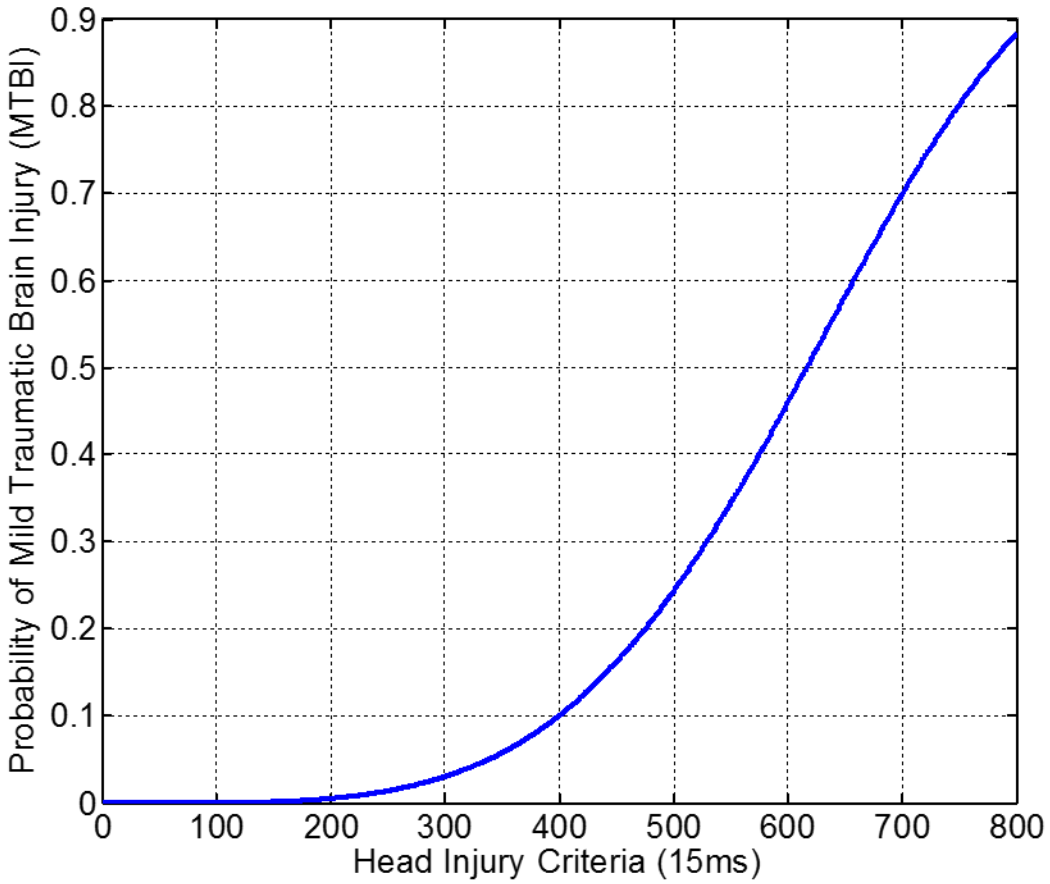

Figure 26. HIC 15 Injury Risk Function [132]

Using the scaling function (Equation 10 and Table 26) proposed by the Alliance of Automobile Manufacturers Association [113, 135], values for the small and large ATDs can be determined (Table 27).

Equation 10. HIC Ratio

$$\lambda_{HIC} = \lambda_{\sigma}^{2.5} \cdot \lambda_{L}^{-1.5}$$

Where:

$\lambda_a = \lambda_\sigma \cdot \lambda_L^{-1}$ is the acceleration ratio
$\lambda_t = \lambda_L$ is the time ratio
λ_L is the head size ratio
λ_σ is the failure stress ratio

TABLE 26. HIC SCALING FACTORS

ATD	λ_L	λ_{σ_f}	λ_t	λ_{HIC}	Nominal HIC	Off-Nominal HIC
Small Female	0.931	1.00	0.931	1.113	375	525
Mid-size Male	1.000	1.00	1.000	1.000	340	470
Large Male	1.030	1.00	1.030	0.957	325	450

TABLE 27: HIC 15 IARVs

HIC 15	Nominal			Off-Nominal		
	Small Female	**Mid-size Male**	**Large Male**	**Small Female**	**Mid-size Male**	**Large Male**
	375	340	325	525	470	450

7.3.2 Rotational Head Acceleration

7.3.2.1 Current HSIR Limits

None

7.3.2.2 Proposed HSIR Limits

Pellman et al. [136] report concussion related to rotational accelerations in professional football players. The IARVs are related to the risk of MTBI that includes concussions. As with HIC 15, the updated limits are based on the injury risk limits shown in Table 23.

Recent data published by Rowson indicate that the Pellman data may be conservative [137]; however, given the age of the subjects in both studies (younger than the current astronaut population), the Pellman injury risk function was chosen (Equation 11).

Equation 11. Head Rotational Acceleration Injury Risk Model

$$p(inj|AIS \geq 1) = \frac{1}{1 + e^{(\alpha - \beta \cdot x)}}$$

Where:

α is regression constant
β is the regression coefficient

TABLE 28. HIC 15 INJURY RISK MODEL COEFFICIENTS

Variable	α	β
AIS≥1	4.939	0.0009

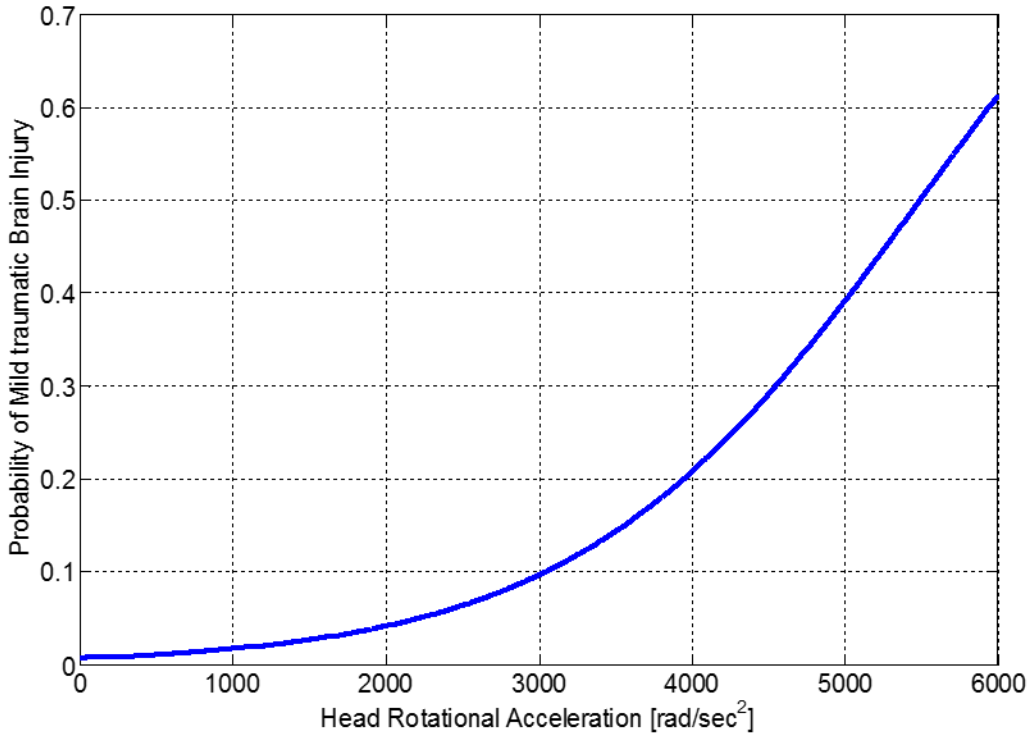

Figure 27. Head rotational acceleration injury risk function (AIS≥1) [136].

TABLE 29. HEAD ROTATIONAL ACCELERATION IARVs

Head CG Rotational Acceleration [rad/s^2]	Nominal [5% risk of MTBI]	Off-Nominal [19% risk of MTBI]
Mid-size Male	2,200	3,800

Using the same scaling function as the HIC (Table 30), values for the small and large ATDs can be determined (Table 31). The head rotational acceleration IARVs are for resultant accelerations at the location of the ATD head accelerometer.

TABLE 30. HEAD CG ROTATIONAL ACCELERATION SCALING FACTORS

ATD	λ_α	Nominal α	Off-Nominal α
Small Female	1.113	2,450	4,230
Mid-size Male	1.000	2,200	3,800
Large Male	0.957	2,100	3,640

TABLE 31. HEAD CG ROTATIONAL ACCELERATION IARVs

Head CG Rotational Acceleration [rad/s^2]	Nominal			Off-Nominal		
	Small Female	Mid-size Male	Large Male	Small Female	Mid-size Male	Large Male
	2,500	2,200	2,100	4,200	3,800	3,600

7.3.3 Limitations of the Proposed Head Injury Assessment

The HIC has been used in the automotive industry for many years; however, there are limitations. The HIC was developed for cases were head impacts occur. Consequently, HIC values without head impacts are not a valid measure of head injury risk. Also, the values proposed are based on football player concussion risk, which may not be an accurate analog to spacecraft occupants. Age is also a factor in predicting concussion risk [138], so the differences in age between the subjects studied and astronaut corps may affect injury risk.

Head rotational acceleration has also been proposed to contribute to concussion; however, there is a wide range of proposed limits for preventing brain injury, so the values proposed here may be conservative. As with HIC, age is a factor in predicting concussion risk [138], so the differences in age between the subjects studied and astronaut corps may affect injury risk.

Finally, the combination of head linear and rotational acceleration may be important in predicting brain injury. Currently, additional research is needed to understand this effect.

7.4 FLAIL LIMIT

To assess flail of the upper extremities, a method of simulating bracing is needed; otherwise, complex restraints would be required to arrest upper limb movement. Because grasping strength is most likely the main inhibitor of arm flail, the following limits were chosen based on values reported in the HSIR document [62]. The values (Table 32) chosen for nominal small-female testing are based on the unpressurized suited grasp strength for other operations (from HSIR Table F4.0-3). The mid-size and large male values are scaled based on ATD mass and values are rounded to 2 significant digits. These values are similar to the values used in military ejection seat testing scaled to similar sized ATDs.

TABLE 32. FLAIL BRACING BREAK CORD FORCE LIMITS

ATD Size	Break Cord Limit [N]
Small Female	490
Mid-size Male	780
Large Male	980

If active bracing is relied on to prevent flail, testing with cord that breaks at the limits shown in Table 32 must be conducted. The design is considered acceptable if the arms do not flail beyond the envelope of the seat.

For lower extremities, grasping strength is not possible, and bracing is most likely insufficient for arresting lower extremity movement. Instead, sufficient restraints are needed to minimize limb movement to less than 25mm in any direction.

7.5 LUMBAR AXIAL COMPRESSION FORCE

Lumbar axial compression force limits are given in the Full Spectrum Crashworthiness Criteria for Rotorcraft [139] and are based on limits derived by Desjardins [140]. These limits correspond to a DR_z of 18.0 (5% risk of lumbar-thoracic spinal fracture), and correspond to the off-nominal BDRC limits. To determine nominal limits, linear scaling was used with the DR_z value of 15.2 (nominal BDRC limit) similar to the method used by Desjardins to scale the lumbar load to higher DR_z values. The deconditioned values were determined by applying the spinal deconditioning factor of 0.86 (from Table 12). Values are rounded to 2 significant digits (Table 33). Because these limits are based on the DR_z, the same limitations discussed in Section 2.0 apply.

TABLE 33. LUMBAR AXIAL COMPRESSION FORCE LIMITS

Peak Lumbar Axial Compression Force [N]	Non-Deconditioned		Deconditioned	
	Nominal	Off-Nominal	Nominal	Off-Nominal
Small Female	3,500	4,200	3,000	3,600
Mid-size Male	5,300	6,200	4,600	5,300
Large Male	6,600	7,800	5,700	6,700

7.6 SUMMARY

Following is a summary of the required ATD assessments and alternate ATD assessments that may be required depending on the design and the alternate verification methods chosen.

TABLE 34. SUPPLEMENTAL ATD ASSESSMENTS. UNSHADED METRICS ARE REQUIRED, SHADED METRIC IS ONLY REQUIRED IF AMPLIFICATION VERIFICATION METHOD IS NOT MET.

ATD Metric	ATD Size	Non-Deconditioned		Deconditioned	
		Nominal	Off-Nominal	Nominal	Off-Nominal
HIC 15	Small female	375	525	375	525
	Mid-size male	340	470	340	470
	Large male	325	450	325	450
Head Rotational Acceleration [rad/sec^2]	Small female	2,500	4,200	2,500	4,200
	Mid-size male	2,200	3,800	2,200	3,800
	Large male	2,100	3,600	2,100	3,600
N_{ij}	Small female	0.5	0.5	0.4	0.4
	Mid-size male	0.5	0.5	0.4	0.4
	Large male	0.5	0.5	0.4	0.4
Peak Neck Axial Tension Force [N]*	Small female	890 - 1,840		765 - 1,580	
	Mid-size male	1,420 - 2,750		1,220 - 2,360	
	Large male	2,000 - 3,390		1,720 - 2,910	
Peak Neck Axial Compression Force [N]*	Small female	890 - 2,310		765 - 1,990	
	Mid-size male	1,420 - 3,510		1,220 - 3,020	
	Large male	2,000 - 4,360		1,720 - 3,750	
Flail	Small female	Pass			
	Mid-size male	Pass			
	Large male	Pass			
Peak Lumbar Axial Compression [N]**	Small female	3,500	4,200	3,000	3,600
	Mid-size male	5,300	6,200	4,600	5,300
	Large male	6,600	7,800	5,700	6,700

* Values in table are evaluated at varying time durations as discussed in Section 7.2.3

** Only applicable if amplification application rule is not met as discussed in Section 5.5

8.0 DESIGN VALIDATION APPROACH

NASA-STD-7009A, Standard for Models and Simulations, defines verification as the process of ascertaining the extent to which a model meets its requirements and specifications, and validation as the process of ascertaining that the model represents reality[141]. Because the current finite element (FE) and mathematical models of the different sizes and versions of ATDs were not developed to simulate the ATD responses in all loading directions and dynamic ranges assessed in spaceflight occupant protection analysis, there is concern that the models are not sufficiently validated for use without physical testing. In addition, there are no validated standard practices to adequately model the ATD-suit-restraint-seat interaction. When referring to the combined model consisting of the ATD, suit elements, restraints, and seat, the term “occupant model” will be used.

To address concerns associated with relying on an invalidated occupant model, a combination of test and analysis is required to determine the occupant-model accuracy and acceptability for demonstrating a spacecraft can meet safety requirements for human-flight certification. This is typically a multi-phased approach with a combination of test and analysis to support model development, validation, and eventually certification. An example of this approach is shown in Figure 28. If an alternate approach is used, sufficient justification and documentation is required to meet the intent of this approach.

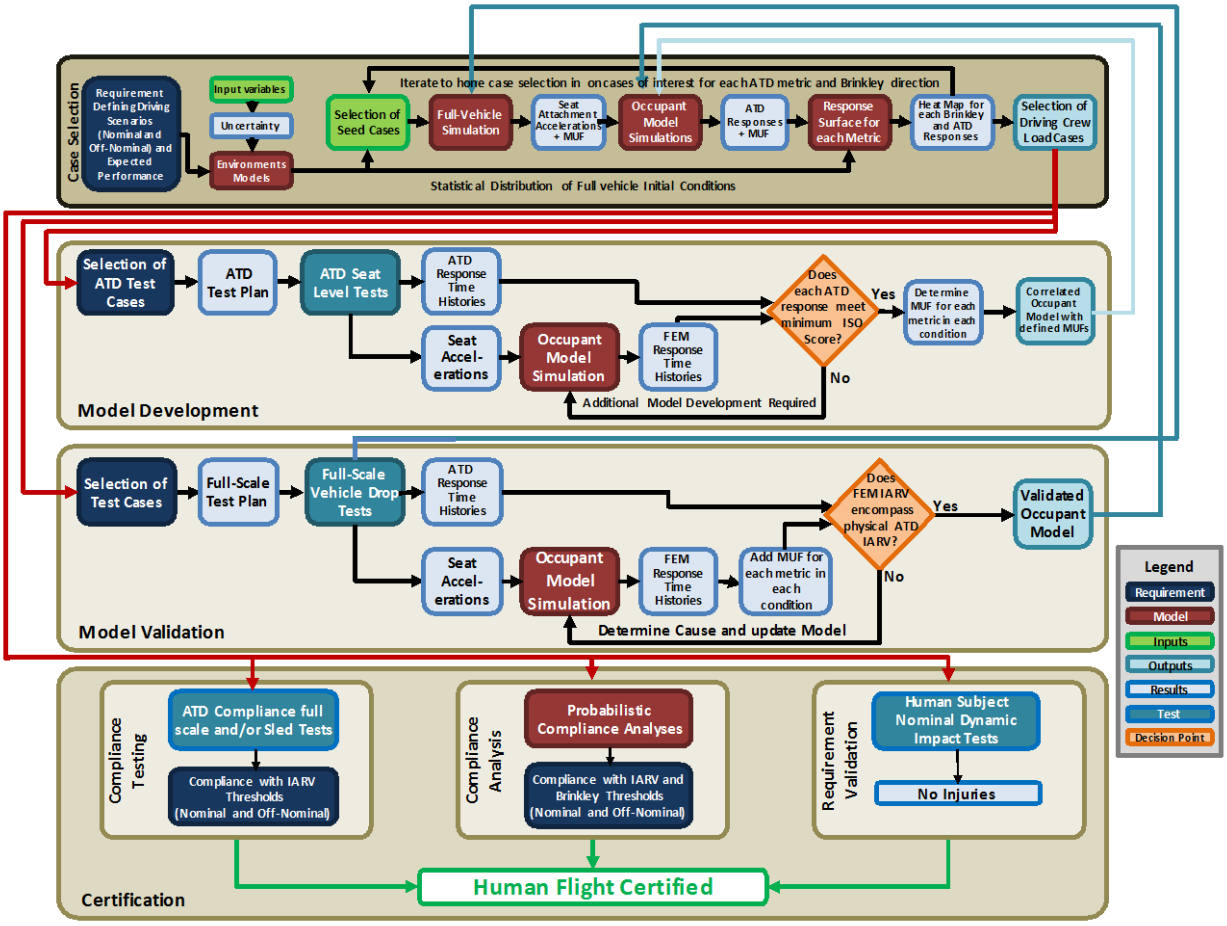

Figure 28. Example process for ATD modeling verification and validation.

We recognize that each spacecraft will have unique environments and hardware configurations that could influence occupant protection results. As the physical and analytical Hybrid III ATDs will be used under multi-axial loading beyond their validation, the quality of the model must be established and meet or exceed minimum credibility-assessment scale (CAS) scores per NASA-STD-7009A as shown in Table 35 [141]. A credibility-assessment score is determined using the descriptions in Table 35 and the resulting model-uncertainty factor (MUFs) for each occupant model. This score may then be used as an overall subjective score to rate the overall quality of the occupant model.

TABLE 35. MINIMUM CREDIBILITY ASSESSMENT SCALE SCORES (GREEN) PER NASA-STD-7009A

	M&S Development			M&S Use (Operations)			Supporting Evidence	
Level	**Data Pedigree**	**Verification**	**Validation**	**Input Pedigree**	**Uncertainty Characterization**	**Results Robustness**	**M&S History**	**M&S Process/Product Management**
4	All data known & traceable to RWS with acceptable accuracy, precision and uncertainty.	Reliable practices applied to verify the end-to-end model; all model errors satisfy requirements.	All M&S outputs agree with data from the RWS over the full range of operation in its real operating environment.	All input data known & traceable to RWS with acceptable accuracy, precision, and uncertainty.	Statistical analysis of the output uncertainty after propagation of all known sources of uncertainty.	Sensitivities known for most parameters; most key sensitivities identified.	Nearly identical model and use.	Controlled processes are applied; measurements used for process improvement.
3	All data known & traced to sufficient referent. Significant data has acceptable accuracy, precision, and uncertainty.	Formal practices applied to verify the end-to-end model; all important errors satisfy requirements.	All key M&S outputs agree with data from the RWS operating in a representative environment.	All input data known & traced to sufficient referent. Significant input data has acceptable accuracy, precision, and uncertainty.	Uncertainty of results are provided quantitatively through propagation of all known uncertainty.	Sensitivities known for many parameters including many of the key sensitivities.	At most minor changes in model and at most minor differences in model use.	Controlled processes are applied; process compliance is measured.
2	Some data known & formally traceable with estimated uncertainties.	Documented practices applied to verify all model features; most important errors satisfy requirements.	Key M&S outputs agree with data from a sufficiently similar referent system.	Some input data known and formally traceable with estimated uncertainties.	Most sources of uncertainty identified, expressed quantitatively, and correctly classified. Propagation of the uncertainties is assessed.	Sensitivities known for a few parameters. Few or no key sensitivities identified.	At most moderate changes in model and at most moderate differences in model use.	Formal processes are applied.
1	Some data known and formally traceable.	Informal practices applied to verify some features of the model and assess errors.	Conceptual model addresses problem statement and agrees with available referents.	Some input data known and formally traceable.	Sources of uncertainty identified and qualitatively assessed.	Qualitative estimates only for sensitivities in M&S.	New model or major changes in model, or major differences in model use; but, model/changes/uses documented.	Informal processes are applied.
0	Insufficient evidence.	Insufficient evidence.	Insufficient evidence.	Insufficient evidence.	Insufficient evidence.	Insufficient evidence.	Insufficient evidence.	Insufficient evidence.

8.1 CASE SELECTION APPROACH

A critical component to validating a design is selection of critical cases. Because ATD responses are nonlinear and sensitive to complex loading kinematics, it is important to use models to adequately explore the range of expected dynamics and estimated ATD responses to determine the cases that elicit the greatest responses. An example approach to selecting the appropriate cases is shown in Figure 29. If an alternate approach is used, sufficient justification and documentation are required to meet the intent of this approach.

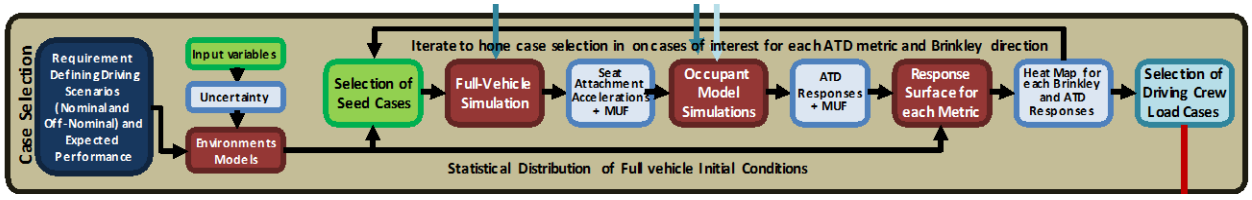

Figure 29. Case selection approach.

The first step of this process is guided by the vehicle level requirements levied on the design for nominal and off-nominal performance. Examples of vehicle level requirements are given in Table 36.

TABLE 36. EXAMPLE PERFORMANCE REQUIREMENTS

Condition		Statistical Level	Cases that must meet the IARVs	Probability of Occurrence
Nominal	No Fault	$\geq 3\sigma$	99.875%	98.9%
Off-Nominal	1 Fault	$\geq 2\sigma$	97.7%	1%
Contingency	2 or more Faults	$\geq 1\sigma$	84.1%	0.1%

In the example given above, assuming a distribution of 10,000 possible landings, a vehicle must have a nominal landing with no faults for more than 9,890 landings, off-nominal landings with 1 fault in less than 100 cases, and contingency landing cases with 2 or more faults in less than 10 cases.

Using all possible nominal (no fault) water landings as an example, 99.875% of these landings would need to pass the ATD IARVs and Brinkley Low criterion or 9,878 cases out of 9,890 landings. For off-nominal landings (e.g., loss of parachute), 98 of 100 landings would be required to pass, and for contingency landings (2 or more faults), 9 of the 10 cases would have to pass. Lower statistical performance levels are allowed for off-nominal and contingency scenarios because their probability of occurrence is much lower.

Using guidance and navigation control (GNC) models, Monte Carlo simulation distributions are generated for the given spacecraft design, expected environments, faults, and performance. From these distributions, nominal and off-nominal cases can be identified with initial conditions defining the state of the vehicle just before water impact. Full-vehicle-mathematical models can be used with these impact conditions to generate seat-specific accelerations and determine occupant response.

To assess spacecraft performance against the requirements listed in Table 36, injury predictions would need to be generated for all possible seated locations, crew sizes, and nominal, off-nominal, or contingency scenarios. We acknowledge that generating occupant-model responses across all locations, crew sizes, and scenarios would be computationally intensive and potentially cost and time prohibitive. Thus, alternate approaches to identifying driving cases, such as development of mathematical or response surfaces, may be utilized [142].

For example, an occupant model can be used to predict responses for a subset of selected cases (black dots in Figure 30). Using these results, a response surface can be created for each occupant response across the design space for a particular scenario (e.g., nominal landings). The ATD injury-metric responses and Brinkley response criterion values can be mapped to individual response surfaces. From these surfaces, high-injury-risk cases can be identified and utilized as the driving cases for selecting test cases for occupant-model development, model validation, and eventually flight certification. Final vehicle certification for Occupant Protection performance will require a similar approach to demonstrate statistical compliance against the requirements shown in Table 36.

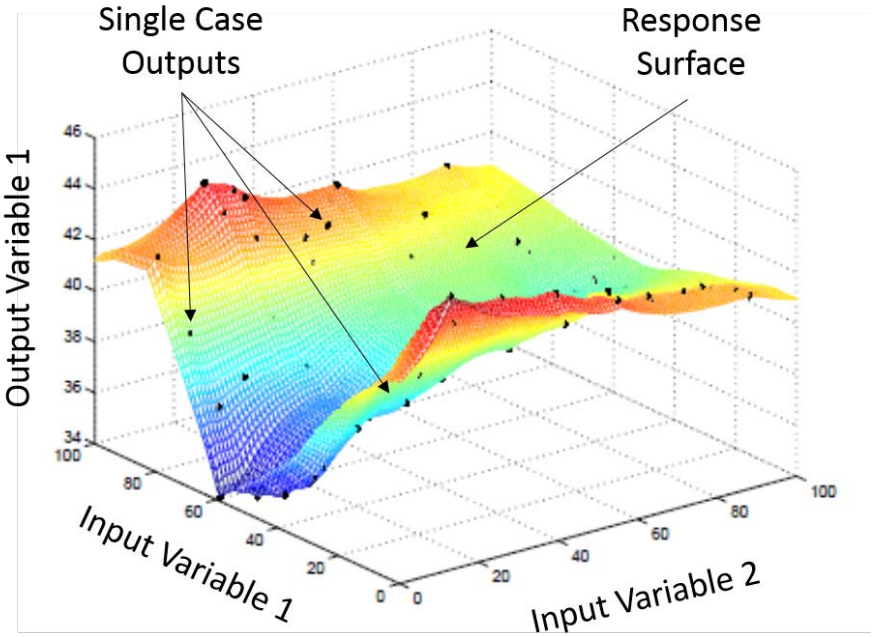

Figure 30. Example of Kriging response surface.

8.2 MODEL DEVELOPMENT APPROACH

Because the ATD models are not validated for spaceflight-like conditions and each spacecraft design has unique seat, restraint, and suit configurations, seat-level ATD testing is required to tune and calibrate each model component and their subsequent interfacing within the occupant model. Although ATD test case selection is driven from simulated driving crew load cases, some adjustments are made to most effectively tune and calibrate the seat, restraint, suit element and ATD model. Adjustments from crew load cases to ATD test cases for model development primarily include simplification to single axis-loading to extract specific model interaction effects (i.e., pure +Z loading to calibrate ATD pelvis to seat interaction and spinal response).

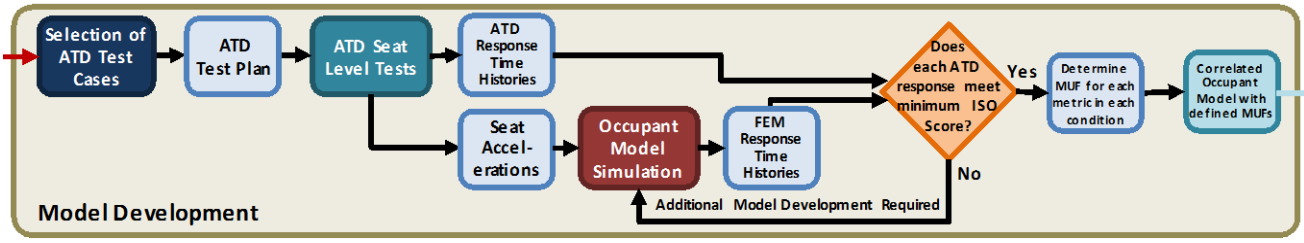

Figure 31. Model development approach.

A sufficient number of ATD tests encompassing selected driving load case conditions are required to cover the design space. Additional load cases are typically required to drive the ATD response to sufficiently exercise the kinematic response of the occupant model. For example rear impact conditions may not drive ATD-injury-metric responses, as neck motion in these cases is limited. Instead, additional frontal impact testing may be required to calibrate neck kinematics, even if these cases fall outside the expected loading conditions. When planning seat-level ATD testing the following criteria must be considered:

- Test repeatability (multiple tests for each condition)
- Crew orientation to impact vector
- Test cases that are sufficient to excite each ATD response near the associated IARV
- Unsuited cases for ATD model tuning, followed by suited cases to aid development of the suit element model

- Multiple peak accelerations and rise times to assess model frequency dependence
- Flight-like seat, suit elements, and restraints must be used
- Multiple ATD sizes must be tested that drive worst case seat and suit element fit

Experience has shown that a more robust seat-level testing campaign is beneficial to reducing the MUF associated with each ATD injury-response metric.

Initial conditions, including the ATD position in the seat and driving accelerations, measured during ATD testing are used to develop and drive occupant-model simulations. Occupant-model response predictions are evaluated against measured ATD and test setup instrumentation (i.e., seat and belt load cells) responses. Observed gross differences are used to initially tune the occupant model. After initial tuning, ATD model responses associated with each injury metric should be evaluated with a quantitative screening method, such as ISO-TR 16250, to determine acceptability before proceeding to assessing MUFs [143]. Because the phase, shape, and magnitude of each response may affect predicted ATD IARVs, a minimum signal correlation threshold is required for acceptability. This threshold should be selected based on the vehicle design, IARV margin, and other considerations. If the acceptability threshold is not met, additional model tuning and calibration is required.

For each ATD model response that meets the established acceptability threshold, a MUF is calculated based on the ratio between the model and test response magnitudes. The MUF calculated for a specific model response may be dependent on load conditions (i.e., G-level, direction of impact, and rise time), ATD type (i.e., small female or large male ATD), or suited versus unsuited. Thus, a statistically derived MUF for each model response as a function of these variables is recommended.

Using the verified occupant model with defined MUFs, driving load cases are resimulated to update the injury-metric-response surfaces and injury-risk heat map with improved results (see Section 8.1). Driving crew load cases, now selected with higher model confidence, are used to select full-vehicle test cases for model validation.

8.3 MODEL VALIDATION APPROACH

To validate the occupant model, full-vehicle testing is needed to replicate the multi-axial loading conditions not reproducible in uni-axial sled testing. The test cases are selected from the updated injury-metric-response surface. At least one driving case should be selected to test each ATD IARV risk scenario in the full-vehicle test. In situations where one test case exercises multiple ATD injury metrics, it is acceptable to conduct a single test to cover the IARV risk. These tests must be conducted with flight-like initial conditions, seat, suit and restraints and should include all applicable ATD sizes.

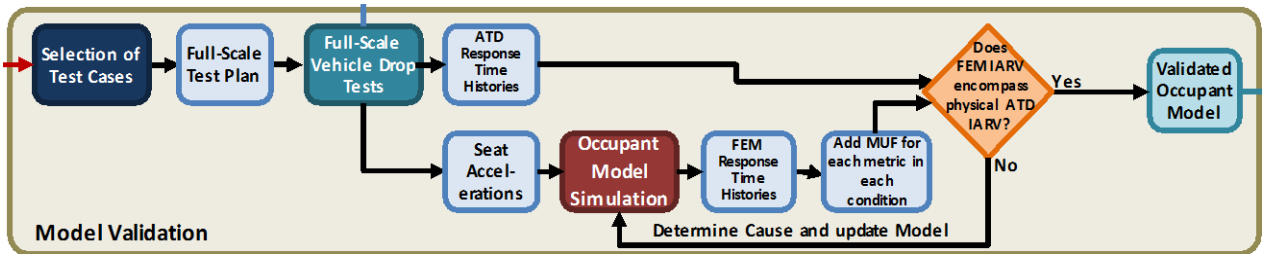

Figure 32. Model validation approach.

Upon completion of the full-vehicle testing, the physical ATD responses should be compared to simulation predictions made by the verified occupant model developed during the model development step and driven by the measured vehicle-seat accelerations. If the models (with associated MUFs) adequately predict the full-vehicle test results, then the model can be considered validated. If the ATD model with MUFs does not adequately predict the physical ATD responses, increased MUFs or additional model tuning and calibration may be needed to address the shortcomings. This model tuning may require additional sled testing to verify modeling gaps not previously addressed. Once the occupant model is acceptable and validated, the final ATD-analysis cycle can be conducted to show design

compliance. In addition to the possible updates to the occupant model, updates to the full-vehicle model may be made based on the full-scale vehicle testing. If model improvements are made during the validation effort, the resultant full-vehicle model and occupant model is used to develop a final set of injury-response surfaces. The resulting IARV and Brinkley response surfaces are then used to select the final bounding crew load cases for vehicle certification.

8.4 DESIGN COMPLIANCE APPROACH

Physical ATD IARV requirement-verification testing, probabilistic design-space analysis, and human subject testing are used in combination to ensure the vehicle both meets all occupant protection certification requirements, and sources of compliance in error are identified and mitigated.

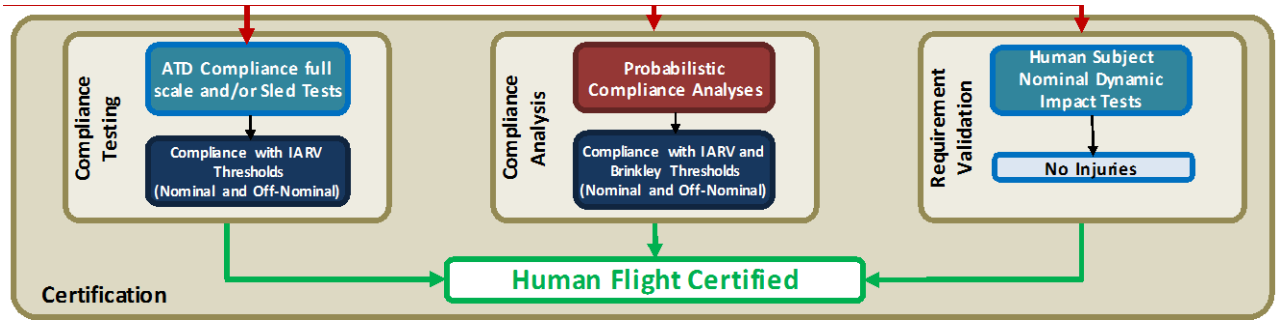

Figure 33. Design compliance approach.

8.4.1 Design Compliance Testing

The ATD IARV requirement verification is performed through physical ATD testing of high-risk design cases, selected from the injury-risk heat map, at or closest to the vehicle specific probability of occurrence boundary. These cases are chosen with the assumption that they adequately bound the injury-risk design space. This assumption is strengthened through confidence in the computational analysis performed with the validated occupant model. Tests are performed with final vehicle design components to show design compliance. Depending on conditions selected, and confidence in transferring the vehicle kinematics to a single-seat environment, ATDs situated in the seat or full vehicle testing may be required. Measured ATD injury response must pass defined IARV metrics to verify the design-risk boundary is adequately covered for human spaceflight certification.

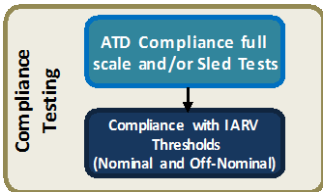

Figure 34. Compliance testing approach.

8.4.2 Design Compliance Analysis

Design compliance analysis is performed to verify the probabilistic vehicle requirements for occupant protection. The vehicle specific nominal and off-nominal injury-risk performance requirements are evaluated against the heat map developed for Brinkley and ATD calculated injury risk. The heat map is divided into the nominal and off-nominal condition sectors from which the initial analysis was derived. The probability of injury within each sector, as determined from IARV and Brinkley limits, is then calculated. The probability of injury for both nominal and off-nominal cases must be below those defined in the injury-risk performance requirements for the vehicle to be human certified.

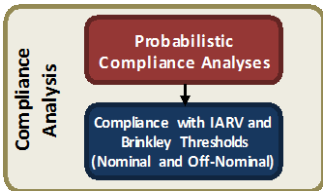

Figure 35. Compliance analysis approach.

8.4.3 Human Volunteer Testing Requirement Verification

All methods for human surrogate testing and analysis have some level of uncertainty associated with their validity in providing an accurate prediction of human response. It is vital to conduct volunteer testing at predicted sub-injurious levels for nominal landing conditions before manned flight, to ensure no injury mechanisms have been missed in the surrogate-model assumptions. After all of the required testing and analysis have been conducted, a final validation with volunteer subjects conducted on a horizontal sled and/or vertical drop tower are required to certify a design. Because the test protocol will be design specific, this section is intended as a general overview of the protocol that must be employed; however, details of the specific testing will vary as necessary. These tests are intended to be NASA-performed validation testing, as levying such requirements without specific insight into the design could be very difficult and burdensome. Although these tests are intended as a final validation of a design, they are critical for assuring the safety of the occupant protection systems. Without such tests, human testing of the system will occur during actual flight operations, where medical assistance and rescue may not be immediately available.

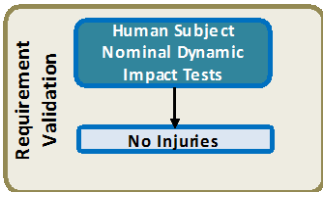

Figure 36. Requirement verification approach.

8.4.3.1 Safety Review

All testing must meet the requirements of the U.S. Code of Federal Regulations Title 14, Part 1230, Protection of Human Subjects, [144]. All test protocols must be reviewed and approved by an appropriate Institutional Review Board (IRB) and must pass a facilities readiness review and test readiness review per JPR 1700.1, JSC Safety and Health Handbook [145]. The IRB evaluates the risk-benefit ratio of the testing to determine whether the risk to the human subjects is justified. All efforts must be made to minimize the risk to the humans during testing. Because of this necessity, only nominal landing loads will be tested.

8.4.3.2 Subject Selection

Subjects must be selected such that they represent the complete range of astronaut population for the specific vehicle program being evaluated. Each vehicle may have different astronaut demographics depending on the nature of the mission. For example, a human Mars mission may include only older astronauts due to the radiation risks. Because older occupants may be at a greater risk of injury, an older subject population would be required for the volunteer testing. Another example may be an asteroid mission, where all of the crewmembers would be required to perform extravehicular activities (EVA). The constraints of the suit would limit the possible anthropometric range for such a mission, so human testing may only need to include a subset of the entire astronaut population's anthropometry.

The number of subjects is also critical for determining the appropriate level of confidence. Based on the risk acceptance of the Program, the number of subjects may range from 10 (low confidence) to 45 subjects (90% confidence that true risk of injury is less than 5%).

In addition to the subject-inclusion criteria stated above, subjects must meet the fitness-for-duty standards specified in NASA-STD-3001, Volume I, Space Flight Human-System Standard, Volume 1: Crew Health [110]. Several exclusion criteria will also be applied to the subject selection process. The following exclusion criteria (Table 37) are imposed as an additional level of safety for the subject as well as to ensure the subject population is similar to the Astronaut Corps.

TABLE 37. SAMPLE SUBJECT EXCLUSION CRITERIA

Subject Exclusion Criteria
Clinically Significant Musculoskeletal Injury
Clinically Significant Degenerative Spinal Condition
Clinically Significant Osteopenia

8.4.3.3 Test Equipment

Testing must consist of all applicable human interfaces including the seat, footrest, restraints, and suit in a flight- or flight-like configuration. In cases where other internal cabin structures are nearby and may interact with the human, they also must be simulated in the testing.

8.4.3.4 Test Protocol

All tests must be conducted based on verified landing loads analysis and test data. Ideally, tests of the maximum nominal loads allowed by the IRB would be desired; however, depending on the particular configuration and landing loads, other loads may be chosen for testing. All possible nominal-landing-load orientations should be considered for testing, but may be constrained due to the total number of tests. Whichever test cases are chosen, testing must begin at low levels and proceed up to the nominal load. The number of increments will be dependent on the nominal loads and the requirements imposed by the IRB to ensure subject safety. Each step to the next higher loading will only be allowed with medical monitor approval.

8.4.3.5 Data Collection

Sled and seat accelerometers to verify sled acceleration peak, rise time, and pulse duration are appropriate for comparison to expected landing loads. Discomfort scale questionnaires must be completed before and after testing. In addition, chest, head, and T1 acceleration should be collected to assess occupant kinematics and dynamics.

8.4.3.6 Acceptance Criteria

Based on a medical assessment of each subject post-test, no injuries occur during any test. A sample decision tree for determining an injury is shown in Figure 37, with definitions given in Table 38.

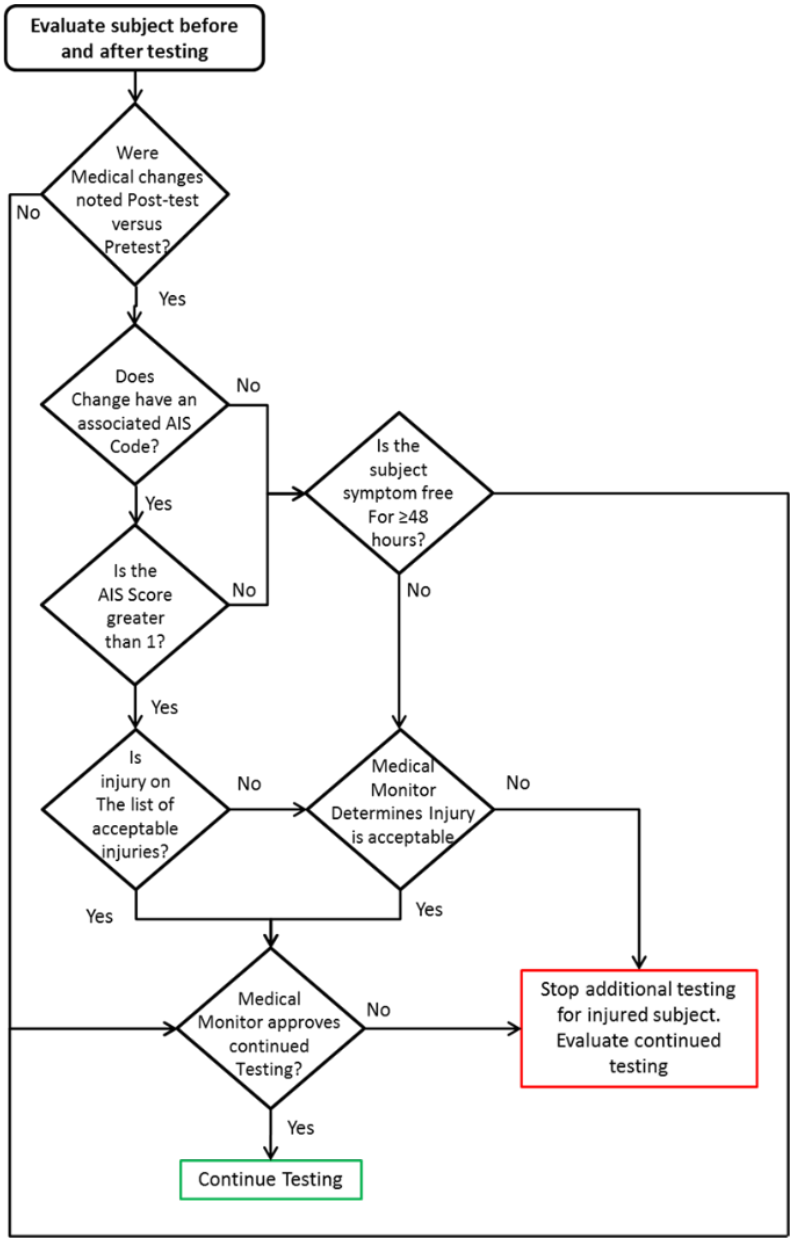

Figure 37. Example injury determination process.

TABLE 38. EXAMPLE DEFINITION OF ACCEPTABLE INJURIES

AIS=1, Acceptable Injury
Headache
Abrasion
Minor Superficial Laceration
Superficial Avulsion
Minor Superficial Penetration Injury
Hematoma
Dizzy
Tinnitus
Minor Musculoskeletal Strain

8.5 ADVERSE OUTCOMES

Any adverse outcome must be reported to the appropriate IRB before continuing any testing. Major injuries must be reported and approval to resume tests must be obtained before further tests can be conducted. A sample decision tree is shown in Figure 38. Adverse outcomes must be included in the final testing report.

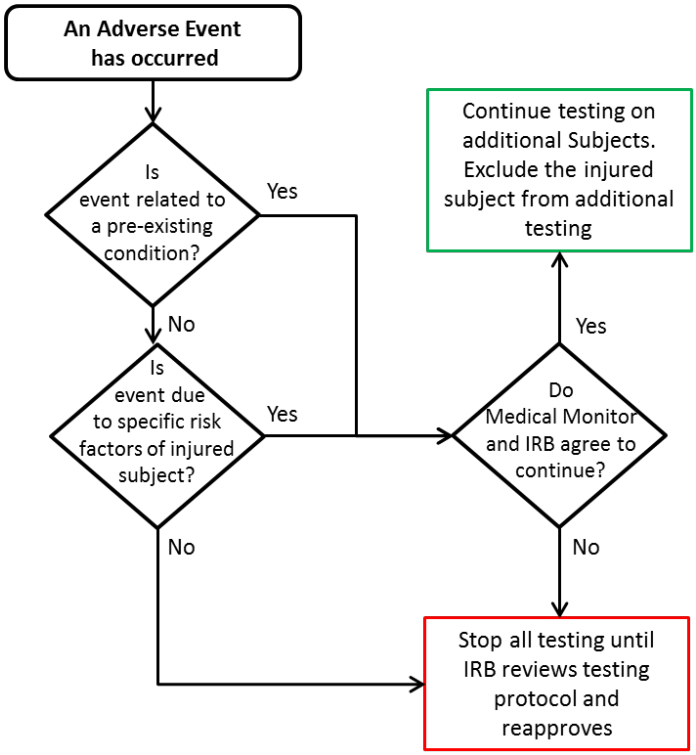

Figure 38. Sample decision tree for continuing testing after an adverse event.

9.0 FORWARD WORK

Although the revised requirements proposed in this document mitigate the risk of injury to crewmembers, there are still considerable limitations to this approach.

First, the BDRC as used today has several limitations for NASA's use. The +X axis model was developed with limited data in regard to the model parameters and the injury risk limits. Because this is expected to be the primary landing load direction, additional work is needed to either revise the model and injury limits, or use more recent developments in the automotive and military injury biomechanics fields to replace the model. The Y axis model has similar limitations. Very few data were used to develop the model and determine the injury levels. Given this limited amount of data, the model would likely not have a high CAS score per NASA-STD-7009A [141]. Although each program or Technical Authority must define the acceptable CAS for a given model, it is anticipated that the decision

consequence for the BDRC would be either a Class I (Catastrophic) or a Class II (Critical), and the results influence would be a 5 (controlling), requiring the model be evaluated using the standard. This work should be conducted to assign a CAS to the BDRC.

As discussed previously, sex differences are of concern because the model was developed with primarily male subjects. Even with the supplemental ATD tests specified, there remains some uncertainty that the proposed requirements offer the appropriate level of protection for returning crewmembers. Age and anthropometry are also areas of further investigation needed to understand how these factors relate to the risk of injury in the orientations expected for future vehicles.

While the Hybrid III Automotive ATD is widely used and readily available and high-fidelity numerical models are available, there are limitations associated with its design. Most notably, the Hybrid III is not intended for lateral testing. Even though the neck is capable of measuring lateral bending moments, it is not biofidelic. In addition, the chest was designed primarily for steering wheel hub interaction and is very stiff compared to humans.

Finally deconditioning due to long-duration spaceflight is a unique challenge that is not directly addressed by any of the methods described here. Because spaceflight deconditioning has the potential to reduce impact tolerance significantly, this area requires further study. In addition, current on-orbit countermeasures have shown promise for mitigating the effects of deconditioning in other areas, so further investigation of the effect on injury biomechanics is needed.

Given sufficient research in these areas, volunteer testing may not be required in the future, which would be a significant benefit to the vehicle programs.

10.0 CONCLUSION

Given the current state of knowledge in the injury biomechanics field, the requirements set out in this document are the best attempt to reduce the risk of injury to future NASA crewmembers. Although not all of the risk is mitigated as discussed above, these requirements represent the best available requirements for protection of crewmembers in future vehicles and at the same time are achievable by spacecraft designers.

Acknowledgements

This work was funded by the NASA Human Research Program, Johnson Space Center (JSC) Health and Human Performance Directorate, and the JSC Engineering Directorate. Portions of the work were performed under the Bioastronautics Contract (NAS9-02078). In addition the authors would like especially thank the NASA Engineering and Safety Center and outside experts for their thorough review of the proposed requirements.

11.0 REFERENCES

[1] C. M. Madsen, "X-38 Parafoil Landing Impact Analysis using Brinkley Dynamic Response Model (EG-DIV-13-34)," NASA Johnson Space Center, Houston, TX, 2013.

[2] NPO Energia, "Report: Supplementary Data on Safety Analysis of Soyuz TM/ACRV Landing by Brinkley Model - Stage CR, Phase B (Document Number C2.1-NPO"E"-001/40061, NASA Contract No. NASW-4727, AP #887)," 1993.

[3] RSC Energia, "Interim Report on Modified Soyuz TMA Descent Vehicle Drop Test Results (Document Number NAS15-10110/CTMA-009-0, NASA Contract No. NAS15, RPO #4181)," 1999.

[4] RSC Energia, "Interim Report on Modified Soyuz TMA Descent Module Airborne Test Results (Document Number NAS15-10110/CTMA-010-0, NASA Contract No. NAS15, RPO #4185)," 1999.

[5] RSC Energia, "Report on Crew Impact Effects During Soyuz TMA Spacecraft Landing by its Test Results (Document Number NAS15-10110/CTMA-014-0, NASA Contract No. NAS15, RPO #3736)," 2000.

[6] RSC Energia, "Report by Results of Statistical Calculations and Analysis of Crew Safety During Soyuz TMA Landing (Document Number NAS15-10110/CTMA-015-0, NASA Contract No. NAS15, EDMS #312017)," 2001.

[7] J. P. Stapp, "Human Exposures to Linear Acceleration: Part II. The Forward-Facing Position and Development of a Crash Harness," Wright-Patterson Air Force Base, Dayton, Ohio AF Technical Report 5912, 1947.

[8] J. P. Stapp, "Human Exposures to Linear Acceleration: Part I. Preliminary Survey of Aft-Facing Seated Position," AF Technical Report 5915, 1949.

[9] H. R. Savely, W. H. Ames, and H. M. Sweeney, "Laboratory tests of catapult ejection seat using human subjects," *ASTIA ATI,* p. 119947, 1946.

[10] R. Shaw, "Human Tolerance to Negative Acceleration of Short Duration," *Journal of Aviation Medicine,* vol. 19, p. 39, 1948.

[11] Air Research and Development Command, "Handbook of Instructions for Aircraft Designers (HIAD) (ARDVM 80-1)," Air Research and Development Command, Wright-Patterson Air Force Base, Ohio, 1960.

[12] M. Eiband, "Human Tolerance to Rapidly Applied Accelerations: A Summary of the Literature," National Aeronautics and Space Administration, Washington, DC, 1959.

[13] J. Baker, *The History of Manned Space Flight*. New York: Crown Publishers, 1982.

[14] G. Holcomb, "Human Experiments to Determine Human Tolerance to Landing Impact in Capsule Systems," in *Ballistic Missile and Space Technology*. vol. I, D. LeGalley, Ed., ed New York, New York: Academic Press, 1960.

[15] R. Headley, J. Brinkley, G. Lokatos, and R. Managan, "Human Factors Responses During Ground Impact," *Aerospace Medicine,* vol. 33, pp. 141-46, 1962.

[16] R. Headley, J. Brinkley, G. Lokatos, and R. Managan, "Human Factors Responses During Ground Impact," Wright-Patterson Air Force Base, WADD Technical Report 60-590, 1960.

[17] M. Kornhauser, "Impact Protection for the Human Structure," in *Advances in Astronautical Sciences,* ed New York: Plenum, pp. Paper 3, Vol. 3, 1958.

[18] J. Brinkley, "Man Protection During Landing Impact of Aerospace Vehicles," in *Ballistic Missile and Space Technology*. vol. I, D. LeGalley, Ed., ed New York, NY: Academic Press, 1960.

[19] J. Brinkley, R. Headley, and K. Kaiser, "Abrupt Accelerations of Human Subjects in the Semi-Supine Position," in *Proceedings of the Symposium on Biomechanics of Body Restraint and Head Protection*, Naval Air Material Center, Aircrew Equipment Laboratory, 1961.

[20] P. Payne, "The Dynamics of Human Restraint Systems," in *Impact Acceleration Stress. Proceedings of the National Academy of Sciences - National Research Council Publication 977*, 1961.

[21] D. Goldman and H. von Gierke, "Effects of Shock and Vibration on Man," in *Shock and Vibration Handbook*. vol. 3, ed New York, NY: McGraw-Hill, pp. 9-19, 1961.

[22] P. Payne, "Personal Restraint and Supprt System Dynamics," Wright-Patterson Air Force Base, Dayton, OH AAMRL-TR-65-127, 1965.

[23] E. L. Stech and P. R. Payne, "Dynamic Models of the Human Body," Wright-Patterson Air Force Base, Dayton, OH, AAMRL-TR-66-157, 1966.

[24] E. Beeding and J. Mosley, "Human Deceleration Tests," AFMDC-TR-60-2, Holloman Air Force Base, New Mexico, 1960.

[25] E. L. Beeding, "Daisy Track Tests: 520-707 (13 July 1959 - 13 April 1960). MDW Test Report No. 60-4," Air Force Missile Development Center, Holloman AFB, NM, 1960.

[26] E. Weis, N. Clarke, and J. Brinkley, "Human Response to Several Impact Acceleration Orientations and Patterns," *Aerospace Medicine,* vol. 34, pp. 1122-1129, 1963.

[27] M. Schulman, G. Critz, F. Highly, and E. Hendler, "Determination of Human Tolerance to Negative Impact Acceleration," NAEC-ACEL-510, Philadelphia, PA, 1963.

[28] J. P. Stapp and E. R. Taylor, "Space Cabin Landing Vector Effects on Human Physiology," *Aerospace Medicine,* vol. 35, pp. 1117-1132, 1964.

[29] W. Brown, J. Rothstein, and P. Foster, "Human Response to Predicted Apollo Landing Impacts in Selected Body Orientations," *Aerospace Medicine,* vol. 37, pp. 394-398, 1966.

[30] A. Zaborowski, "Lateral Impact Studies: Lap Belt Shoulder Harness Investigations," in *9th Stapp Car Crash Conference, Society of Automotive Engineers*, Warrendale, PA, pp. 93-1227, 1966.

[31] H. W. Klopfstein, "Compression Fracture of the Seventh Thoraic Vertebrae Caused by Experimental Impact: A Case Report," in *40th Annual Meeting, Aerospace Medical Association*, San Francisco, 1969.

[32] J. Brinkley, "Personal Communication," 2010.

[33] B. F. Hearon, J. W. Brinkley, R. Luciani, and H. E. von Gierke, "F/FB 111 Ejection Experience (1967-1980) – Part I: Evaluation and Recommendations (AFAMRL-TR-66-113)," Air Force Research Laboratory, 1981.

[34] J. Brinkley, "Development of Aerospace Escape Systems," *Air University Review,* vol. XIX, pp. 34-49, 1968.

[35] J. Brinkley and J. Schaffer, "Dynamic Simulation Techniques for the Design of Escape Systems: Current Applications and Future Air Force Requirements," AMRL-TR-71-29, Wright-Patterson Air Force Base, Dayton, OH, 1971.

[36] G. C. Mohr, J. W. Brinkley, L. E. Kazarian, and W. W. Millard, "Variations of Spinal Alignment in Egress Systems and Their Effect," *Aerosp.Med.*, vol. 40, pp. 983-988, 1969.

[37] R. J. Baumann, J. W. Brinkley, and A. Brandau, "Back Injuries Experienced During Ejection Seat Testing, AMRL-TR-68-82," Aerospace Medical Research Laboratory, Wright-Patterson Air Force Base, Ohio, 1968.

[38] J. Brinkley and J. Rock, "Advanced Concepts and Biotechnology for Future Escape Systems," in *Medical Service Digest*. vol. XXXIV, ed, 1983.

[39] J. Brinkley, "Personnel Protection Concepts for Advanced Escape System Design," in *Human Factors Considerations in High Performance Aircraft*, 1984.

[40] J. W. Brinkley, "Acceleration Exposure Limits for Escape System Advanced Development," *SAFE Journal*, vol. 15, pp. 10-16, 1985.

[41] J. Brinkley, L. J. Specker, and S. Mosher, "Development of Acceleration Exposure Limits for Advanced Escape Systems," in *Implications of Advanced Technologies for Air and Spacecraft Escape, NATO AGARD Proceedings*, 1990.

[42] Air Force Research Laboratory. (2012, 6/1/2012). *Collaborative Biomechanics Data Network*. Available: http://www.biodyn1.wpafb.af.mil/

[43] J. W. Brinkley, S. Johnston, C. Cerimele, J. A. Jones, and J. McMichael, "Informational Briefing: Crew Exploratory Vehicle Project Control Board," ed. Houston, TX: NASA Johnson Space Center, 2008.

[44] J. Buhrman and C. Perry, "Brinkley Dynamic Response Model Parameters," J. Somers, Ed., ed, 2013.

[45] J. Brinkley, J. Raddin, B. Hearon, L. McGowan, and J. Powers, "Evaluation of a Proposed, Modified F/FB-111 Crew Seat and Restraint System," AFAMRL-TR-80-52, Wright-Patterson Air Force Base, Dayton, OH, 1981.

[46] R. R. Coermann, "The Mechanical Impedance of the Human Body in Sitting and Standing Positions at Low Frequencies," Aerospace Medical Laboratory, Wright-Patterson Air Force Base, OH, 1961.

[47] A. J. Yorra, "The Investigation of the Structural Behavior of the Intervetebral Disc," Master's Thesis, Massachusetts Institute of Technology, Cambridge, MA, 1956.

[48] S. Ruff, "Brief Acceleration: Less than One Second," in *German Aviation Medicine in World War II*. vol. I, ed: Department of the Air Force, 1950.

[49] O. Perey, "Fracture of the Vertebral End-Plate in the Lumbar Spine," *An Experimental Biomechanical Investigation, Acta orthod Scand., Supp. 25*, 1957.

[50] J. Buhrman and S. Mosher, "A Comparison of Male and Female Acceleration Responses During Laboratory +Gz Impact Tests,," in *Proceedings of the 37th Annual SAFE Symposium*, Altanta, GA, 1999.

[51] Department of Defense, "Military Specification: General Specification for Aircraft Upward Ejection Seat System," vol. MIL-STD-9479B, ed. Wright-Patterson Air Force Base, OH: US Air Force, 1971.

[52] National Aeronautics and Space Administration, "NASA Space Flight Human-System Standard," in *Volume 2: Human Factors, Habitability, and Environmental Health* vol. NASA-STD-3001 Volume 2, ed. Washington, D.C., 2011.

[53] SAE International, "Restraint Systems for Civil Aircraft," vol. AS-8043B, ed. Warrendale, PA, 2008.

[54] SFI Foundation Inc., "Driver Restraint Assemblies," vol. SFI Specification 16.1, ed. Poway, CA, 2006.

[55] Department of Defense, "Seat System: Crash-Resistant, Non-Ejection, Aircrew, General Specifications," vol. MIL-S-58095A, ed, 1986.

[56] H. J. Asbun, H. Irani, E. J. Roe, and J. H. Bloch, "Intra-Abdominal Seatbelt Injury," *J Trauma,* vol. 30, pp. 189-93, Feb 1990.

[57] T. B. Sato, "Effects of seat belts and injuries resulting from improper use," *J Trauma,* vol. 27, pp. 754-8, 1987.

[58] SFI Foundation Inc., "Seatbelt Installation Guide for Upright Seating," Poway, CA, 2012.

[59] R. DeWeese, D. Moorcroft, T. Green, and M. Philippens, "Assessment of Injury Potential in Aircraft Side-Facing Seats Using the ES-2 Anthropomorphic Test Dummy," DOT/FAA/AM-07/13, Federal Aviation Administration, Washington, DC, 2007.

[60] Federal Aviation Administration, "Shoulder Harness - Safety Belt Installations (FAA Advisory Circular 21-34)," ed, 1993.

[61] R. Bandstra, U. Meissner, C. Warner, S. Monoghan, R. Mendelsohn, and D. MacPherson, "Seat-Belt Injuries in Medical and Statistical Perspectives," in *Proceedings of the 16th International Enhanced Safety of Vehicles Conference (98-S6-W-25).* Windsor, Ontario, 1998.

[62] National Aeronautics and Space Administration, "Orion Multi Purpose Crew Vehicle Program: Human-Systems Integration Requirements," Johnson Space Center, Houston, TX, 2012.

[63] B. Hearon and J. Brinkley, "Comparison of Human Response in Restraint Systems With and Without a Negative G Strap," *Aviation, Space, and Environmental Medicine,* vol. 57, 1986.

[64] N. Clarke, E. Weis, J. Brinkley, and W. Temple, "Lateral Impact Tolerance Studies in Support of Apollo," AMRL Memo M-29 Wright-Patterson Air Force Base, Dayton, OH, 1963.

[65] D. G. Schall, "Non-ejection cervical spine fracture due to defensive aerial combat maneuvering in an RF-4C: a case report," *Aviat Space Environ Med,* vol. 54, pp. 1111-6, 1983.

[66] C. Perry, D. Bonetti, and J. Brinkley, "The Effect of Variable Seat Back Angles on Human Responses to +Gz Impact Accelerations," AL-TR-1991-0110, Wright-Patterson Air Force Base, 1991.

[67] C. L. Ewing and A. I. King, "Structural considerations of the human vertebral column under +Gz impact acceleration. NAMRL-1178," Naval Aerospace Medical Research Laboratory, Pensacola, FL, 1975.

[68] A. I. King and C. L. Ewing, "Mechanism of spinal injury due to caudocephalad acceleration," *Orthopedic Clinics of North America*, vol. 6, pp. 19-31, 1975.

[69] National Aeronautics and Space Administraion, "CEV System Requirements Specification Rev. E," P. Orion, Ed., ed. Houston, TX: National Aeronautics and Space Administration, 2015.

[70] C. Perry, "Impact Evaluation of a Proposed B-2 Seat Cushion," *SAFE Journal,* vol. 27, pp. 24-31, 1997.

[71] B. Hearon and J. Brinkley, "Effect of Seat Cushions on Human Response to +Gz Impact," *Aviation, Space and Environmental Medicine,* vol. 57, 1986.

[72] Z. Cheng and J. Pellettiere, "Evaluation of the Safety Performance of Ejection Seat Cushions," in *SAFE Symposium*, Salt Lake City, UT, 2004.

[73] K. Miller and L. Morelli, "Ejection Tower Evaluation of the Rate-Dependent Foam Cushions for the NACES Seat," Naval Air Systems Command, Department of the Navy, Washington, D. C. NAWCADWAR-93078-60, 1993.

[74] K. A. Danelson, J. H. Bolte, and J. D. Stitzel, "Assessing astronaut injury potential from suit connectors using a human body finite element model," *Aviat Space Environ Med*, vol. 82, pp. 79-86, Feb 2011.

[75] S. McFarland and M. Dub, "Suited Occupant Injury Potential During Dynamic Spacecraft Flight Phases (AIAA 2010-6230)," in *40th Internation Conference on Environmental Systems*, Barcelona, Spain, 2010.

[76] T. Radford, J. Hongliang, M. Parthasarathy, P. Kosarek, R. Watkins, and J. Santini, "Next Generation Space Suit Injury Assessment (AAIA 2011-5107)," in *Proceedings of the 41st International Conference on Environmental Systems*, Portland, OR, 2011.

[77] A. Nahum and J. Melvin, *Accidental Injury Biomechanics and Prevention*, Second Edition ed. New York: Springer Science and Business Media, 2002.

[78] American National Standards Institute, "American National Standard for Protective Headgear - for Motor Vehicular Users - Specifications," vol. Z90.1-1992, ed. New York, NY: American National Standards Institute, 1992.

[79] D. L. Belavy, G. Armbrecht, U. Gast, C. A. Richardson, J. A. Hides, and D. Felsenberg, "Countermeasures against lumbar spine deconditioning in prolonged bed rest: resistive exercise with and without whole body vibration," *J Appl Physiol*, vol. 109, pp. 1801-11, Dec 2010.

[80] L. Vico, P. Collet, A. Guignandon, M. Lafage, T. Thomas, M. Rehaillia, *et al.*, "Effects of Long-Term Microgravity Exposure on Cancellous and Cortical Weight-Bearing Bones of Cosmonauts," *Lancet*, vol. 355, pp. 1607-1611, 2000.

[81] A. LeBlanc, L. Shackelford, and V. Schneider, "Future Human Bone Research in Space," *Bone*, vol. 22, pp. 113S-116S, May 1998.

[82] J. H. Keyak, A. K. Koyama, A. LeBlanc, Y. Lu, and T. F. Lang, "Reduction in proximal femoral strength due to long-duration spaceflight," *Bone*, vol. 44, pp. 449-53, 2009.

[83] W. Thornton and J. Rummel, "Muscular deconditioning and its prevention in spaceflight," in *Biomedical Results of Skylab*. vol. NASA SP-377, R. S. Johnston and L. F. Deitlein, Eds., ed Washington, DC: NASA, pp. 191-197, 1977.

[84] T. Stein, "Nutrition and muscle loss in humans during spaceflight," *Adv Space Biol Med*, vol. 7, pp. 49-97, 1999.

[85] A. LeBlanc, C. Lin, L. Shackelford, V. Sinitsyn, H. Evans, O. Belichenko, *et al.*, "Muscle Volume, MRI relaxation times (T2), and body composiition after spaceflight," *J Appl Physiol*, vol. 89, pp. 2158-2164, 2000.

[86] M. Zhou, H. Klitgaard, B. Saltin, R. Roy, V. Edgerton, and P. Gollnick, "Myosin heavy chain isoforms of human muscle after short-term spaceflight," *J Appl Physiol*, vol. 78, pp. 1740-1744, 1995.

[87] V. Edgerton, M. Zhou, Y. Ohira, H. Klitgaard, B. Jinag, G. Bell, *et al.*, "Human Fiber Size and Enzymatic Properties After 5 and 11 Days of Spaceflight," *J Appl Physiol*, vol. 78, pp. 1733-1739, 1995.

[88] K. J. Hackney and L. L. Ploutz-Snyder, "Unilateral lower limb suspension: integrative physiological knowledge from the past 20 years (1991-2011)," *Eur J Appl Physiol,* vol. 112, pp. 9-22, Jan 2012.

[89] J. D. Sibonga, "Spaceflight-induced bone loss: is there an osteoporosis risk?," *Curr Osteoporos Rep,* vol. 11, pp. 92-8, Jun 2013.

[90] B. Lewandowski, E. Nelson, J. Myers, D. Griffin, and A. Licata, "Risk Assessment of Bone Fracture During Space Exploration Missions to the Moon and Mars," in *Space Systems Engineering and Risk Management Symposium*, Los Angeles, CA, 2008.

[91] T. Lang, A. LeBlanc, H. Evans, Y. Lu, H. Genant, and A. Yu, "Cortical and trabecular bone mineral loss from the spine and hip in long-duration spaceflight," *J.Bone Miner.Res.,* vol. 19, pp. 1006-1012, 2004.

[92] J. Buhrman, C. Perry, and S. Mosher, "A Comparision of Male and Female Acceleration Responses During Laboratory Frontal -Gx Axis Impact Tests," AFRL-HE-WP-TR-2001-0022, United States Air Force Research Laboratory, Wright-Patterson AFB, Dayton, OH, 2000.

[93] L. Evans and P. H. Garrish, "Gender and age difference on fatality risk from the same physical impat determined using two-car crashes," Society of Automotive Engineers, Warrendale, PA SAE 011174, 2004.

[94] L. Evans, "Female Compared with Male Fatality Risk from Similar Physical Impacts," *J Trauma,* vol. 50, pp. 281-88, 2001.

[95] R. Allnutt, "Gender Effects in Traumatic Injury," *SAFE Journal,* vol. 37, 2007.

[96] F. A. Pintar, N. Yoganandan, and L. Voo, "Effect of age and loading rate on human cervical spine injury threshold," *Spine (Phila Pa 1976),* vol. 23, pp. 1957-62, 1998.

[97] B. Stemper, N. Yoganandan, F. Pintar, D. Maiman, M. Meyer, D. J, *et al.*, "Anatomical Gender Differences in Cervical Vertebrae of Size-Matched Volunteers," *SPINE,* vol. 33, pp. 44-49, 2008.

[98] H. Gallagher, J. Buhrman, S. Mosher, C. Perry, and D. Wilson, "A Comparison of Cervical Stress and BMD as Related to Gender and Size During +Gz Acceleration," in *Proceedings of the 44th SAFE Symposium*, 2006.

[99] H. Gallagher, J. Buhrman, S. Mosher, C. Perry, and D. Wilson, "An Analysis of Vertebral Stress and BMD During +Gz Impact Accelerations," Wright-Patterson Air Force Base AFRL-HE-WP-TR-2007-0085, 2007.

[100] R. W. Nightingale, J. H. McElhaney, D. L. Camacho, M. Kleinberger, B. A. Winkelstein, and B. S. Myers, "The Dynamic Responses of the Cervical Spine: Buckling, End Conditions, and Tolerance in Compressive Impacts," Society of Automotive Engineers, Warrendale, PA 973344, 1997.

[101] R. W. Nightingale, B. A. Winkelstein, K. E. Knaub, W. J. Richardson, J. F. Luck, and B. S. Myers, "Comparative strengths and structural properties of the upper and lower cervical spine in flexion and extension," *J Biomech,* vol. 35, pp. 725-32, 2002.

[102] R. W. Nightingale, V. Carol Chancey, D. Ottaviano, J. F. Luck, L. Tran, M. Prange, *et al.*, "Flexion and extension structural properties and strengths for male cervical spine segments," *J Biomech,* vol. 40, pp. 535-42, 2007.

[103] C. Perry, J. Buhrman, E. Doczy, and S. Mosher, "The Effects of Variable Helmet Weight on Head Response and Neck Loading during Lateral +Gy Impact," in *Proceedings of the 41st Annual SAFE Symposium*, Jacksonville, FL, 2003.

[104] L. Mosekilde and L. Mosekilde, "Sex differences in age-related changes in vertebral body size, density and biomechanical competence in normal individuals," *Bone,* vol. 11, pp. 67-73, 1990.

[105] F. A. Pintar, N. Yoganandan, T. Myers, A. Elhagediab, and A. Sances, Jr., "Biomechanical properties of human lumbar spine ligaments," *J Biomech,* vol. 25, pp. 1351-6, 1992.

[106] D. Foust, D. Chaffin, R. Synyder, and J. DBaurn, "Cervical Range of Motion and Dynamic Response and Strength of Cervical Muscles," Society of Automotive Engineers International Journal 730975, 1973.

[107] E. N. Ebbesen, J. S. Thomsen, H. Beck-Nielsen, H. J. Nepper-Rasmussen, and L. Mosekilde, "Age- and gender-related differences in vertebral bone mass, density, and strength," *J Bone Miner Res,* vol. 14, pp. 1394-403, Aug 1999.

[108] K. Singer, S. Edmondston, R. Day, P. Breidahl, and R. Price, "Prediction of thoracic and lumbar vertebral body compressive strength: correlations with bone mineral density and vertebral region," *Bone,* vol. 17, pp. 167-74, 1995.

[109] C. E. Cann, H. K. Genant, F. O. Kolb, and B. Ettinger, "Quantitative computed tomography for prediction of vertebral fracture risk," *Bone,* vol. 6, pp. 1-7, 1985.

[110] National Aeronautics and Space Administration, "NASA Space Flight Human-System Standard," in *Volume I: Crew Health* vol. NASA-STD-3001 Volume 1, ed. Washington, D.C., 2007.

[111] SAE International, "Instrumentation for Impact Test - Part 1 - Electronic Instrumentation," Warrendale, PA J211/1, 2007.

[112] National Highway Traffic Administration, "Federal Motor Vehicle Safety Standards and Regulations.," Washington, DC, 2008.

[113] H. Mertz, "Injury Risk Assessments Based on Dummy Responses," in *Accidental Injury: Biomechanics and Prevention,* J. Melvin and A. Nahum, Eds., ed New York: Springer-Verlag, pp. 89-102, 2002.

[114] H. Mertz, "Anthropometric Test Devices," in *Accidental Injury: Biomechanics and Prevention*, A. Nahum and J. Melvin, Eds., ed New york: Springer-Verlag, pp. 72-88, 2002.

[115] H. J. Mertz and L. M. Patrick, "Strength and Response of the Human Neck (SAE Paper 710855)," *15th Stapp Car Crash Conference Proceedings,* 1971.

[116] L. M. Patrick and C. C. Chou, "Response of the Human Neck in Flexion, Extension and Lateral Flexion," VRI 7.3, 1976.

[117] M. Shea, R. H. Wittenberg, W. T. Edwards, A. A. White, 3rd, and W. C. Hayes, "In vitro hyperextension injuries in the human cadaveric cervical spine," *J Orthop Res,* vol. 10, pp. 911-6, 1992.

[118] N. Yoganandan, F. A. Pintar, D. J. Maiman, J. F. Cusick, A. Sances, Jr., and P. R. Walsh, "Human head-neck biomechanics under axial tension," *Med Eng Phys,* vol. 18, pp. 289-94, 1996.

[119] J. B. Lenox, A. K. Ommaya, M. Haffner, K. D. Carey, and H. W. Huntington, "Development of Neck Injury Tolerance Criteria in Human Surrogates. I. Static Tensile Loading in the Baboon Neck: Preliminary Observations," in *Ninth International Technical Conference on Experimental Safety Vehicles,* Washington, DC, pp. 279-286, 1984.

[120] P. Prasad and R. P. Daniel, "A biomechanical analysis of head, neck and torso injuries to child surrogates due to sudden torso acceleration," *Stapp Car Crash J,* vol. 28, 1984.

[121] K. D. Klinich, "NHTSA Child Injury Protection Team. Techniques for Developing Child Dummy Protection Reference Values. NHTSA Docket No. 74-14, Notice 97, Item 069.," National Highway Traffic Safety Administration, Washington, DC, 1996.

[122] M. Kleinberger, E. Sun, R. Eppinger, S. Kuppa, and R. Saul, "Development of Improved Injury Criteria for the Assessment of Advanced Automotive Restraint Systems," National Highway Traffic Safety Administration, Washington, DC, 1998.

[123] R. Eppinger, E. Sun, F. Bandak, M. Haffner, N. Khaewpong, M. Maltese, *et al.*, "Development of Improved Injury Criteria for the Assessment of Advanced Automotive Restraint Systems - II," National Highway Traffic Safety Administration, Washington, DC, 1999.

[124] R. Eppinger, E. Sun, S. Kuppa, and R. Saul, "Supplement: Development of Improved Injury Criteria for the Assessment of Advanced Automotive Restraint Systems - II," National Highway Traffic Safety Administration, 2000.

[125] J. P. Nichols, "Overview of Ejection Neck Injury Criteria," in *Proceedings of the 44th Annual Safe Symposium*, Reno, NV, pp. 159-171, 2006.

[126] A. Dibb, R. Nightingale, V. Chancey, L. Fronheiser, L. Tran, D. Ottaviano, *et al.*, "Comparative Structural Neck Responses of the THOR-NT, Hybrid III, and Human in Combined Tension-Bending and Pure Bending," *Stapp Car Crash Journal*, vol. 50, pp. 567-581, 2006.

[127] J. G. Paver, D. Friedman, G. Mattos, and J. Caplinger, "The Development of IARV's for the Hybrid III Neck Modified for Dynamic Rollover Crash Testing," in *Proceedings of the 7th International Crashworthiness Conference, ICRASH*, 2010.

[128] L. M. Patrick, H. R. Lissner, and E. S. Gurdjian, "Survival By Design - Head Protection," in *Proceedings of the 7th Stapp Car Crash Conference*, Springfield, IL, 1965.

[129] C. Gadd, "Use of Weighted Impulse Criterion for Estimating Injury Hazard," in *Proceeding of the 10th Stapp Car Crash Conference*, 1966.

[130] J. Versace, "A Review of the Severity Index," in *Proceedings of the 15th Stapp Car Crash Conference*, pp. 771-796, 1971.

[131] V. Hodgson, Thomas LM., "Effect of Long-Duration Impact on the Head," in *Proceedings of the 16th Stapp Car Crash Conference*, New York, pp. 292-295, 1972.

[132] J. Funk, S. Duma, S. Manoogian, and S. Rowson, "Biomechanical risk estimates for mild traumatic brain injury," *Annu Proc Assoc Adv Automot Med*, vol. 51, pp. 343-61, 2007.

[133] J. Funk, S. Rowson, R. Daniel, and S. Duma, "Validation of concussion risk curves for collegiate football players derived from HITS data," *Ann Biomed Eng*, vol. 40, pp. 79-89, 2012.

[134] J. Somers, J. Melvin, A. Tabiei, C. Lawrence, R. Ploutz-Snyder, B. Granderson, *et al.*, "Development of Head Injury Assessment Reference Values Based on NASA Injury Modeling," *Stapp Car Crash Journal*, vol. 55, pp. 49-74, 2011.

[135] Alliance of Automotive Manufacturers, "Proposal for dummy response limits for FMVSS 208 compliance testing. AAMA comments to docket 98-4405, notice 1.," 1998.

[136] E. J. Pellman, D. C. Viano, A. M. Tucker, I. R. Casson, and J. F. Waeckerle, "Concussion in professional football: reconstruction of game impacts and injuries," *Neurosurgery*, vol. 53, pp. 799-814, 2003.

[137] S. Rowson, S. M. Duma, J. G. Beckwith, J. J. Chu, R. M. Greenwald, J. J. Crisco, *et al.*, "Rotational head kinematics in football impacts: an injury risk function for concussion," *Ann Biomed Eng*, vol. 40, pp. 1-13, 2012.

[138] A. Mallory, R. Herriott, and H. Rhule, "Subdural Hematoma and Aging: Crash Characteristics and Associated Injuries (11-0399)," in *22nd International Technical Conference on the Enhanced Safety of Vehicles*, Washington, DC, 2011.

[139] A. Bolukbasi, J. Crocco, C. Clarke, E. Fasanella, K. Jackson, P. Keary, *et al.*, "Full Spectrum Crashworthiness Criteria for Rotorcraft," U.S. Army Research, Development and Engineering Command, Ft. Eustis, VA RDECOM TR 12-D-12, 2011.

[140] S. Desjardins, "Establishing Lumbar Injury Tolerance for Energy Absorbing Seats," in *American Helicopter Society Forum 64*, Montreal, Canada, 2008.

[141] National Aeronautics and Space Administration, "Standard for Models and Simulation," vol. NASA-STD-7009A, Ch 1, ed. Washington, D.C.: National Aeronautics and Space Administration, 2016.

[142] L. G. Horta, B. H. Mason, and K. H. Lyle, "A computational approach for probabilistic analysis of water impact simulations," *International Journal of Crashworthiness*, vol. 15, pp. 649-665, 2010.

[143] International Organization for Standardization, "Road Vehicles - Objective Rating Metrics for Dynamic Systems," ISO/TR 16250:2013, 2013.

[144] "Protection of Human Subjects," in *14 CFR 1230*, ed. United States of America: Code of Federal Regulations, 2013.

[145] National Aeronautics and Space Administraion, "JSC Safety and Health Handbook," in *Facility Readiness Review for Hazardous or Critical Facilities* vol. JPR 1700.1, ed. Houston, TX: Johnson Space Center, 2008.

[146] National Aeronautics and Space Administration, "NASA Defense Purchase Request T-9643(G)," 1962.

[147] E. Hershgold, "Roentgenographic Study of Human Subjects During Transverse Accelerations," *Aerospace Med*, vol. 31, p. 213, 1959.

[148] J. P. Stapp, "Personal Communication."

[149] F. Robinson, R. Hamlin, W. Wolfe, and R. Coermann, "Response of the Rhesus Monkey to Lateral Impact," *Aerospace Medicine*, vol. 34, pp. 56-62, 1963.

[150] E. Hixson, "Mechanical Impedance and Mobility," in *Shock and Vibration Handbook*. vol. I, C. Harris and C. Crede, Eds., ed New york: McGraw-Hill, 1961.

[151] National Aeronautics and Space Administraion, "Human Integration Design Handbook (HIDH)," Washington, D.C. NASA/SP-3020-3407/REV1, June 5, 2014.

APPENDIX A - SUMMARY OF OCCUPANT PROTECTION IMPACT TESTS CONDUCTED TO SUPPORT JOINT USAF AND NASA SPACECRAFT LANDING STUDIES

Addressing Complex Multi-directional Accelerations

Based upon survived accidents, experimental data from tests with volunteers, tests with animals [17], and theoretical work based on the laws of mechanics, AFRL laid out an initial plan to investigate the acceleration profiles with high rates of onset using experimental and analytical approaches. NASA joined this effort to investigate human tolerance to landing impact conditions with rates of onset higher than had previously been considered safe.

To begin to address this problem, Headley et al. [15, 16] and Brinkley et al. [18, 19] conducted experiments with volunteer subjects to explore the human responses to the complex waveforms associated with emergency escape capsule impact and the Project Mercury module launch abort landing impact. These experimental data demonstrated several relationships between the higher rates of acceleration onset, acceleration magnitude, and impact velocity change in the +Z- and +X-axes. During these experiments, Brinkley et al. [18] investigated the beneficial effects of an individually contoured body support constructed of fiberglass compared to a body support liner filled with plastic microballoons that could be formed to fit the occupant (Figure 39). Preliminary tests using dummies explored the safety of these body support and restraint systems. These tests included a net couch that had been demonstrated to be especially effective in protecting volunteers to sustained acceleration levels up to 16 G. The net couch proved to be unacceptable during impact tests. The elasticity of the couch caused amplification of the impact loads.

The individually contoured couch and the form-fitted liner proved equally effective in protecting the volunteers during impact tests [18]. Thirty-two impact tests were completed with volunteers at the time of Brinkley's report. The couches were designed to hold the subject's body in a semi-supine posture and were mounted on top of a wooden heat shield structure. The subject's unhelmeted head and torso were inclined at 12° from horizontal. The restraint system is shown in Figure 39. Dropping the test vehicle on compacted sand created the impact acceleration of the heat shield structure with vertical impact velocities ranging from 10 to 30 ft/s. The impact of the couches was attenuated by 8 inches of highly crushable aluminum honeycomb mounted under the couch. The impact accelerations were increased in increments up to a maximum of 36.5 G with rates of onset up to 11,200 G/s. Accelerations were measured on the subject's chest and forehead as well as on the couch and wooden heat shield. The highest acceleration measured on the subject was 54.5 G. There were no injuries reported as a result of these experiments. A few of the volunteers experienced brief headaches soon after the tests.

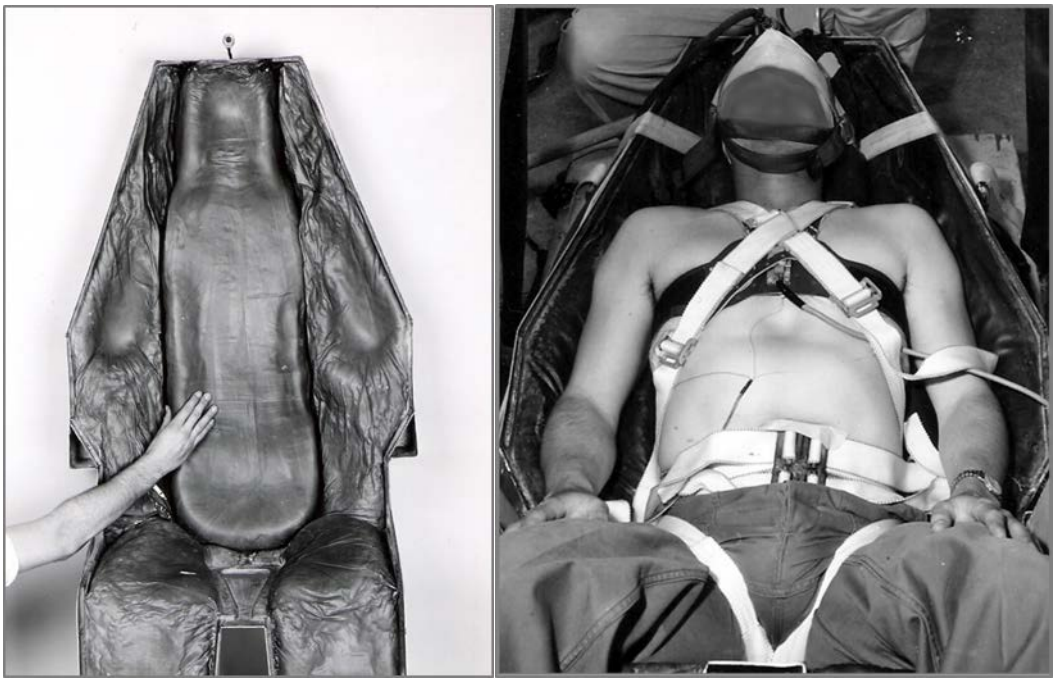

Figure 39. Photographs of a volunteer subject prepared for an impact test supported by couch with a form-fitting liner and a top view of the liner formed to fit the test subject. (Credit: USAF)

During this same period, Payne [20] used the extensive human and animal impact exposure data assembled by Eiband [12], and Goldman and von Gierke [21] to study the feasibility of developing simple, lumped-parameter dynamic models that might describe more adequately the human response and likelihood of injury based on the experimental data. Payne developed numerical models of restraint and support systems to show the effects of their mechanical properties on the human responses to complex acceleration profiles.

In 1962, NASA began to organize efforts to design the Apollo crew systems. One of the efforts included the development of a crew module landing impact system human tolerance criteria. Initially, crew protection system designers were forced to accept a maximum acceleration of 10 G and a rate of onset of 250 G/s as the limiting crew acceleration exposure criteria. A major analytical and experimental program was organized by the NASA Manned Spacecraft Center (later renamed the Johnson Space Center [JSC]) and was implemented by AFRL, the Naval Air Engineering Center, and the Armed Forces Institute of Pathology to identify potential critical modes of injury and likely adverse physiological responses, and to explore the effects of higher level multi-directional impacts "to assure astronaut functionality immediately after landing" [146].

The most immediate problem was to explore the human responses to sideward (Y-axis) impact. At that time, knowledge of human response to sideward acceleration was limited to the results of centrifuge experiments conducted by AFRL at sustained acceleration levels up to 10 G [147]. In a study using a centrifuge, Hershgold examined the displacement of the volunteer subjects' internal organs during steady-state acceleration. His radiographs showed extensive displacement of thoracic and abdominal viscera to the dependent side of the body under sustained accelerations as small as 6 G. This finding differed from previous studies by Stapp [148], in which he did not observe injuries to chimpanzees at calculated accelerations to 47 G with durations estimated to be 140 ms at the peak G level.

During this same time, impact tests of the B-58 encapsulated ejection seat were conducted with volunteer subjects by Holcomb [14]. The capsule was dropped with vertical velocities to 27 ft/s. The capsule landed on its back bulkhead with its occupant in a semi-supine position. The tests were conducted without detectable injury. During tests not reported in this article, the capsule was impacted with horizontal velocities to 34 ft/s. An undetermined amount of energy was dissipated in tumbling

and skidding of the capsule, making use and extrapolation of these data difficult. However, these tests demonstrated the tolerance to sideward impact was probably higher than the 10 G that had been investigated under steady-state acceleration of 10 G by Hershgold [147].

In preparation for a joint agreement with NASA to study the feasibility of higher impact exposure limits, Robinson et al. [149] conducted impact tests with Rhesus monkeys with sideward impacts to 75 G at terminal velocities to 32 ft/s, with and without contoured body support systems. No post-mortem injuries were observed. Electrocardiographic evidence of transient abnormalities in conduction and rhythm were found following higher-level accelerations and impact velocities. Radiographs taken before and after the impacts showed an increase in the total heart shadow on the dependent side of the midline. Sequential radiographs revealed that the heart returned to normal within 3 hours after impact.

Under the agreement between NASA and the DoD, Schulman et al. [27], explored the effects of downward acceleration (–Z-axis) to 18.5 G with rates of onset to 1,540 G/s. This research supplemented and extended USAF research that had been conducted with animals and volunteers to define criteria for downward ejection seats [10].

AFRL conducted impact tests to investigate the dynamic responses of military volunteers using a vertical deceleration tower. Acceleration, forces, physiological reactions, and subjective responses of volunteers were measured for sideward (Y-axis) impacts ranging to 21.5 G with rates of onset to 1,350 G/s and impact velocities to 25.5 ft/s [64]. An individually fitted, semi-rigid body support was used with torso and extremity restraints. The subjects in these tests wore a Mercury pressure-suit helmet weighing 2.7 kg. Plastic foam (0.5-inch thick pads were placed behind the helmet earphones and across the chin bar. The helmet was prevented from pitching motion, but not vertical motion by a 1.75-inch strap. The helmet microphone was removed. The impacts were tolerated by the male volunteer subjects.

A second series of impact tests jointly sponsored by the USAF and NASA were conducted to study the effects of seven impact vector directions and six acceleration profiles ranging in acceleration from 3 to 26 G, impact velocities ranging from 5 to 28 ft/s, and onsets ranging from 200 to 2,000 G/s. The seven seat orientations including forward, upward, and sideward (right and left) acceleration components in 45-degree increments were used on a vertical deceleration tower. A drawing of the orientations, designated as vectors A through G, is shown in Figure 40 [26]. Force, acceleration, and physiological data were collected and analyzed. The volunteers were contained by an experimental restraint system and supported by a flat seat and seat back, and side panels to support the pressure-suit helmet, shoulders, and upper legs. The previously used liner filled with small beads was not used in this second series of tests. The subjects needed assistance to ensure that the liner was adequately formed about their bodies and they were more confident in the support provided by a rigid seat. A test subject is shown restrained within the multi-directional impact test vehicle in Figure 41. The seat and its frame are attached to the AFRL vertical deceleration tower by rods that are instrumented with force measurement cells (see Figure 41). The restraint system is shown in Figure 42.

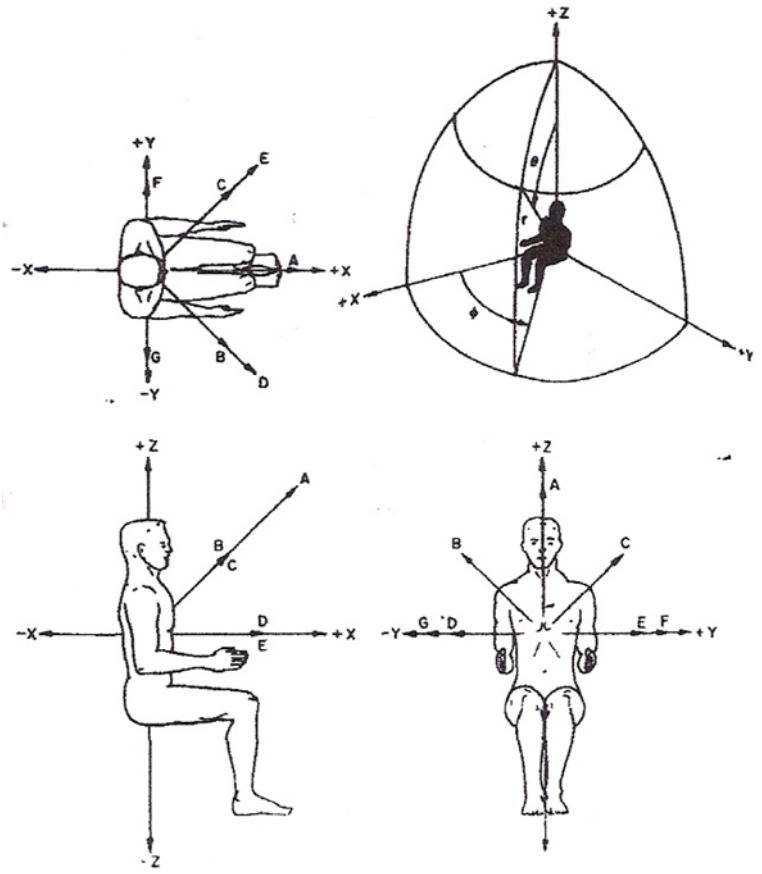

Figure 40. Acceleration vectors [26].

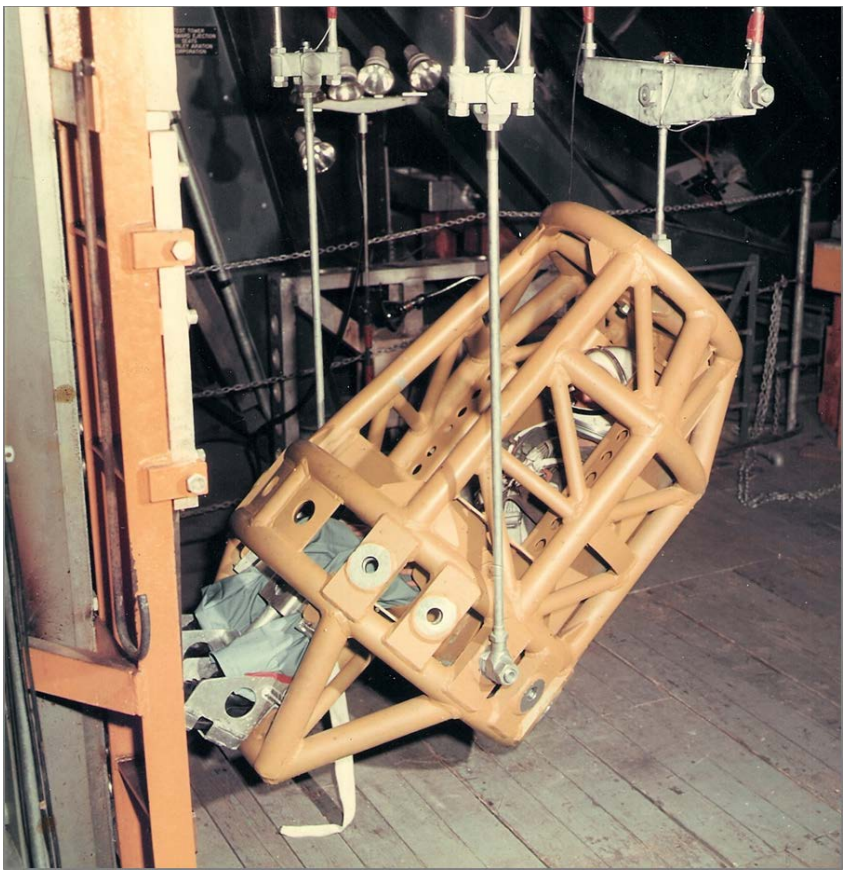

Figure 41. Multi-directional impact vehicle showing seat and volunteer subject. (Credit: USAF)

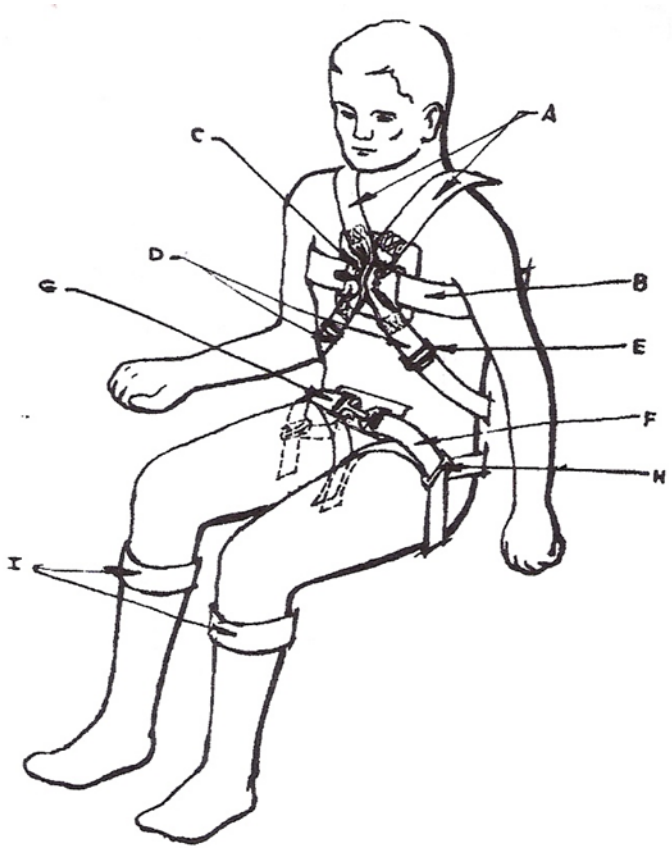

Figure 42. Restraint system configuration [26].

The subject panel included 20 male USAF subjects. The acceleration and force data were subjected to extensive mathematical analysis based upon the Fourier Transformation [150]. The relationship between the measured forces and impact velocity, called mechanical impedance, was used to identify the human body DR properties in terms of resonances similar to those of linear, second-order, spring-mass-damper systems. Broad, low-amplitude resonances were identified at 3.5, 5.5, 7.2, and 11.7 Hz. There was no gross distinction in the impedance magnitude or phase angle among the orientations studied. The subject impedance magnitude increased linearly with frequency to about 35 Hz. The analysis was not valid beyond this frequency because the velocity pulse did not contain significant frequency components beyond 35 Hz. Physiologic and subjective response data that were collected indicated abrupt cardiac rhythm changes at the higher acceleration levels, wind knocked out, and various sites of transient pain including the head. The investigators concluded the head would present a problem at higher impact levels. However, no voluntary tolerance limit was specified [26].

The USAF accomplished further tests as part of its joint effort with NASA using a horizontal deceleration track at Holloman AFB, New Mexico. Stapp and Taylor [28] explored 16 different seat orientations with 58 male volunteers ranging in age from 18 to 42 years old, 165.1 to 190.5 cm in height, and 52.2 to 94.8 kg in weight. A total of 146 tests were conducted to explore the effects of accelerations ranging in magnitude from 10 to 25 G, rates of onset from 1,000 to 2,000 G/s, and durations from 60 to 130 ms. A pneumatic piston accelerated a sled and subject, allowing it to coast and impact a water-filled decelerator at velocities ranging from 18 to 46 ft/s. The subjects wore Mercury pressure-suit helmets and were restrained by the same developmental restraint system used by [26] at AFRL. The seat was constructed of flat panels to support and constrain the subject's movement in the rearward and sideward directions [28] (see Figures 43-44). For smaller subjects, panels were used to ensure that there were no gaps between the subject and the seat.

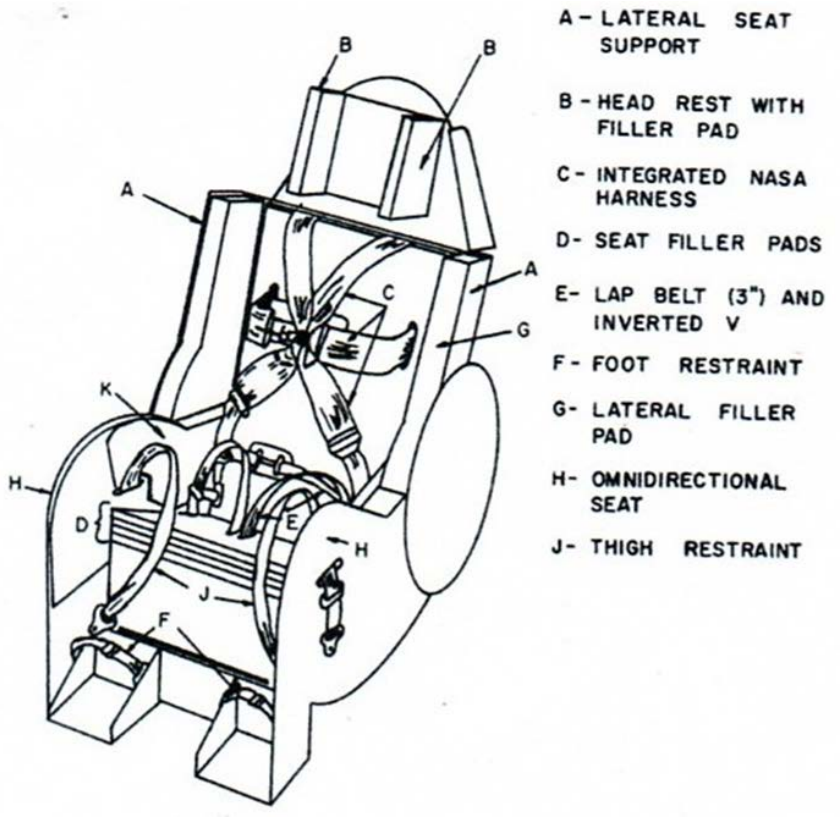

Figure 43. Seat and Restraint System [29].

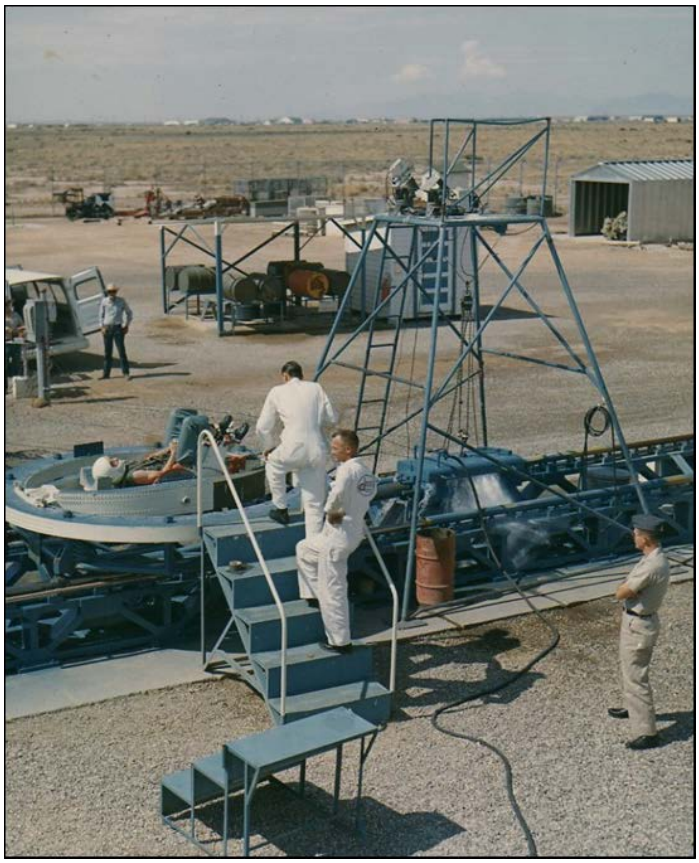

Figure 44. Photograph of horizontal deceleration test facility and subject restrained within the multi-directional test apparatus. (Credit: USAF)

All body positions and impact conditions were tolerated without injury except the forward-facing 45-degree reclining position at 25.4-G sled acceleration with a rate of onset of 960 G/s and 97-ms duration. The subject experienced soft tissue pain and stiffness in the area of the 6th through 8th thoracic vertebrae for 60 days. Bradycardia was experienced in 55 electrocardiograms immediately after impact. The bradycardia was triggered by headward impact vectors due to stimulation of the carotid sinuses, dropping the heart rate as much as 90 beats per minute for 10 to 30 seconds. The restraint looseness was found to be a contributing factor. Persistent or severe pain was absent in 146 of 163 tests.

Brown et al. [29] extended the research of Weis et al.[26], and Stapp and Taylor [28] by conducting 288 impact tests with 79 young adult male volunteers (18 to 42-years old, 167.6 to 190.5 cm height, and 52.6 to 95.0 kg weight) using the horizontal deceleration track to explore the responses of the nervous, cardiovascular, respiratory, and musculoskeletal systems. Twenty-four acceleration vector directions in 45-degree increments were studied (see Figure 45) using the same helmet, body support, and restraint in the two studies described above. Seventy-nine subjects participated in this experimental study. At each seat orientation, the impact level was increased in increments of 2 to 5 G until the occurrence of an adverse reaction based upon the evaluation of the subjective, clinical, and physiological responses by the medical monitor, determined the maximum impact levels. Two tests were accomplished at each combination of position, acceleration level, and onset rate. The sled acceleration ranged from 5.5 to 30.7 G, the rate of onset was varied from 300 to 2,500 G/s, and the impact velocity ranged from 9.3 to 45 ft/s. The highest impact levels were achieved in positions 19 and 23, whereas lower levels were limited to 11.8 and 11.1 in positions 9 and 13, respectively. The +Z- and -Z-axes orientations of positions 9 and 13 had been explored more thoroughly in the earlier tests by Schulman et al. [27], Weis et al. [26], and Stapp and Taylor [28].

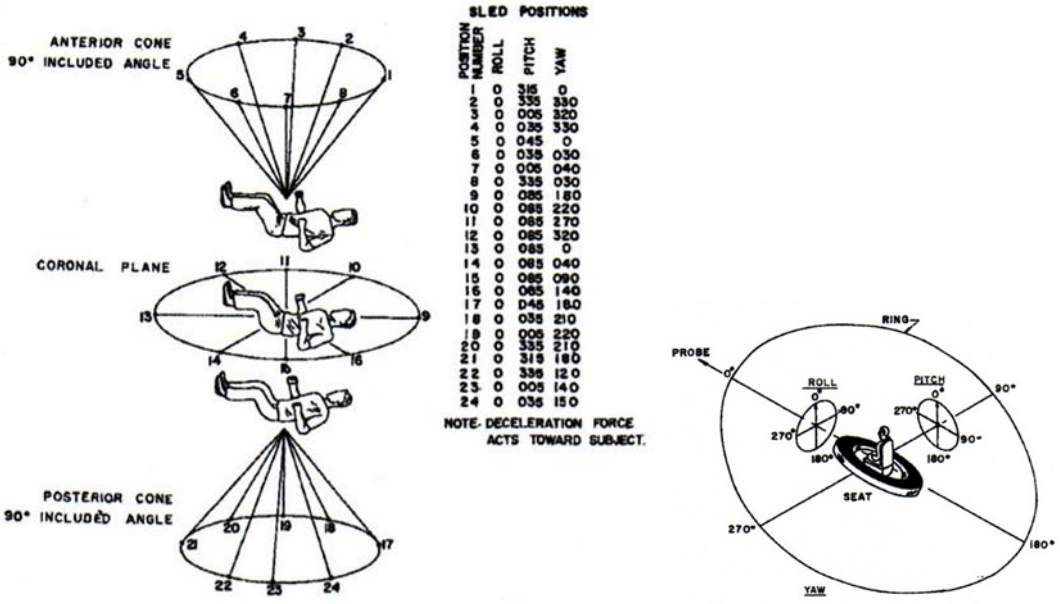

Figure 45. Force vectors orientation applied to the volunteers [29].

The neurological effects observed were momentary stunning and disorientation, which lasted no more than 2 minutes. In one case, this response was noted at an impact level as low as 17.4 G, where the impact force vector was in orientation 17. Headaches lasting several hours were noted in nine tests. Shortness of breath and chest pain was experienced by the subjects in more than one-half of the higher-level tests. Musculoskeletal complaints resulted primarily from muscle spasms and strains of the neck, back, and lower extremities.

APPENDIX B - NASA SIGN CONVENTION

The coordinate system used by NASA is shown in Figure 46 as given in the NASA/SP-2010-3407, NASA Human Integration Design Handbook, [151]. To be consistent with the original derivation of the Brinkley Dynamic Response Criterion (BDRC), this report uses the ±X, ±Y, ±Z nomenclature (acting acceleration) instead of the ±Gx, ±Gy, and ±Gz nomenclature (inertial responses) used in the NASA Standard (Figure 47).

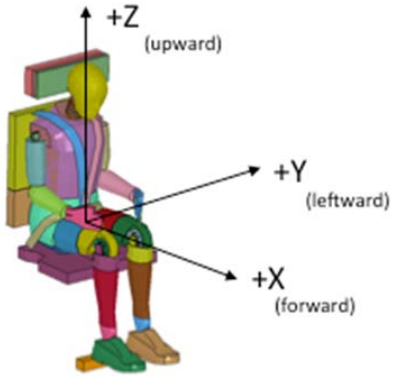

Figure 46. Acting Acceleration Directions

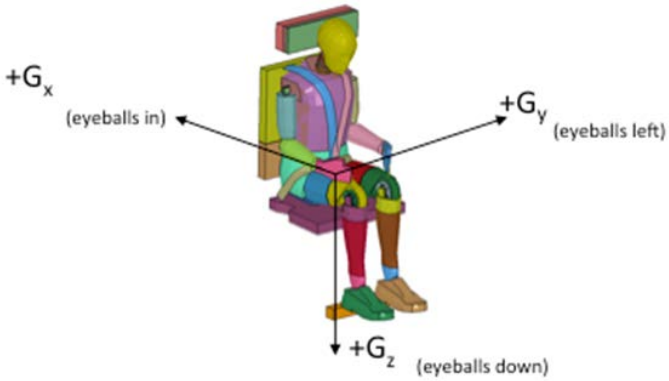

Figure 47. Inertial Responses

APPENDIX C - ACRONYMS AND ABBREVIATIONS

ACRV	Assured Crew Return Vehicle
AFB	Air Force Base
AFRL	Air Force Research Laboratory
AIS	Abbreviated Injury Scale
ATD	Anthropomorphic Test Device
BDRC	Brinkley Dynamic Response Criterion
BMD	bone mineral density
CAS	credibility assessment scale
CBDN	Collaborative Biodynamics Network
$_{CE}$	compression-extension
$_{CF}$	compression-flexion
$_{CL}$	compression-lateral
DAI	diffuse axonal injury
DoD	Department of Defense
DOF	degree-of-freedom
DR	dynamic response
DRI	Dynamic Response Index
EVA	Extravehicular Activity
FE	Finite Element
GSI	Gadd Severity Index
HIC	Head Injury Criteria
HSIR	Human-System Integration Requirements
Hz	Hertz
IARV	injury assessment reference values
IRB	Institutional Review Board
IRC	Injury Risk Criterion
ISS	International Space Station
lbf	Pounds (force)
JSC	Johnson Space Center
JSF	Joint Strike Fighter
MTBI	mild traumatic brain injury
NASA	National Aeronautics and Space Administration
$_{TE}$	tension-extension
$_{TF}$	tension-flexion
$_{TL}$	tension-lateral
USAF	United States Air Force
WSTC	Wayne State Tolerance Curve

APPENDIX D - DOCUMENTATION

JPR 1700.1	JSC Safety and Health Handbook
MIL-S-58095A	Military Specification Seat System: Crash-Resistant, Non-Ejection, Aircrew General Specification
MIL-S-9479B	Military Specification Seat System, Upward Ejection, Aircraft, General Specification
NASA/SP-2010-3407	NASA Human Integration Design Handbook
NASA-STD-3001, Volume I	Space Flight Human-System Standard, Volume 1: Crew Health
NASA-STD-3001, Volume II	Space Flight Human-System Standard Volume 2: Human Factors, Habitability and Environmental Health
NASA-STD-7009	Guidance Document for Human Health and Performance Models and Simulations
NHTSA FMVSS 208	Occupant Crash Protection
SAE AS-8043B	Restraint Systems for Civil Aircraft
SFI Specification 16.1	Driver Restraint Assemblies
U.S. Code of Federal Regulations Title 14, Part 1230	Protection of Human Subjects